MODELING OF CONTINUOUS COMPOSITE PARTIALLY REINFORCED GIRDERS WITH CFRP

BY

MOHAMMAD ABDUL RAHMMAN SAMAANEH

A Thesis Presented to the
DEANSHIP OF GRADUATE STUDIES

KING FAHD UNIVERSITY OF PETROLEUM & MINERALS

DHAHRAN, SAUDI ARABIA

In Partial Fulfillment of the
Requirements for the Degree of

MASTER OF SCIENCE

In

CIVIL ENGINEERING

MAY, 2012

KING FAHD UNIVERSITY OF PETROLEUM AND MINERALS

DHAHRAN 31261, SAUDI ARABIA

DEANSHIP OF GRADUATE STUDIES

This thesis, written by **MOHAMMAD A. SAMAANEH** under the direction of his thesis advisor and approved by his thesis committee, has been presented to and accepted by the Dean of Graduate Studies, in partial fulfillment of the requirements for the degree of **MASTER OF SCIENCE IN CIVIL ENGINEERING**

Thesis Committee

Dr. Alfarabi M. Sharif (Advisor)

Dr. Muhammed Baluch (member)

Dr. Abul Kalam Azad (member)

27 MAY 2012

Dr. Nedal T. Ratrout
Chairman, Civil Engineering Department

Dr. Salam Zummo
Dean of Graduate Studies

29/5/12

Date

IN THE NAME OF ALLAH, THE MOST GRACIOUS, THE MOST MERCIFUL

Dedicated

To

My Beloved parents

ACKNOWLEDGMENTS

All praise be to ALLAH Subhanahu wata'ala for bestowing me with health, opportunity, patience and knowledge to complete thesis research. May the peace and blessing of ALLAH (S.W.T) be upon prophet Mohammad (PBUH), his family and his companions.

I would like to thank my parents, sisters and all of my family for their continuous love, encouragement, prayer, emotional and moral support throughout my life. Words fall short in conveying my gratitude towards them. A prayer is the simplest way I can repay them – May ALLAH (S.W.T) give them good health and give me ample opportunity to be of service to them throughout my life.

I would like to acknowledge KFUPM for the support extended towards my research through its remarkable facilities and for providing me the opportunity to pursue graduate studies.

I acknowledge, with deep appreciation, the inspiration, encouragement, remarkable assistance and continuous support given by my thesis advisor Prof Alfarabi M. Sharif. His valuable suggestions made this work interesting and a great learning experience for me. I am deeply indebted to my committee members, Prof. Mohammed Baluch, Prof. Abul Kalam Azad for their constructive support and encouragement.

I would like to acknowledge my friends at KFUPM, Palestine, and everywhere for their support and love.

TABLE OF CONTENT

LIST OF TABLES

LIST OF FIGURES

THESIS ABSTRACT

NAME: **MOHAMMAD ABDUL RAHMMAN SAMAANEH**
TITLE: **MODELING OF CONTINUOUS COMPOSITE PARTIALLY REINFORCED GIRDER WITH CFRP**
Major Field: **CIVIL ENGINEERING**
Date of Degree: **MAY 2012**

The continuous composite steel-concrete girders are commonly used in bridges and building systems. The negative moment over the interior supports plays an important role in designing the continuous composite steel-concrete girders. The loss of composite action at the negative moment region reduces the capacity of the girder. The capacity of the girder at the negative moment region is evaluated based on one of the following:

i) The steel section alone neglecting the concrete slab in tension
ii) Considering the composite action between steel section and steel reinforcement of the slab.
iii) Pre-stressing the concrete at the negative moment region using external or internal tendons, so that the composite action between steel and concrete is maintained.

The principal objective of this research work is to investigate a new method of maintaining the composite action of continuous fully composite steel-concrete girders at the negative moment region. Carbon Fiber Reinforced Plastics (CFRP) sheets bonded to the top of concrete slab at the negative moment region. The girder modeled using finite element software (ANSYS) to study it's behavior, and to evaluate the effect of partial Reinforcement of CFRP on the capacity of the section. This research included studying the effect of CFRP length and thickness on the ultimate capacity and recommendations for the best length and thickness of CFRP.

MASTER OF SCIENCE

KING FAHD UNIVERSITY OF PERTOLUEM AND MINERALS
Dhahran, Saudi Arabia

THESIS ABSTRACT (ARABIC)

ملخص الرسالة (باللغة العربية)

الاســــــــــم: محمد عبد الرحمن سماعنه

عنوان الرسالة: نمذجة الكمرات المستمرة المركبة والمسلحة جزئيا باستخدام البوليمير المدعم بألياف الكربون

التخصـــــص: هندسة مدنية (إنشاءات)

تاريخ التخـرج: جمادى الآخر ١٤٣٣هـ (الموافق مايو ٢٠١٢)

تستخدم الكمرات المستمرة في الجسور وأنظمة البناء بشكل شائع. يؤثر عزم الدوران السالب فوق الدعامات الداخلية بشكل رئيسي في تصميم الكمرات المتصلة المركبة من الفولاذ والخرسانة. كما أن فقدان الخرسانة في منطقة عزم الدوران السالب يقلل من قوة الكمرات المستمرة. هذا علماً أن قوة تحمل الكمرات المستمرة في منطقة عزم الدوران السالب يمكن حسابها باستخدام أحد الخيارات التالية:

i. قوة تحمل مقطع الفولاذ وحده مع إهمال الخرسانة التي تتعرض للشد.
ii. الأخذ في الاعتبار التأثير المركب بين مقطع الفولاذ وحديد التسليح الموجود داخل البلاطة الخرسانية.
iii. استخدام حديد التسليح الخارجي أو الداخلي مسبق الشد للحفاظ على التأثير المركب بين الخرسانة والحديد.

يهدف هذا البحث بشكل رئيسي إلى دراسة طريقة جديدة للحفاظ على التأثير المركب بين الخرسانة والحديد في منطقة عزم الدوران السالب للكمرات المركبة من الخرسانة والحديد. تم تثبيت صفائح البوليمر المدعم بألياف الكربون على السطح العلوي للخرسانة في منطقة العزم السالب. كما تم القيام بنمذجة الكمرات باستخدام برنامج العناصر المحدودة (ANSYS) لدراسة تأثير التسليح الجزئي للكمرات باستخدام صفائح البوليمر المدعم بألياف الكربون على قوة تحمل الكمرات. وقد تضمن هذا البحث دراسة تأثير طول صفائح ألياف الكربون المدعم وسماكتها على قوة التحمل القصوى للكمرات بالاضافة إلى التوصيات المتعلقة بالطول والسماكة المناسبة للاستخدام.

درجة الماجستير في العلوم
جامعة الملك فهد للبترول والمعادن
الظهران ، المملكة العربية السعودية

CHAPTER ONE

INTRODUCTION

1.1 GENERAL

Composite steel-concrete structures are commonly use in bridges and buildings. The use of composite steel-concrete structures reduces the construction cost and efficiently utilizes materials properties, considering the high compressive and tensile strengths of concrete and steel respectively [1]. Composite steel-concrete girders have some advantages such as reducing the weight and the required depth of the steel section, in addition to the increasing of the floor stiffness which gives opportunity to increase the span length of the member.

The composite steel-concrete structures composed of cast in place concrete slab and steel girder. The composite action could be formed using of shear connectors, headed studs which are usually welded to the upper surface of the top flange of the steel girders to maintain the interaction and to prevent the relative slip between the concrete slab and the steel girder. Bonding materials could be used in addition or instead of the headed studs to achieve the composite action between concrete and steel which reduces the stress concentration due to shear connectors [2].

Experimental tests carried out by Bouazaoui et al. (2007) indicated that the bonded connection decreased the stress concentrations at steel-concrete connection. The first crack started at the mid-span of the concrete slab in the transverse direction. The mid-span had the maximum tensile stress, and this stress decreases towards the end of the beam. No problem in the adhesive material in the steel–adhesive–concrete composite system. It is possible to realize a bridge or footbridge by using such a bonded steel–concrete composite structure. Yielding of steel girder in addition to concrete cracking is the observed failure in this bonded composite beam.

Adhesive materials had no problem in this composite beam so that the adhesion strength between the concrete slab and steel beam is ensured. Vertical deflection of the steel beam in addition to the concrete slab cracking is the observed failure of this beam that connected by polyurethane adhesive. Mechanical behavior and the ultimate load capacity depend strongly on the adhesive's properties [3].

Finite element (FE) models and numerical analysis offer better versatility compared with the generic models. FE software could be used to analyze large steel-concrete composite structures including material and geometrical nonlinearities. Assumptions that increase the difference between the model and the actual case are not required [4][5].

1.2 COMPOSITE ACTION

The composite action of composite steel-concrete girders plays an important factor to determine the stresses distribution in the composite members as shown in figure (1). The depth of the neutral axis and the element in which the neutral axis located are greatly affecting the capacity of the composite member [6]. Fully composite girders have significant increase in the strength compared to the strength of the components acting separately. In continuous spans, the composite interaction at the negative moment region could be neglected, or only steel reinforcement could be considered. Other approach is to use an external force to overcome the negative moment and to maintain the composite action between steel and concrete.

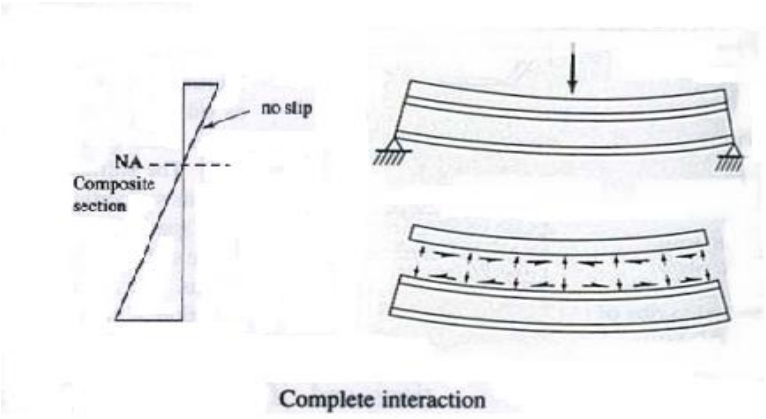

Figure 1- 1 Fully Composite Action of composite Steel-Concrete beam

In fully interacted steel-concrete girder, the system considers no relative displacement (slip) between the concrete slab and the steel beam. Shear forces acts on the lower surface of the slab to cause compression and shorten of the surface as shown in figure (1-1), where as they act on the upper surface of the steel beam to cause elongation, so that single neutral axis for the composite section.

1.3 NEED FOR THE RESEARCH

The composite action between steel and concrete in bridges has a lot of advantages in reducing cost, materials, and depth of the members. In simple span, the concrete slab under compression, where the compression capacity of the concrete is high. Continuous spans have many advantages in reducing the deflection of the member, long spans and economical sections. The negative bending moment over the interior supports in the continuous spans put the concrete in tension. Therefore the composite action lost and the capacity of the section is reduced. Including the composite action at the negative moment region leads to more economical girders with longer spans and less depth.

Most of the research works focused on the composite action between steel and concrete using analytical and numerical analysis with experimental verification. In continuous span, at the negative moment region, either the concrete slab is neglected or considering the composite action between the slab reinforcement and steel section. Several researchers used external prestressing tendons to increase the capacity of the section at the negative moment region.

This study used finite element analysis to investigate the use of CFRP to partially reinforced continuous fully composite steel-concrete girder. CFRP sheet bonded to the top of concrete slab at the negative moment region of the girders. The study focused in the benefit of CFRP in maintaining the composite action at the negative moment region and the behavior of the continuous composite girders up to failure.

1.4 OBJECTIVES OF THE STUDY

The main objective of the proposed study is to model continuous composite steel-concrete girder using finite element software " ANSYS ". At the negative moment region, CFRP sheet bonded to the top of concrete slab to utilize the composite action.

The following investigation have been carried out in this study

1) Literature review for continuous composite steel-concrete girders related to full composite action and techniques used for maintaining the composite action at the negative moment region. In addition to some CFRP applications.

2) Finite element modeling of fully continuous composite steel-concrete girder strengthened by carbon fibers at the negative moment region. The girder is composed of continuous W- shape section fully composite with the concrete slab. At the negative moment region CFRP sheet bonded to the concrete slab to maintain the composite action

3) Evaluation of the effect of CFRP in maintaining the composite action at the negative moment region, and evaluate the behavior of the composite girder up to failure.

1.5 RESEARCH PROGRAM

This study investigated the composite behavior of continuous steel-concrete girders reinforced with CFRP sheet that bonded to the top of concrete slab at the negative moment region. The research work was conducted in the following parts

i) At first, A comprehensive literature survey in the following areas:

1) Finite Element Analysis of Composite steel-concrete girder.
2) Improving Strength of continuous composite girder.
3) Improving strength of structures using CFRP.

ii) Secondly, Modeling of Continuous Composite Girder.

Finite element analysis of a continuous steel-concrete composite girder to evaluate the capacity of the composite girder. At the negative moment region, the reinforced concrete slab considered compositely acting with steel section up to it's cracking load. Once slab is cracked then composite action considered between steel reinforcement and steel section.

Finite element Software (ANSYS) was used to analyze the continuous steel-concrete girder. Suitable element selected for modeling concrete slab and steel section. Concrete element must be capable of cracking in tension and crushing in compression "like SOLID65 in ANSYS", whereas the steel element must be able to simulate plasticity and large strain "Like SOLID45 in ANSYS". Geometry and materials nonlinearity included in the model.

iii) Thirdly, Modeling of continuous fully composite girder partially reinforced with CFRP.

Finite element analysis of the composite continuous steel-concrete beam with CFRP sheet bonded to the concrete slab at the negative moment region. The model evaluated the girder behavior up to failure. The composite action between the concrete and CFRP sheet as well as thickness and length of CFRP sheet are investigated.

This part includes the modeling of continuous steel-concrete girder strengthened with CFRP sheet. CFRP sheet bonded to the top of the concrete slab at the negative moment region. The concrete slab is fully composite with the steel section. Suitable element selected for modeling CFRP sheet. A solid element used for modeling of CFRP "SOLID46 in ANSYS". Properties of adhesive material between concrete and CFRP induced to the program in the model. Geometry and materials nonlinearity included in the model.

iv) Fourth, Finite element results, and discussion of the results

Discuss the finite element results on the use of partial strengthening of continuous composite girders using CFRP sheet. Then based on the results, the required detail of CFRP sheets at the negative moment region to maintain the composite action are recommended.

v) Simplified Analytical Solution

This section included simple analysis to get a simplified design equation. Equations for designing girder partially reinforced with CFRP are included in this part. Plastic analysis for the girder and comparison between analytical and FE results also included.

CHAPTER TWO

LITERATURE REVIEW

2.1 FINITE ELEMENT ANALYSIS OF COMPOSITE STEEL-CONCRETE GIRDER

Nowadays, finite element modeling and numerical procedures become one of the most important techniques in research and developing new structural models. It can be used to analyze composite steel-concrete structures including all materials and geometrical nonlinearities in the analysis. The degree of accuracy depends on the number of elements in the model, the selected elements, and accuracy of the assumptions before start modeling.

Finite element modeling and analytical study of simply supported composite girders carried out by Zona and Ranzi (2007). The study assured that the relative displacement must be included in the model to have suitable representation of the composite action [7]. The steel-concrete connection should be included in the study as an important parameter such as materials and geometry.

Ayoub (2005) conducted finite element analysis to simulate the composite action of steel-concrete composite members. The study provided that the slab is acting as an integral part of the girder because of the shear connectors which welded to the top surface of the steel flange [5]. In continuous steel-concrete girder, the situation is different because of the negative moment, and the tensile stresses in the concrete.

Finite element analysis used in studies to predict the behavior of the composite action under different conditions. FE modeling results showed agreement with experimental results [8]. Ranzi and Tahmasebini (2011) carried a three-dimensional FE modeling to predict the response of composite steel-concrete beams up to failure. Simply supported composite beams and continuous two spans in addition to three spans beams were modeled using FE software. The results showed that "it's not required to describe the nonlinear behavior of the connectors because the particularity of the proposed model relies on its ability to model the shear connectors as solid elements" [9].

Parametric study carried out by Yakel et al. (2005), the study investigated the important parameters in the composite steel-concrete beams. It concluded that the depth of the neutral axis is important, but the element in which the neutral axis is also affecting the strength of the structure. In continuous span girder, the location of the neutral axis is important such that it will determine the tension stresses in slab as well as compression stresses. The study provided two sets of predictive equations based on the location of the neutral axis, if it's below the mid-depth of the compression flange or above the mid-depth of the compression flange which predict to have higher strength [6].

Luo et al. (2011) did a 3-D finite element modeling using ANSYS to simulate material nonlinearity of bonded steel-concrete girder. (SOLID65) used to model concrete, and 8-node solid element (SOLID45) used for steel [4]. The study assured that the bonding material can be used to maintain the composite action of the composite girder, and the bonding materials are efficient to allow a large plastic strain without shear failure. Good agreement between finite element results and experimental results.

Non linear finite element model carried out by Jurkiewiez et al. (2011). It showed that similar behavior of composite action of composite girder that had normal strength concrete with a bonding connection and composite steel-concrete girder with mechanical connectors [1].

Analytical model for steel-concrete composite beams including the shear deformability of the steel component carried out by Ranzi and Zona (2007). Continuous shear connection used to provide the composite action which enabled relative longitudinal displacements to occur between the two components [7]. "The steel beam modeled as linear elastic whereas slab modeled as linear viscous–elastic integral type constitutive law". Numerical analyses of simple span and continuous three span composite beams were done to study the effect of shear deformability of the steel beam on the overall composite beam. The results compared with other beams where the shear deformability not included. The study concluded that the shear deformability of steel beam must be included because of the difference of the results.

FE model carried out by Porco et al. (1994) to predict deformations and stresses in composite steel-concrete beams. The effect of cracking and tension stiffening were taken into account in addition to the longitudinal slip between the concrete slab and steel beam due to the partial interaction of the connectors. A parametric study was done to investigate the effects of the geometrical and mechanical variables as boundary conditions and the slip modulus of the connectors. The finite element analysis compared with available experimental data to validate the results and showed good agreement [10].

Most of the research work focused on improving the composite action or to increase the capacity of composite simply supported spans. Sallam et al. (2010) used carbon fiber reinforced polymers (CFRP) to increase the load carrying capacity of simple span composite steel-concrete girders. The ultimate capacity of composite steel-concrete girders improved by bonding fiber reinforced polymers (FRP) laminates to the tension flange of the steel girder. CFRP has great ability for the repair and strengthening of steel girders due to high strength to weight ratio in addition to corrosion resistance and high fatigue properties [11].

2.2 IMPROVING STRENGTH OF CONTINUOUS COMPOSITE GIRDER

Degree of continuity (mainly in building) is one of the parameters in the design of continuous composite steel-concrete beams. Fabbrocino et al. (2002) presented some computational aspects related to the modeling of continuous and semi-continuous composite flexural members [12].

Vasseghi (2009) carried out nonlinear finite element analysis for continuous span girder. The study used a simple reinforcement to change the mechanism of failure for the continuous girder by forming plastic hinges over the interior support and at mid-span. Longitudinal stiffeners or plates used on the opposite sides of the web near the interior support to prevent local buckling. Strength in addition to the ductility of the composite girder were greatly improved by changing failure mechanism. This new section "prevented local buckling, rotated inelastically, and reached the plastic moment capacity with good ductility allowing the second hinge to form at mid-span" [8].

Chen and Jia (2008) derived equations for continuous composite beams of uniform composite section to find the required moment redistribution to enable full plastic mechanism. Continuous composite girders must have available moment redistribution greater than the required moment redistribution to develop full plastic capacity. The required moment redistribution for continuous girder increased as the ratio of negative to positive moment resistance reduced, and decreased as the difference of load in the two spans increased [13].

The rotational capacity used as a method to evaluate the required moment redistribution over the interior support. It proposed new method of increasing the capacity of the section, it's mainly depends about changing the failure mechanism by assuring enough rotational capacity of the interior support. The study provided a design approach to increase the ultimate capacity for a continuous composite girder of two spans based on the available moment redistribution and rotation. An economical design is capable in most cases. The results showed agreement to the experimental results and computer simulations [13].

Chen et al. (2009) investigated experimentally two spans and three spans continuous composite girders. Each group had one non-prestressed composite girder and one prestressed composite girder with external tendons. The cracking behaviors, local buckling and the ultimate strength of the beams were investigated experimentally. Type of failure was concrete crushing at the mid-span and web local buckling over the support. The study showed that a significant increasing in the cracking moment resistance achieved for composite beam prestressed with external tendons. The yielding moment at the negative moment region of the beam not always increases. Lateral, distortional and local buckling occurred in the compression flanges and web of two span composite girders, whether prestressed or non- prestressed [14].

Even lateral or distortional buckling occurred in the hogging moment regions; girder achieved full plasticity at the mid-span section. Also higher sagging moment achieved by the prestressed beam compared with non- prestressed beam at the mid-span. For Three span composite hirders, lateral torsional buckling and local buckling initiated in the web and in the compression flanges. Plastic hinges were developed at the mid-span and the internal support section in the hogging moment regions as two span girders. A design proposal based on moment redistribution to evaluate the ultimate capacity of continuous composite girders prestressed using external tendons was proposed in the study [14].

Chen et al. (2009) carried out FE modeling and experimental study to investigate the increasing capacity of using prestressed tendons in continuous composite beams. The study considered the full composite section up to the first crack appeared in the concrete. The first crack in the two span girder occurred transversely across the concrete slab over the interior support in the non prestressed beams, and subsequent cracks were developed immediately adjacent to the first crack. Distortion in the web and lateral buckling occurred in the bottom flange and significant web buckling and bottom flange buckling noted after crushing of concrete. The prestressed continuous beams had the same observations but with much higher load than non-prestressed continuous beam.

Nakamura et al. (2002) investigated several new steel concrete composite bridges constructed in Japan. The study assured that "steel girders are relatively vulnerable against the compressive forces". At the same time, "the concrete filled pipe girders and the partially encased I-girders that investigated in the study can greatly improve the

bending strength". Local buckling of plates in compression could be resisted by concrete when it's filled in the section. Steel girders filled by concrete are good for damping and it can reduce noise and vibration levels of the bridge. "This work presented new railway bridge system using steel pipe girders filled with concrete, new structural forms using concrete filled pipes or rolled H-girders, a composite bridge with rolled H girders, in addition to partially concrete filled I-girders" [15].

Partially encased composite girder proposed by HAYASH et al. as a new type of steel-concrete composite bridge. Reinforcing bars were welded to the steel flanges whereas concrete filled into the areas surrounded by the flanges and web. The results proved experimentally. High ultimate bending strength and shear strength for encased composite girder compared to the conventional steel I-girder. This method is recommended for retrofitting or rehabilitation of wide flange steel girder subjected to damage or deformed by buckling. Bending and combined bending and shear test carried out simultaneously on the steel I-girder and the encased composite girder retrofitted by this method [16]. In this way, enough ultimate strength of the partially encased composite girder can be achieved. "The new structure was so valuable to retrofit the steel I-girder even if it was deformed excessively. But, it is important also to investigate the effectiveness and availability for retrofitting fatigue crack and corrosion".

Nie et al. (2011) carried out a loading capacity analysis for prestressed continuous steel-concrete girder. The cracking, yielding, and ultimate capacity of continuous prestressed composite girder under concentrated loads were presented and extended to general cases.

"The variation of tendon force is considered and the adopted limit equilibrium approach only requires the development of equilibrium equations". Also, nonlinear behavior of prestressed continuous composite beams was simulated by finite element model using finite element software. Materials and geometrical nonlinearities were considered in the numerical model. The model reflects the complicity in the behaviors of prestressed two span composite girders during the loading process. "The increment of tendon forces, slip effect, curvature distribution, formation of plastic hinges, redistribution of internal forces, and the stress distribution were the most complexities in the model". Comparisons between experimental and analytical, numerical results showed that the analytical method provided reliable and convenient method for a routine design practice. Finite element model provided excellent numerical simulation for the nonlinear behavior of prestressed continuous composite girders [17].

External post-tensioning strengthening is an effective technique to restore the ultimate load carrying capacity of many types of bridges. Choi et al. (2009) expressed a systematic procedure of external post-tensioning technique for strengthening or rehabilitation of existing bridges. Virtual work principle used for derivation of analytical expressions for the increment of the initial tendon force in the study. Choi introduced a new rating equation for bridges considering the initial tendon force in addition to its increment [18]. Systematic procedures could be used to find number of strands in external tendons in addition to the initial tendon force using the proposed rating equation.

Experiments results and finite element analysis used to verify the analytical expressions for the increment of a tendon force and showed good agreement. The study showed that the proposed method is suitable for strengthening of existing bridges with external post-tensioning technique. More economical design may be feasible by considering the increment of tendon force.

2.3 IMPROVING STRENGTH OF STRUCTURES USING CFRP

Nowadays carbon fiber reinforced polymer (CFRP) uses for strengthening members in flexure and shear. It can be used because of the properties of this material which can provide high strength with low weight. The plasticity of the material gives ability to use it in relative high deformation. Sallam et al. (2010) used CFRP and steel plates to increase the capacity of composite steel-concrete beam (simple span beam). Two different patterns of CFRP sheet were used, I-beam wrapped with CFRP around the flange whereas the second the flange and part of the web was wrapped with CFRP. Both of them were checked by testing four different strengthened steel-concrete composite girders. Two composite girders were strengthened by CFRP sheet with the two different patterns, whereas the others were bonded with steel plate of 50 mm length and flange width at the bottom surface of the bottom flange. The experimental results showed that increasing in the capacity achieved by using CFRP sheets and steel plates. CFRP sheet participated in increasing the capacity of the beam significantly after yielding of the bottom flange [11].

Ibrahim and Mahmood (2009) used finite element software ANSYS to model reinforced concrete beams reinforced externally with FRP laminates. Smeared cracking approach used to model concrete and 3-D layered elements to model FRP composites. Experimental data for six beams with different conditions from researches used to verify the results obtained from ANSYS [19].

Load-deflection curves at mid-span and ultimate load carrying capacity were used for comparison. The behaviors of the FE models showed agreement with results that obtained from the experimental full scale beam tests. The load-deflection curves from the finite element analysis have will agreement with the experimental results in the linear range, but the FE result was slightly stiffer than that from the experimental results. Change in the failure mechanism observed by using addition FRP reinforcement.

Shifting in the failure mode of the control beam from shear failure near the ends to flexure failure at the mid-span was noted in the study. "The obtained results demonstrated that carbon fiber polymer is efficient more than glass fiber polymer in strengthening the reinforced concrete beams for shear". FE model could be used with additional studies to develop design rules for strengthening reinforced concrete members using FRP laminates.

The ultimate capacity of a composite steel-concrete girder can be enhanced significantly by bonding CFRP laminates to its' tension flange. Tavakkolizadeh and Saadatmanesh (2003) conducted a study on the behavior of steel-concrete composite girders strengthened with CFRP sheets under static loading. "Three composite girders made of A36 steel beam and 75 mm thick by 910 mm wide concrete slab were prepared and tested. Constant thickness of the CFRP sheet with different number of layers of 1, 3, and 5 were used in the specimens" [20]. The results showed that bonding CFRP sheet increased the ultimate strength of composite steel-concrete girders and traditional methods could be used to predict the behavior conservatively. The ultimate load carrying capacity improved significantly for all three retrofitted girders considered in this study.

Case study carried out by Soliman Khudeira (2010) on one of the Lake Shore Drive bridges in Chicago. "Strengthened of this bridge is preferred rather than replaced for various reasons, such as resolving existing structural deficiencies to resist seismic forces, to increase member capacity in order to carry new traffic loads, and to make repairs within budget constraint, and to fulfill immediate safety or capacity requirements". External posttensioning system used for strengthening the existing bridge. The external posttensioning systems provided many benefits including improved strength, service performance, and durability [21].

The rehabilitation of steel girders using advanced composite materials offered a smart solution for short-term retrofit or long-term rehabilitation. Several laboratory studies conducted shown that CFRP plates can be used to effectively strengthen steel bridge girders.

Miller et al. (2001) verified that CFRP cover plates can be used to restore reasonable losses of stiffness and strength in deteriorated bridge girders. "10-37% increasing in stiffness achieved for the corrosion-damaged bridge girders. The development length was found to be on the order of 100 mm. The results indicated an 11.6% increase in flexural stiffness due to the retrofit" [22]. The results showed well agreement with estimated values found using transformed sections.

Majid Kadhim (2012) studied the behavior of beam strengthened with CFRP plate in addition to the effect of strengthening length. Finite Element Software ANSYS used to model simply supported steel beam using the same data of an experimental work. Comparison between modeling and experimental result showed that ANSYS is capable of modeling and predicting the actual deformation behavior for steel beam. Continuous steel beam modeled also using Finite element software ANSYS and strengthened using different length of CFRP plate as a ratio of beam length. FE result showed that "the increase of CFRP plate length bonded in sagging region only increased the ultimate strength of beam until reach 40% length of beam span [23]. But the increase of CFRP plate length bonded in hogging region only increased the ultimate strength of beam until

reach 60% length of total beam". The corresponding increasing in capacity is 70% more than ultimate strength of un strengthened beam.

Liu et al. (2001) discussed strengthening and repairing of corroded steel members of composite girders using (FRP) material. The experimental results showed that an improvement in stiffness and plastic load of corroded steel members can be achieved by applying CFRP laminates to the tension flange of corroded steel members. Peel off of FRP laminates was the observed failure mode of the retrofitted girders. This was due to high stress concentrations near the girders mid-span [24].

Galal et al. (2011) investigated the effectiveness of using CFRP in retrofitting deteriorated steel beams. The study included using of two thicknesses of CFRP, 0.27 mm and 1.4 mm. The study showed that increasing the post-yield carrying capacity for retrofitting deteriorated steel beams with bonded CFRP. Sudden failure due to either peeling off CFRP or CFRP rapture is the observed failure mode of steel beams retrofitted using CFRP. The results showed that adhesive material has a slight influence on the load at yield, but it has a significant effect on the ultimate flexural capacity in addition to mode of failure of the CFRP retrofitted beams [25].

Retrofitting beams using anchorage system could prevent peel off of the CFRP sheet at early stage to enhance the flexural performance of the CFRP retrofitted steel beams. No significant influence on eliminating or delaying the debonding of CFRP plates by using transverse wrapping of the CFRP longitudinal retrofit plates using CFRP sheets wrapped

around the bottom flange at both ends. The end detail of the unbonded CFRP sheets in a ductile anchorage system has a significant influence on the efficiency of retrofitting scheme.

Lau et al. proposed a theoretical model to estimate shear and peel-off stresses. The theoretical solution is based on some assumptions such as elastic behavior of concrete, adhesive material, and FRP, perfect bonds between FRP plate and the concrete, thin layers of FRP and adhesive material, and no change with thickness. The research considered the axial stresses in a concrete beam strengthened by FRP including variation in FRP plate fiber orientation. Theoretical predictions validated using an experimental FE model. The results showed that maximum shear and peel off stresses were at the end region of plate.

The maximum shear stress increased by increasing the amount of fibers aligned in the beam's longitudinal axis, the modulus of adhesive material and the number of laminate layers. Also, increasing layer thickness of adhesive material decreases the maximum peel-off stress. Lau found that peeling at the plate-glue-concrete interface is rare due to strong chemical bonding of adhesive material to the concrete, but high peel-off stress may cause the FRP and concrete to separate [26].

CHAPTER THREE

FINITE ELEMENT ANALYSIS

Finite element Analysis of a continuous composite steel-concrete girder carried out in this study. The girder used in this study was tested experimentally by Chen et al. (2009) [14], so that it used to verify FE results. As part of the experimental investigation, Chen et al strengthened the girder by external prestressed tendons to maintain the composite action at the negative moment region. Two tendon cables with 274.8 mm^2 used to prestress the girder as shown in figure (3-1). This work included comparison of the strengthening done by chen and strengthening done in this work using CFRP at the negative moment region.

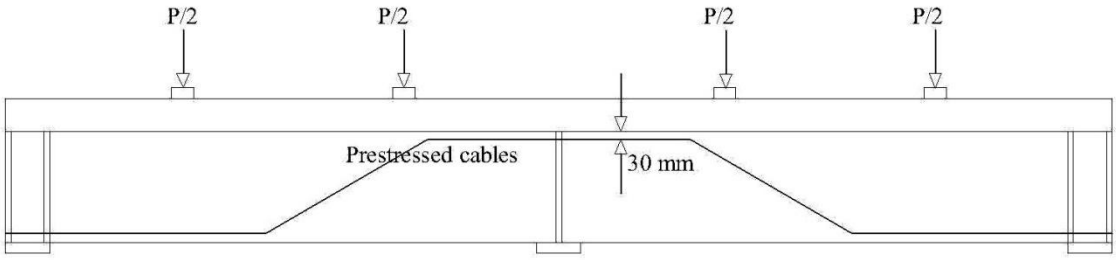

Figure 3-1 Cable profile of prestressed girder

Load-deflection curve, cracking load, ultimate load, and deflection at failure used for comparison. Also, results used to compare the increasing in the ultimate load capacity of composite steel-concrete girder strengthened by prestressed cables and by using CFRP.

3.1 GEOMETRY OF GIRDERS

Continuous two spans composite steel-concrete girder of 9.9 m. Each span has a length of 4.8 m as shown in figure (3-2). The girder has a fully composite steel-concrete section as shown in figure (3-3). Concrete slab of 550 mm width and 90 mm depth, and a steel section of 279 overall depth. Top flange of 120 mm width and 10 mm thickness whereas bottom flange of 120 mm width and 14 mm thickness. Concrete slab reinforced by 8#16 mm in two layers. This girder named as CSC in this study.

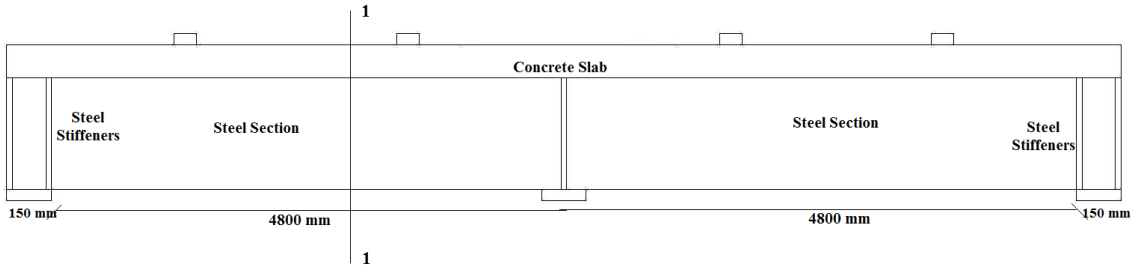

Figure 3-2 Composite steel-concrete girder

Bearing steel plates of 150 * 120 mm and 50 * 120 mm are used at supports and point load respectively. Stiffeners 10 mm in thickness are used at the supports as shown in figure (3-2).

The vertical and horizontal displacements are prevented for the end support whereas vertical displacement and out of plane horizontal displacement are prevented for the 2nd and 3rd supports.

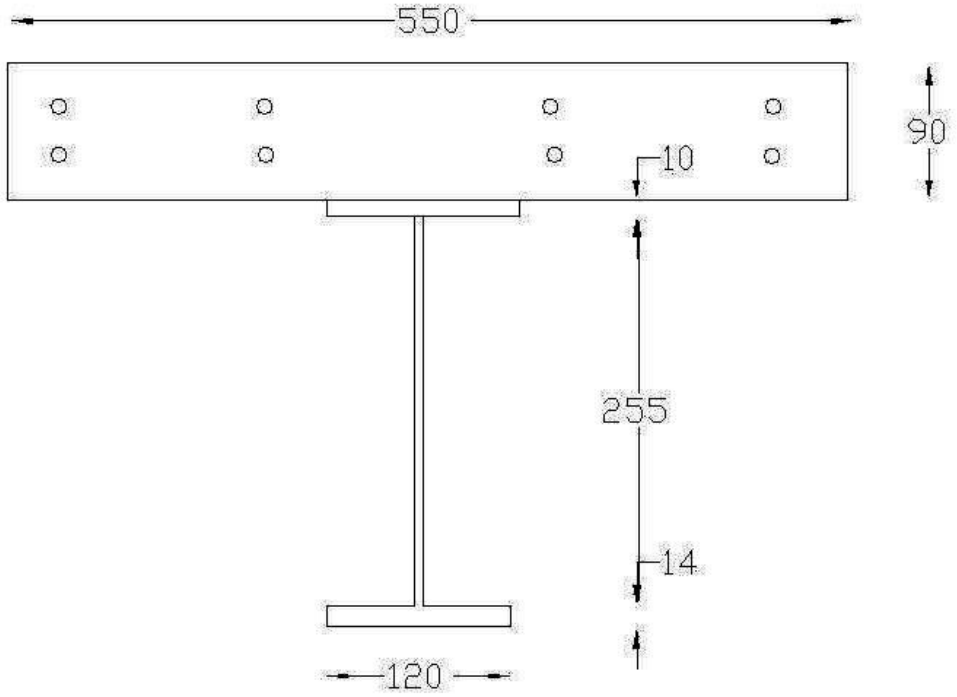

Figure 3-3 Section1-1 steel-concrete section (mm)

CFRP thickness, length of CFRP, and location of the neutral axis are the main parameters considered in the study. Different five thicknesses of CFRP sheets bonded to the concrete slab over the negative moment region to study the effect of CFRP thickness on the composite action of steel-concrete girders and the ultimate strength, in addition to optimize the better use of CFRP. These models named as CSCC1, CSCC2, CSCC3, CSCC4, and CSCC5. CSCC2Y girder is a girder with higher ultimate capacity of steel to investigate the effect of the steel section capacity on the tensile stress of CFRP. Typical steel-concrete girder and section of the girder are shown in figures (3-4) and (3-5) respectively.

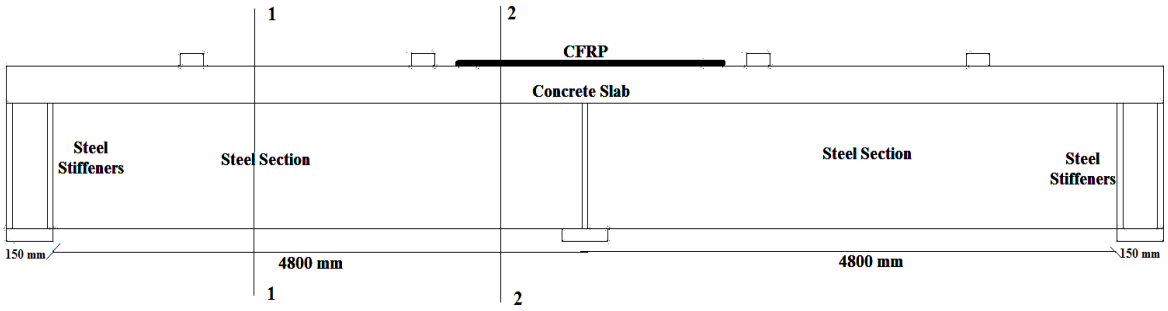

Figure 3-4 Steel-Concrete girder with CFRP

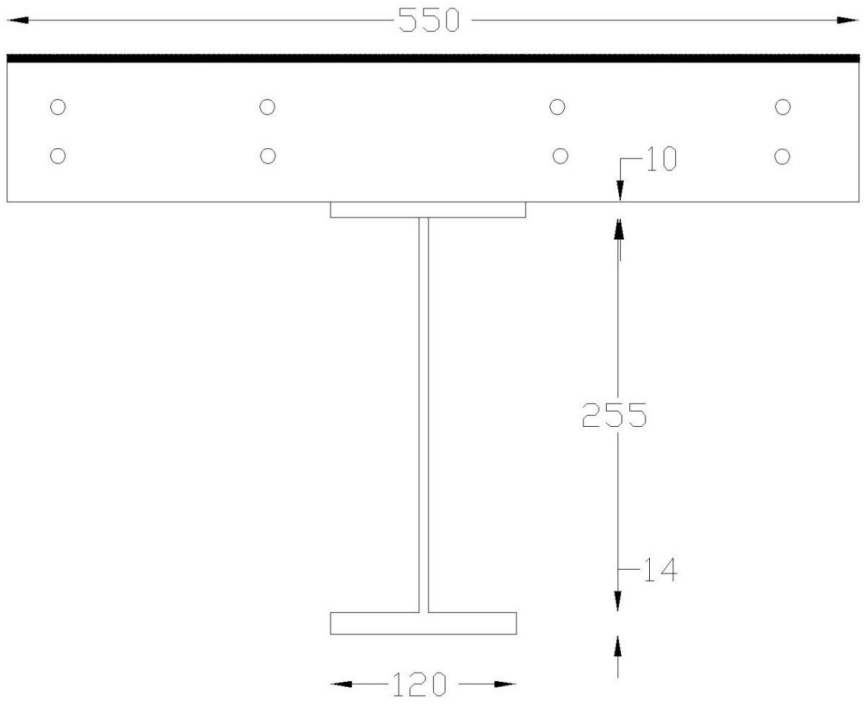

Figure 3-5 Section 2-2, Steel-Concret section with CFRP

The location of the neutral axis is varied by changing thickness of slab. Slab thickness of 90 mm as experiment considered, so that the neutral axis located in the steel web. Also thickness of 120 mm modeled in this study and named as CSCC2T, so that the neutral axis shifted to the concrete slab.

Another model named as CSCC6 with an idealized stress-strain diagram of steel considered to compare FE results with analytical solution. Table (3-1) summarizes all girders modeled in the study.

Girder	Steel Stress-Strain curve	CFRP thickness (mm)	Length of CFRP (mm)	Slab thickness (mm)
CSC	Multilinear curve	-	-	90
CSC1	Multilinear curve	-	-	120
CSCC1	Multilinear curve	0.15	2360	90
CSCC2	Multilinear curve	0.25	2360	90
CSCC3	Multilinear curve	0.5	2360	90
CSCC4	Multilinear curve	1.0	2360	90
CSCC5	Multilinear curve	3.0	2360	90
CSCC2Y	Multilinear curve with higher yielding and ultimate stress	0.25	2360	90
CSCC2L1	Multilinear curve	0.25	2800	90
CSCC2L2	Multilinear curve	0.25	3150	90
CSCC2L3	Multilinear curve	0.25	1560	90
CSCC2T	Multilinear curve	0.25	2360	120
CSCC6	Idealize stress-strain curve	0.25	2360	90

Table 3-1 Summary of modeled girders

3.2 MATERIAL PROPERTIES

Steel:

The yielding stress of steel sections equal to 383 MPa and the ultimate stress (F_u) equal to 530 MPa, whereas Poisson ratio is 0.3. The stress-strain diagram of steel is shown in figure (3-6)

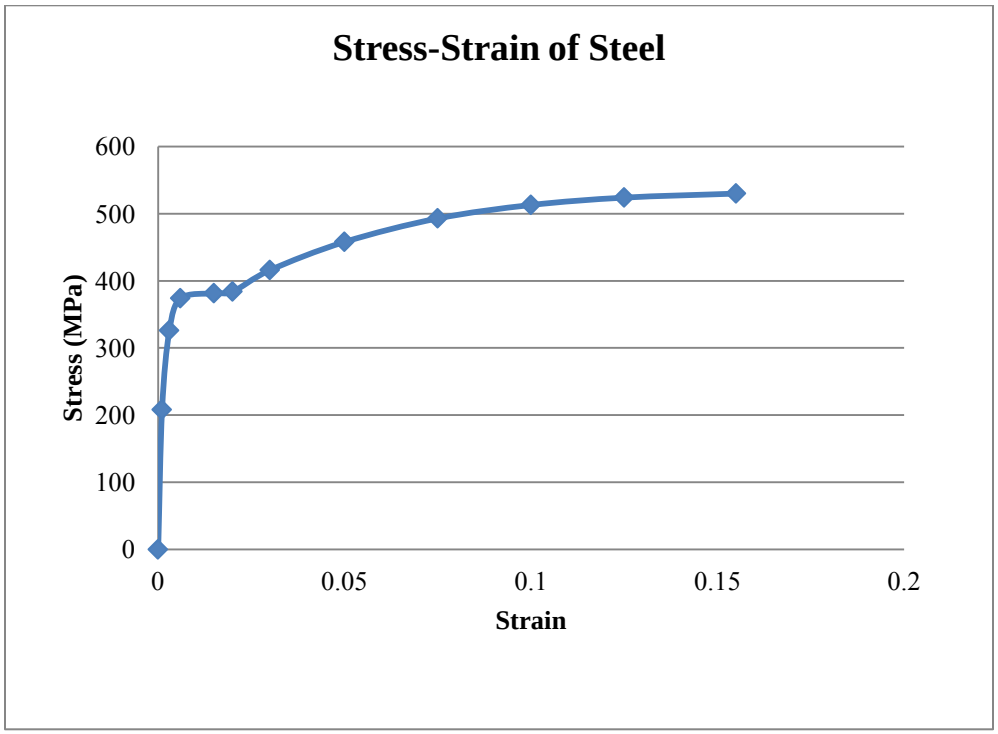

Figure 3-6 Stress-strain diagram of Steel

Concrete:

The compressive strength of Concrete f'_c equal to 34 MPa, and it has an elastic modulus of 31.5 GPa. Also the tensile strength of the concrete is equal to 2.4 Mpa. Stress-strain diagram of concrete is shown in figure (3-7).

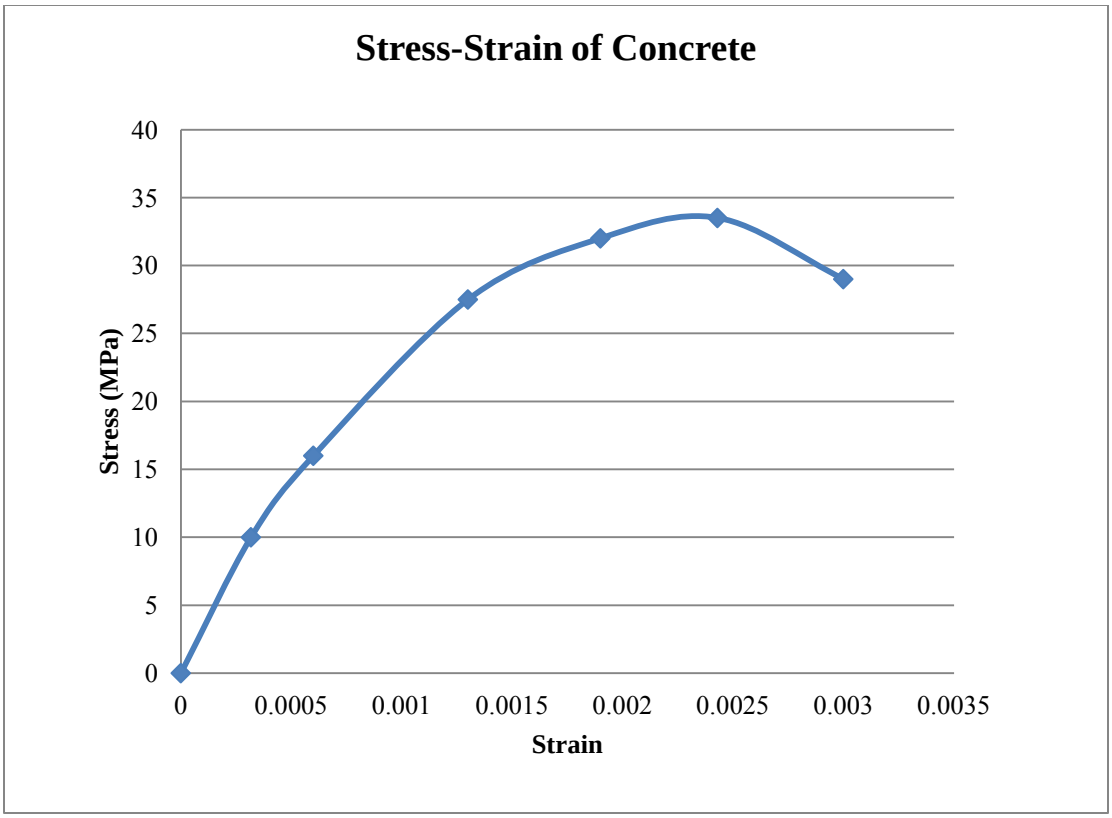

Figure 3-7 Stress-strain diagram of Concrete

Steel Reinforcement

Te yield strength of steel reinforcement is 350 MPa and the tangential modulus is 20^{o}. The concrete slab reinforced by 8*16 (201 mm^2) longitudinal reinforcement in two layers and #8 (50.26 mm^2) shear reinforcement each 300 mm. The stress-strain diagram of steel reinforcement shown in figure (3-8).

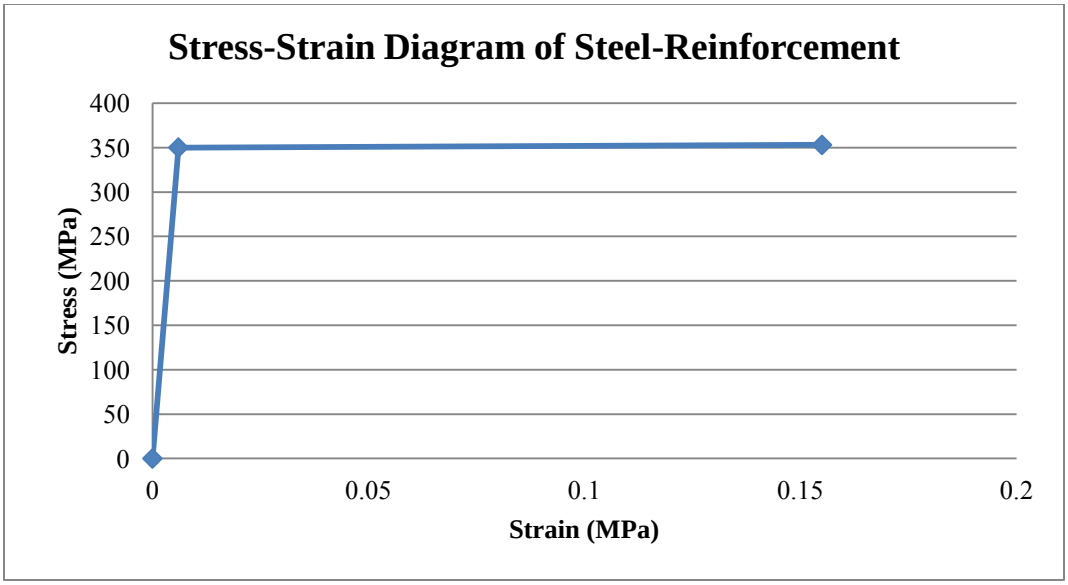

Figure 3-8 Stress-strain diagram of steel reinforcement

Carbone fiber reinforcement polymer "CFRP"

Carbon-fiber-reinforced polymer (CFRP) has a strong and light fiber-reinforced polymer that contains carbon fibers

CFRP has many uses such as:

- Increasing the load capacity of structures which include slabs, beams, and bridges for shear and bending, or columns.
- Improving capacity of damaged elements such as steel reinforcement corrosion, and vehicle impact.
- Useful in service improvements such as reduced deflection and crack width reduction.
- Change in structural system such as removal of walls or columns and removal of slab sections for openings.

The characteristic of CFRP has some advantages such as:

- ❖ Very high strength.
- ❖ Flexibility of surface geometry (Beams, columns, chimneys, piles, walls, silos)
- ❖ Lightweight and low density.
- ❖ Non corrosive.
- ❖ Combinations of high strength and modulus of elasticity available.
- ❖ Excellent durability.
- ❖ Easy to install, especially overhead.
- ❖ Economical compared to traditional techniques

CFRP bonded to the concrete slab over the negative moment region. A mid strength carbon fibers with fiber orientation of 0^o (Unidirectional) was selected.

This fiber has a fiber density of 1.8g/cm^3, the tensile strength is 3800 N/mm^2 and elongation at break is 1.64%. The tensile E-modulus is 63 KN/mm$^{2.}$

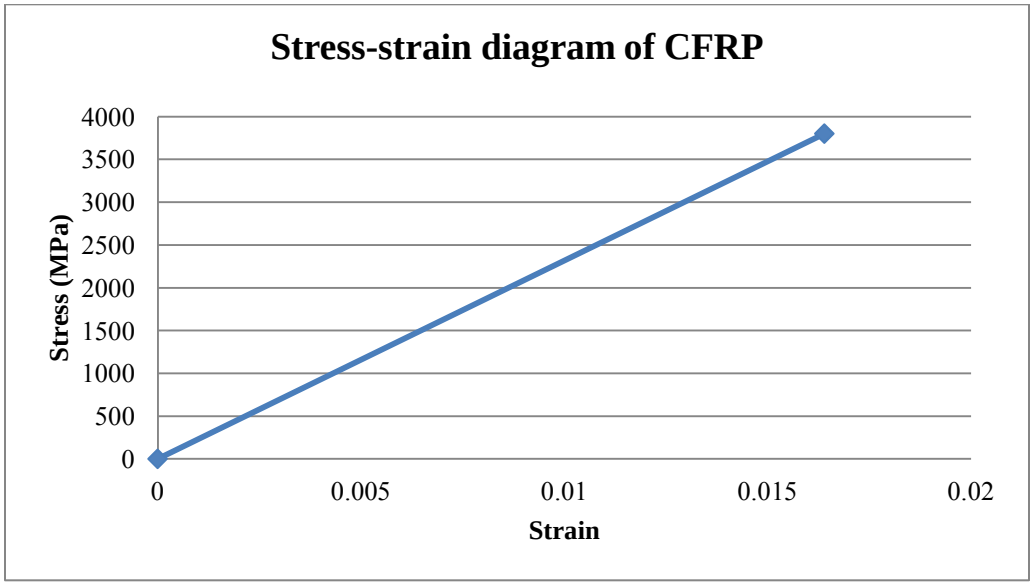

Figure 3-9 Stress-strain diagram of CFRP

Adhesive material

Adhesive materials (epoxy) use to make the interaction between structural elements and CFRP. Many types of adhesive materials could be used to connect concrete with CFRP such as 2-part epoxy impregnation resin, and Adhesive for bonding reinforcement.

2-part epoxy impregnation resin has some properties that make it proper for connecting CFRP with concrete such as:

- ✓ Easy mix and application by trowel and impregnation roller.
- ✓ Manufactured for manual saturation methods.
- ✓ Excellent application behavior to vertical and overhead surfaces.
- ✓ High mechanical properties
- ✓ No separate primer required
- ✓ Solvent free

CFRP bonded to the concrete slab using 2-part epoxy impregnation resin. The tensile strength of this material is 30 N/mm^2 and elongation at break is 0.9%. The flexural Elastic modulus is 3800 N/mm^2, and Tensile E-modulus is 4500 N/mm^2, also the shear strength of the epoxy is 22 N/mm^2.

3.3 FINITE ELEMENT MODELING

A three-dimensional Non-linear finite element models developed using ANSYS 12.1 to analyze composite steel-concrete girder and composite steel-concrete girders with CFRP over the negative region. Both material and geometric nonlinearities considered in the study.

Elements of the model

The flanges, web, and stiffener plates of the steel girder modeled using a 3-D eight nodes element SOLID45, this element has three degree of freedom at each node. Figure (3-10) shows the geometry of SOLID45. "SOLID45 has a plasticity, creep, stress stiffening, and large strain capability".

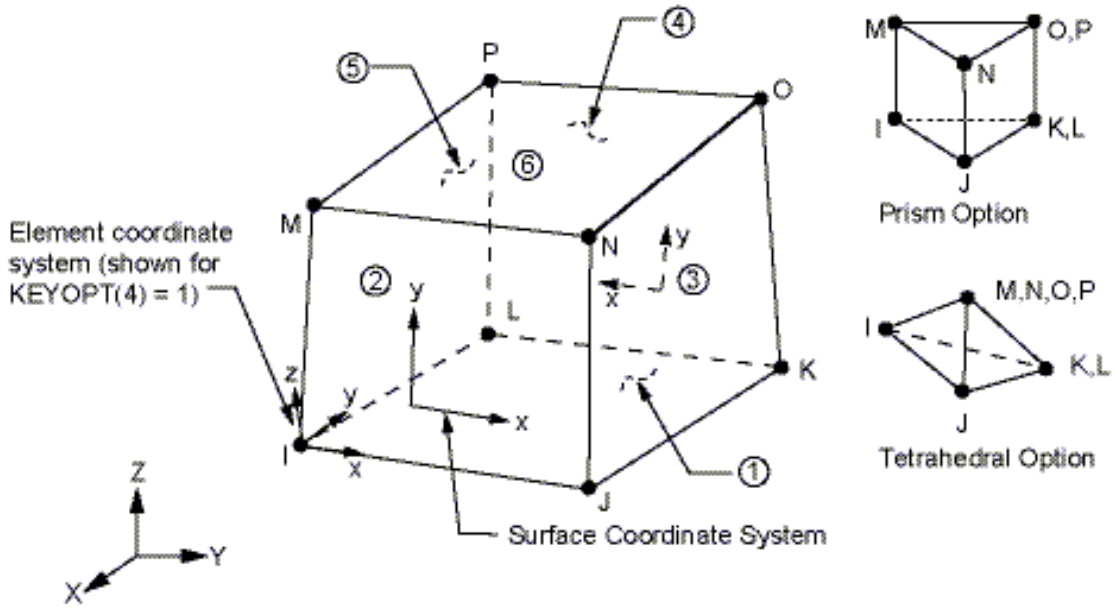

Figure 3-10 Geometry of SOLID45

The concrete slab modeled using 3-D element SOLID65. "This element is capable of cracking in tension and crushing in compression as concrete. One of the important aspects of this element is the treatment of nonlinear material properties". Geometry of SOLID65 is shown in figure (3-11).

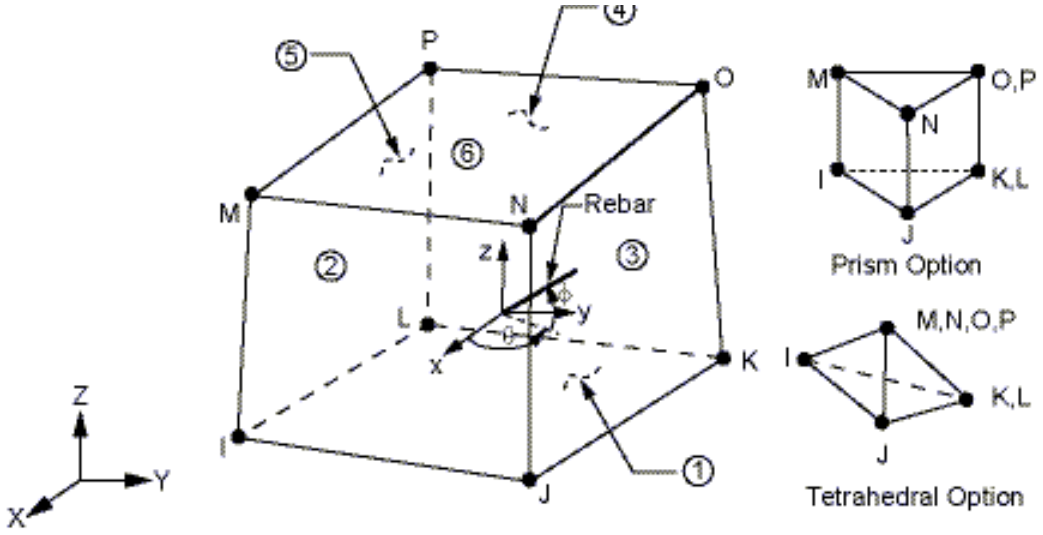

Figure 3-11 Geometry of SOLID65

Longitudinal and shear steel reinforcement modeled using LINK8 element. "This element can be used to model trusses, sagging cables, links, springs, etc. The 3-D spar element is a uniaxial tension-compression element with three degrees of freedom at each node; translations in the nodal x, y, and z directions. LINK8 includes Plasticity, creep, swelling, stress stiffening, and large deflection capabilities". Figure (3-12) below shows the geometry of the element.

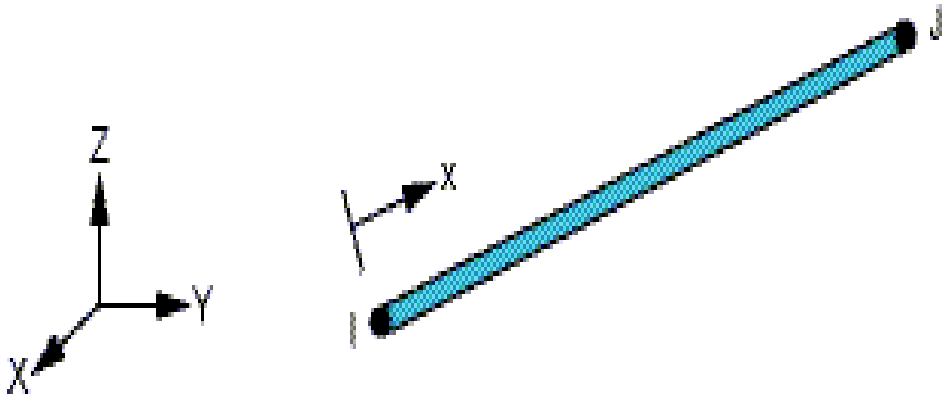

Figure 3-12 Geometry of LINK8

CFRP and adhesive material modeled using SOLID46. "This element is a layered version of the 8-node structural solid SOLID45 designed to model layered shells or solids. The element allows up to 250 different material layers". The following figure shows the geometry of the element. Figure (3-13) shows geometry of the element.

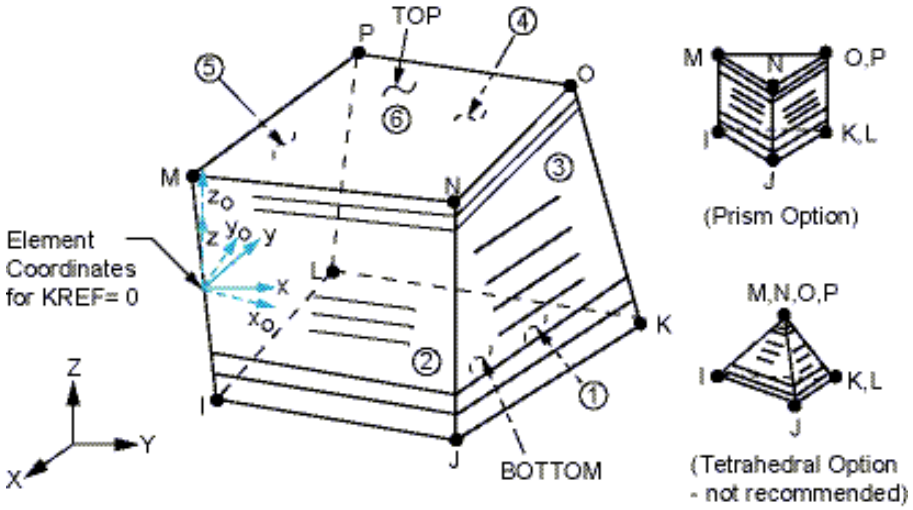

Figure 3-13 Geometry of SOLID46

The element types for the models summarized in the following table

Element	**ANSYS Element**
Steel girder Stiffeners Plates	**SOLID45**
Concrete	**SOLID65**
Steel Reinforcement	**LINK 8**
CFRP and Adhesive material	**SOLID46**

Table 3- 2 ANSYS elemnt types

Model meshing

The meshing size was selected to insure proper matching of the element nodes at the interface between stiffeners, steel girder and concrete slab, in addition to the CFRP and adhesive material as shown in figure (3-14) and (3-15). The concrete slab, steel girder, and steel plates were divided such that elements nodes of concrete slabs matched and interacted with steel reinforcement nodes as shown in figure (3-16).

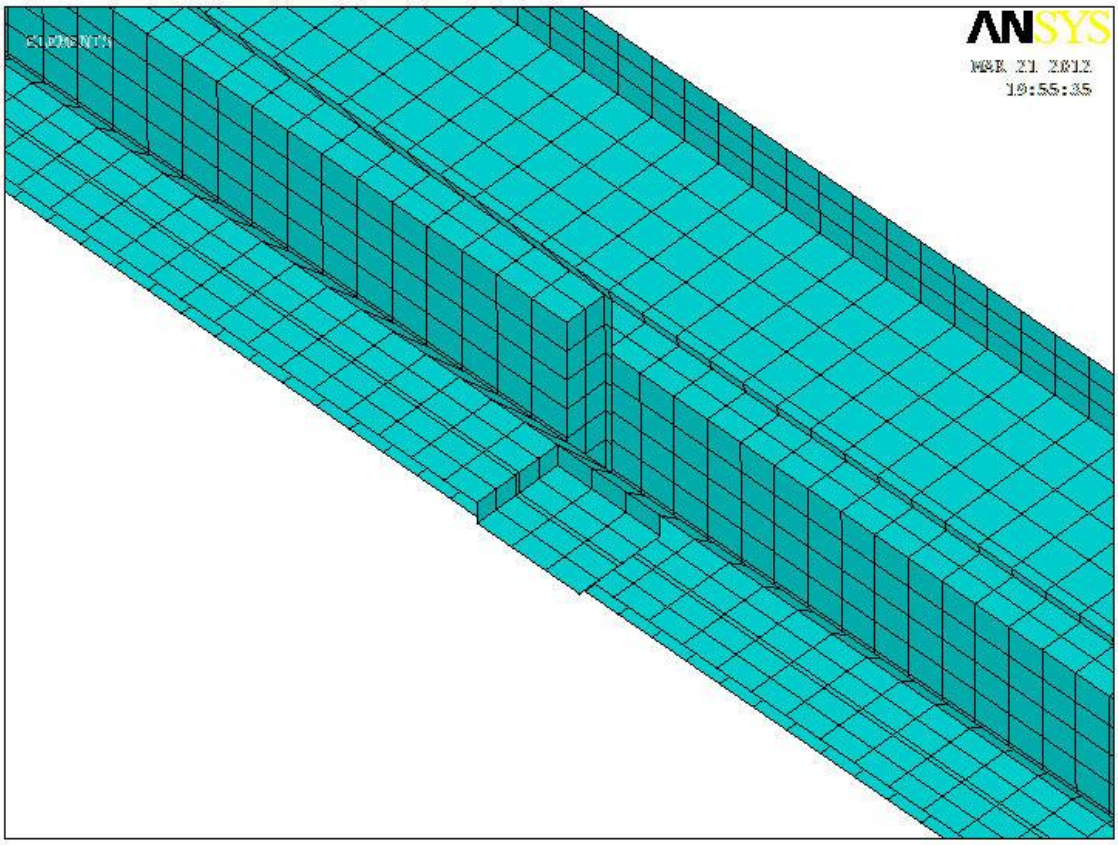

Figure 3-14 Element meshing

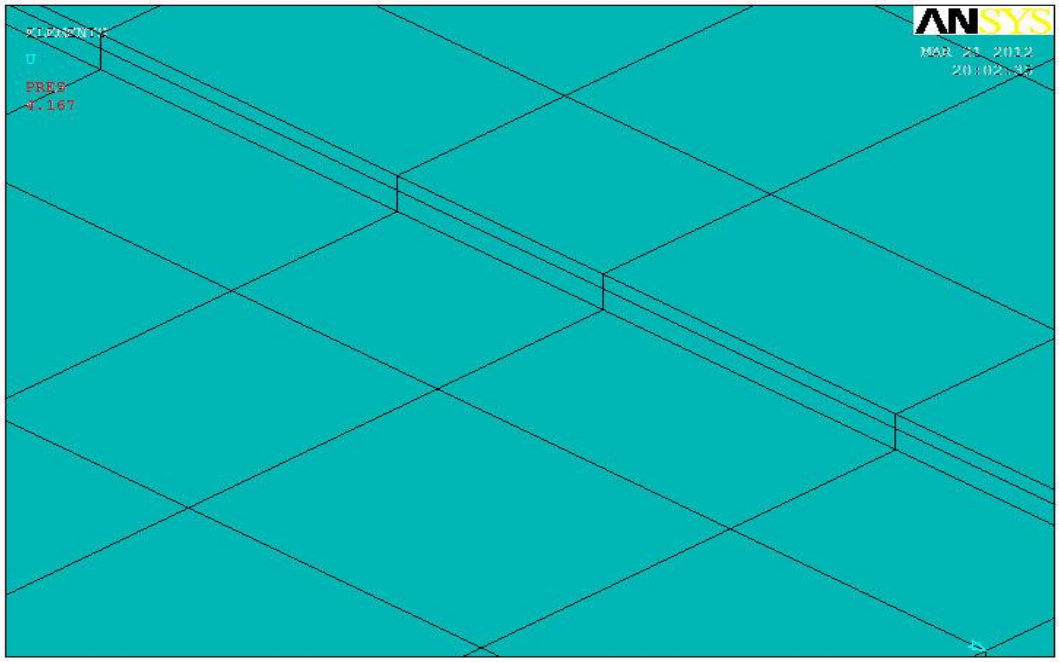

Figure 3-15 Meshing Interaction between CFRP and concrete slab

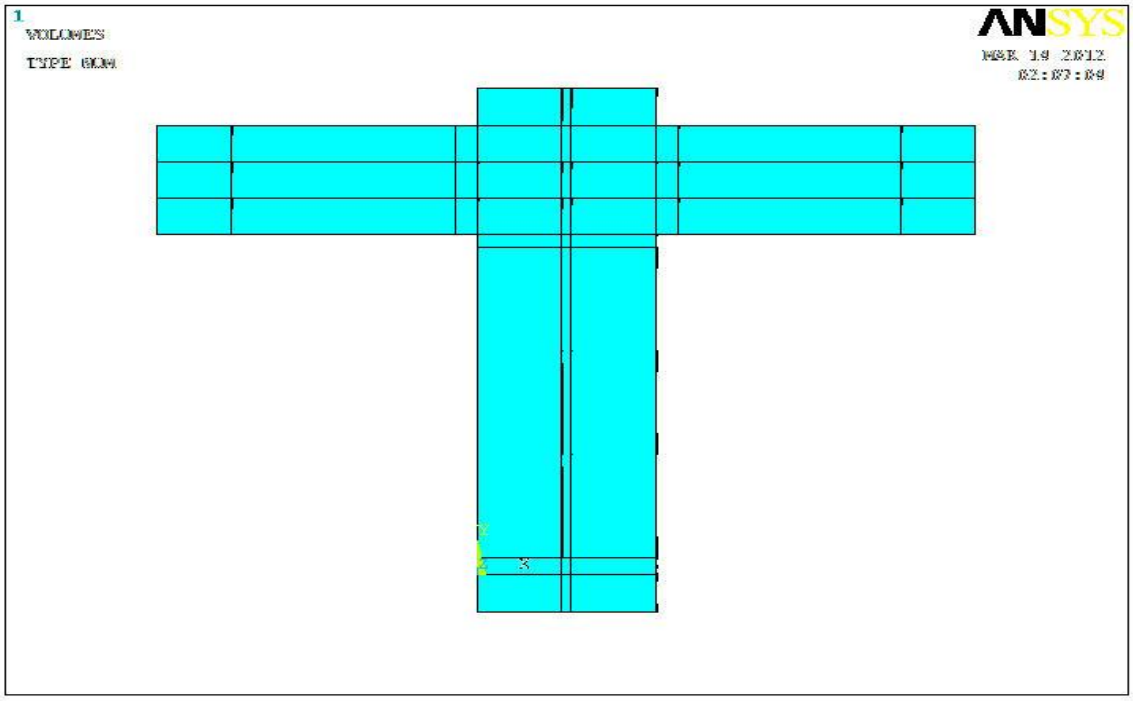

Figure 3-16 Division of the section

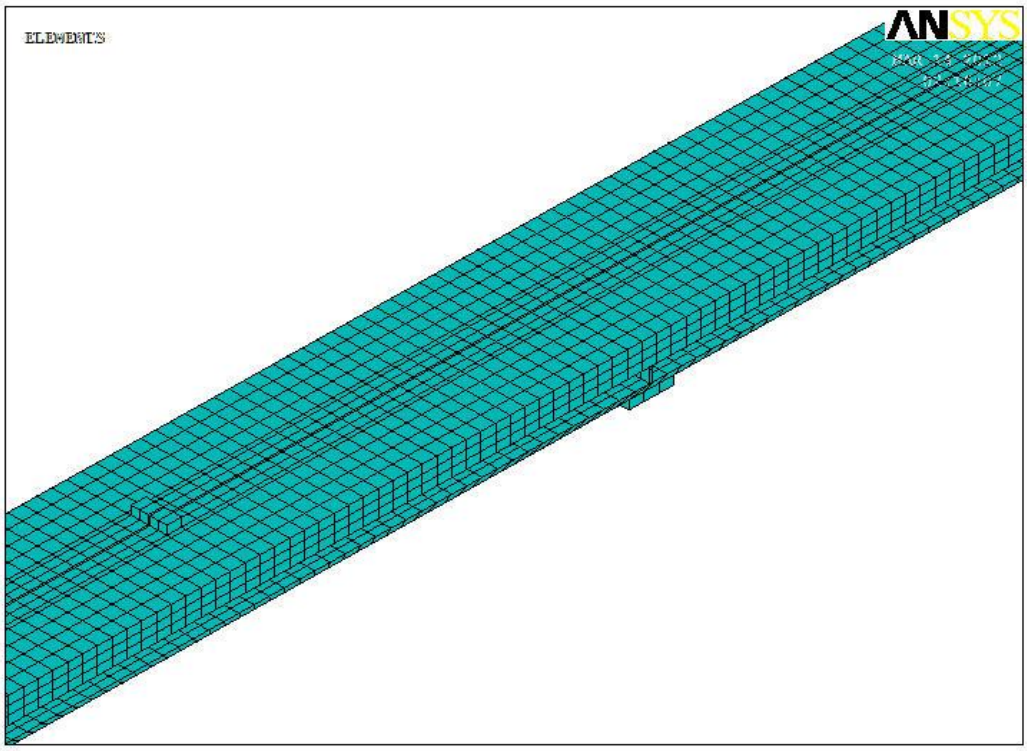

Figure 3-17 Typical girder meshing

Non-linear Finite element modeling

In this study, steel modeled as elastic-plastic multilinear material. The multilinear isotropic material uses von Mises failure criterion. Concrete slab modeled using SOLID65 element. This element requires linear isotropic in addition to multilinear isotropic material properties to model concrete. Willam and Warnke (1974) model used to define the failure of the concrete. CFRP modeled as linear elastic material with rupture failure.

Willam and Warnke (1974) material model required different parameters [27]. Table (3-3) summarizes these parameters in addition to the corresponding values.

Constant	Value
Shear transfer coefficients for an open crack	**0.3**
Shear transfer coefficients for a closed crack	**1**
Uniaxial tensile cracking stress	**2.4**
Uniaxial crushing stress	**34**
Biaxial crushing stress	**0**
Ambient hydrostatic stress state	**0**
Biaxial crushing stress (positive) under the ambient hydrostatic stress state	**0**
Uniaxial crushing stress (positive) under the ambient hydrostatic stress state	**0**
Stiffness multiplier for cracked tensile condition	**0**

Table 3- 3Willam and Warnke material model parameters

Typical shear transfer coefficients range from 0.0 to 1.0, with 0.0 representing a smooth crack (complete loss of shear transfer) and 1.0 representing a rough crack (no loss of shear transfer) [27] . Value of 0.3 selected for Shear transfer coefficients for an open crack (Reasonable for convergence), and 1.0 for closed crack. The Uniaxial tensile cracking stress is 2.4 MPa, and Uniaxial crushing stress is 34 MPa. Default value used for the remaining parameters.

Failure criteria of the materials were induced to ANSYS program. These criteria are the max compressive stress, max tensile strength and the corresponding strains, in addition to the max shear stress for steel, concrete, CFRP, and adhesive material.

Stages of Loading

Two point loads (P/2) applied at each span at one-third and two-third of the span length. The first stage of loading was considered close to the cracking load of concrete. Then load was increased incrementally up to yielding of top flange of steel section over the interior support and then up to failure. Number of substeps was increased as the loading approach the inelastic range. Failure criteria were recorded at different stages of loading.

CHAPTER FOUR

RESULTS AND CONCLUSION

4.1 RESULTS OF CSC AND VALIDATION

The FE results of the continuous composite steel concrete girder (CSC) validated using experimental results carried by Chen et al.(2009) [14]. Figure (4-1) shows load deflection curve of CSC experimentally and using ANSYS. The results showed good agreement in the elastic and plastic range. The ultimate capacity of girder is 558 KN experimentally, and the corresponding FE result is 568 KN with 1.8% difference. The deflection at failure is 52 mm experimentally whereas its 52.5 mm using FE ANSYS software.

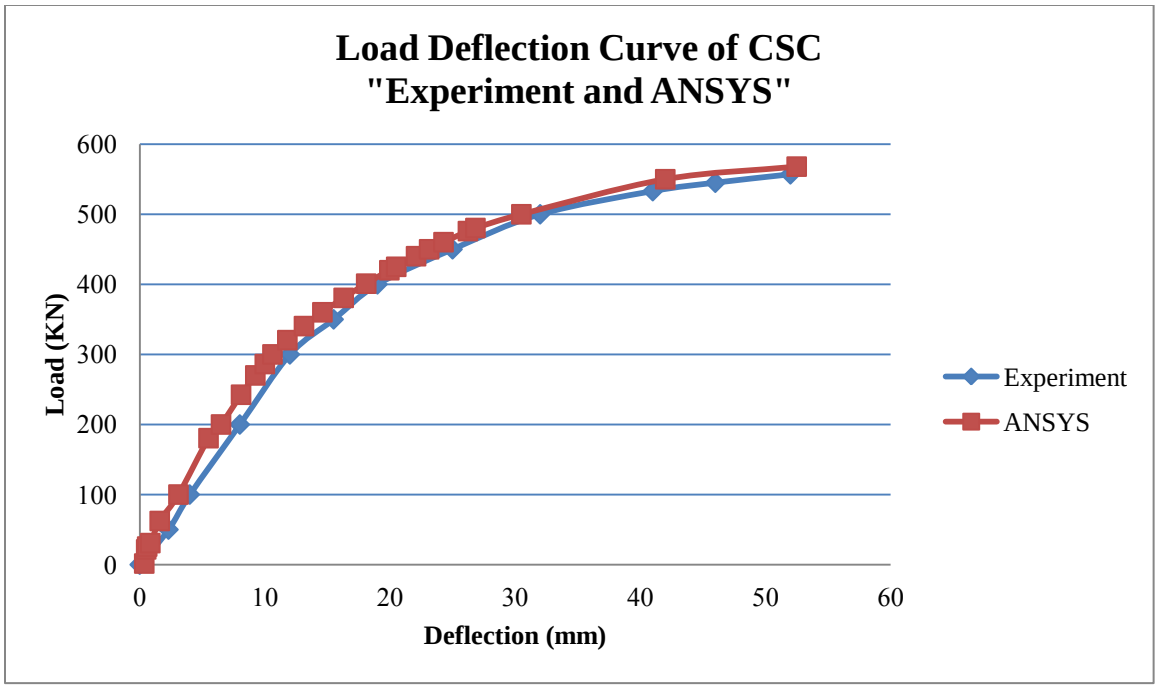

Figure 4-1 Comparison between load deflection curve experimentally and ANSYS

The failure mechanism started by cracking of concrete over the interior support at early stage of loading. The cracks started at the top surface of concrete over the interior support, then propagate to cover the whole slab depth. As the load increased, cracks extended over the entire negative moment region as shown in figure (4-2).

The section over the interior support reached its capacity then followed by developing the capacity of section at the positive moment region. It was noted that steel section at the positive moment region and concrete slab reached ultimate capacity approximately at the same load. This means that ultimate capacity of steel section reached while concrete slab between the point loads starts crushing as shown in figure (4-3). At ultimate load, the compression stress in steel reinforcement at positive moment region is 50% of yielding stress. Experimental results showed the same stages of failure with close load corresponding to each stage. Table (4-1) summarizes failure mechanism stages and

corresponding loads for CSC experimentally and by ANSYS. Load corresponding to the capacity of section over interior support is 69% and 61% of the ultimate load capacity of girder for ANSYS and experimental results respectively.

Failure mechanism stage	Load (KN) ANSYS	Load (KN) Experiment
Starting Concrete cracking	27	30.7
Yielding of bottom flange over the interior support	321	347
Yielding of steel reinforcement at the negative moment	370	-
Yielding of top steel flange over the interior support	379	-
Ultimate capacity of section over the interior support	393	341
Failure	568	558

Table 4-1 Loads corresponding to failure mechanism stages of CSC

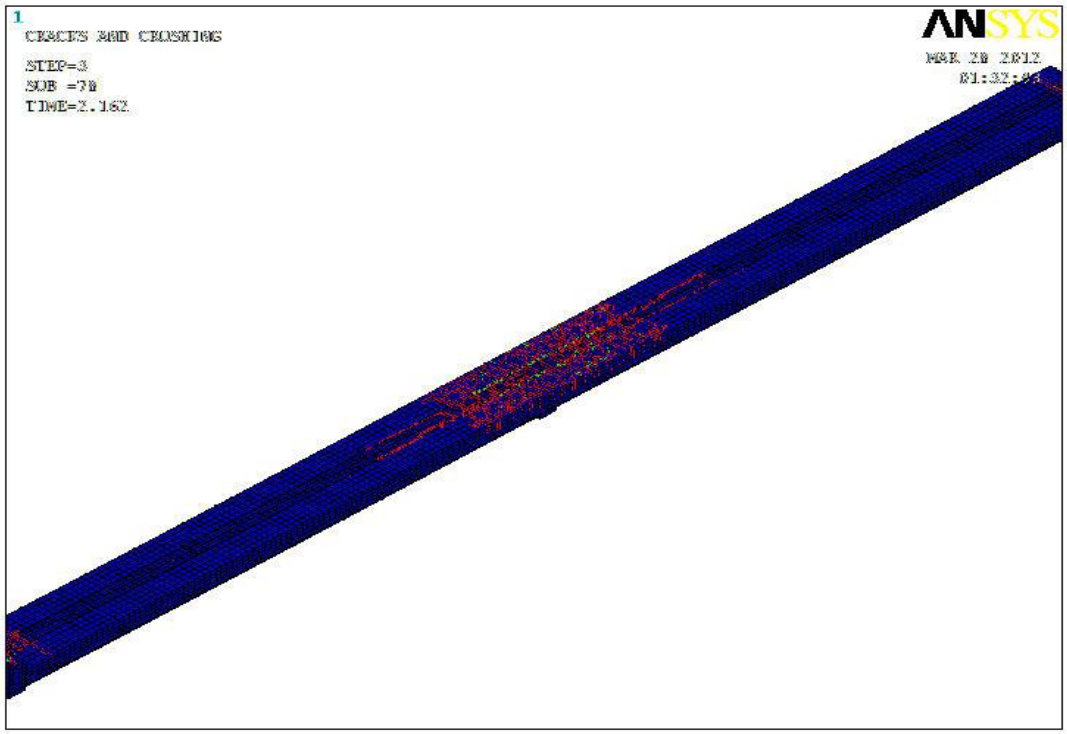

Figure 4-2 Concrete cracking of CSC

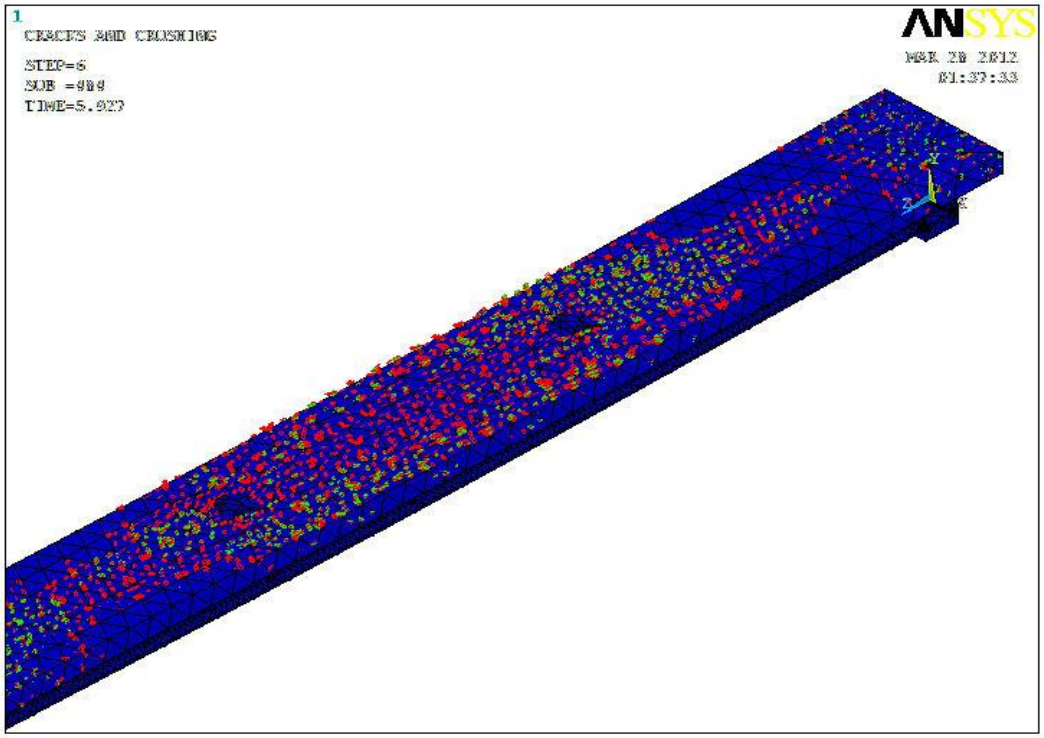

Figure 4-3 Concrete crushing at ultimate load for CSC

The stress distribution along negative moment region and over interior support before concrete cracking are shown in figures (4-4) and (4-5) respectively.

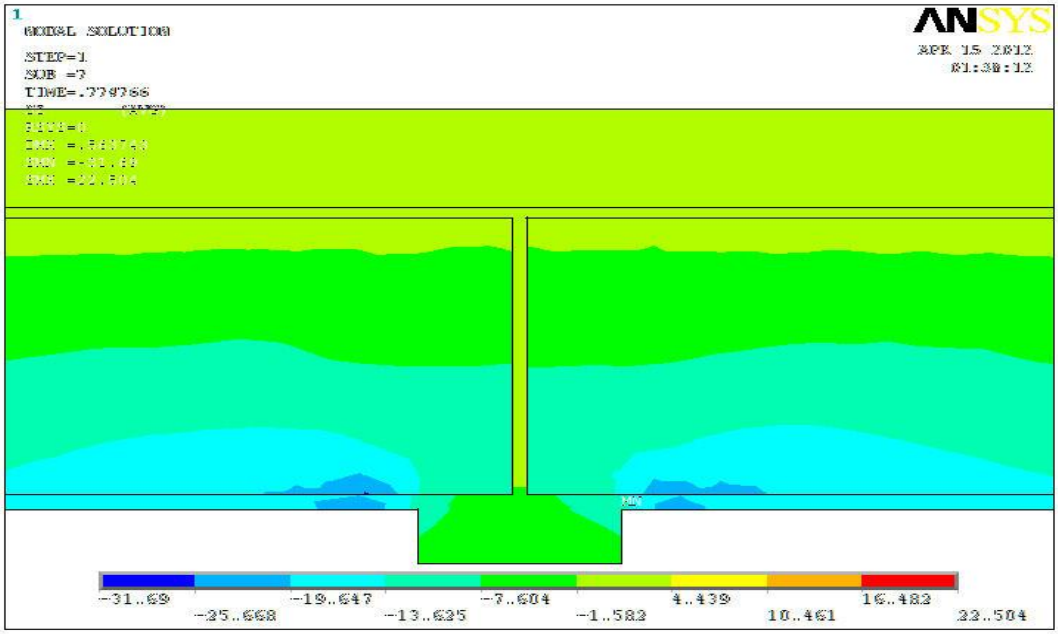

Figure 4-4 Stress distribution along negative moment region before concrete cracking for CSC girder

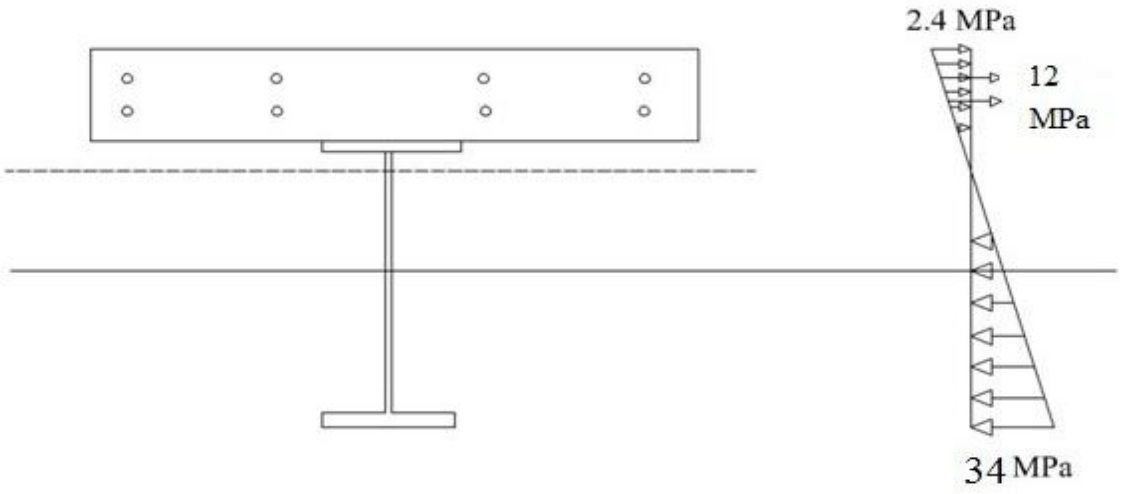

Figure 4-5 Stress distribution over interior support region before concrete cracking for CSC girder

The stress distribution along negative moment region and for section 1-1 at yielding of bottom flange over interior support are shown in figures (4-6) and (4-7) respectively.

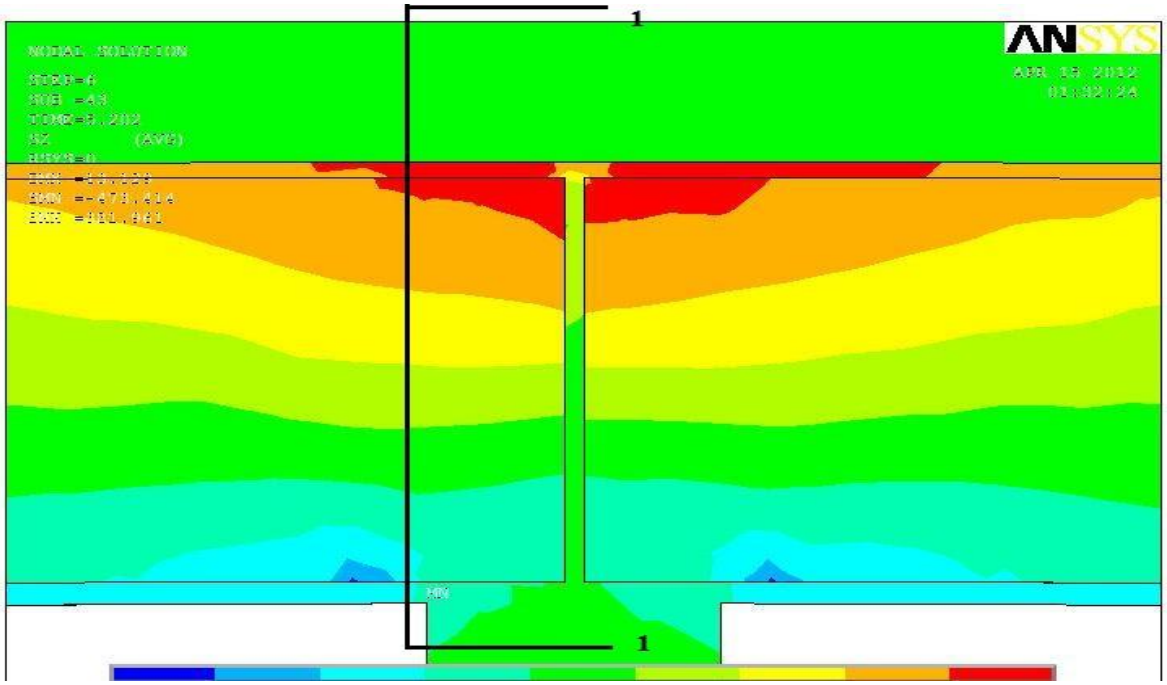

Figure 4-6 Stress distribution along negative moment region at yielding of bottom steel flange for CSC girder

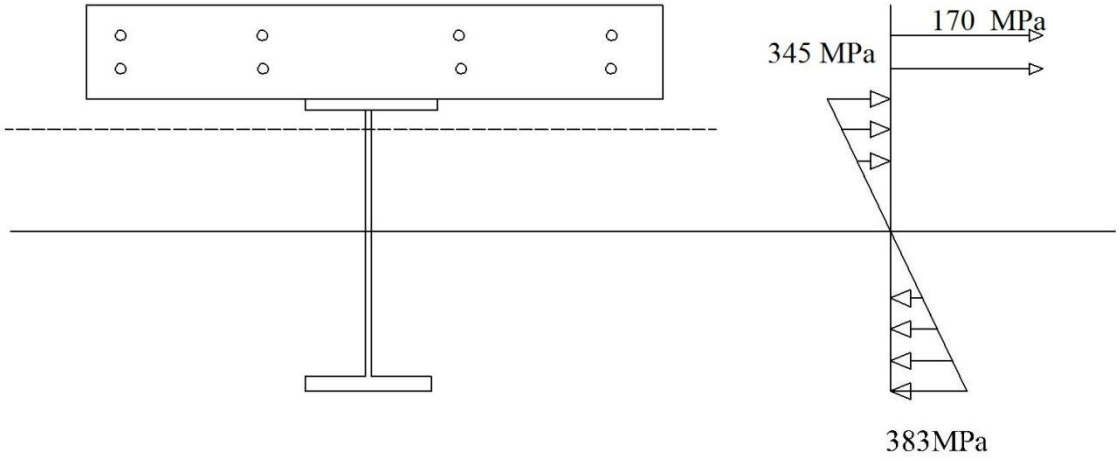

Figure 4-7 Stress distribution at section 1-1 at yielding of bottom steel flange for CSC girder

The stress distribution along negative moment region and for section 1-1 at ultimate capacity of section are shown in figures (4-8) and (4-9) respectively.

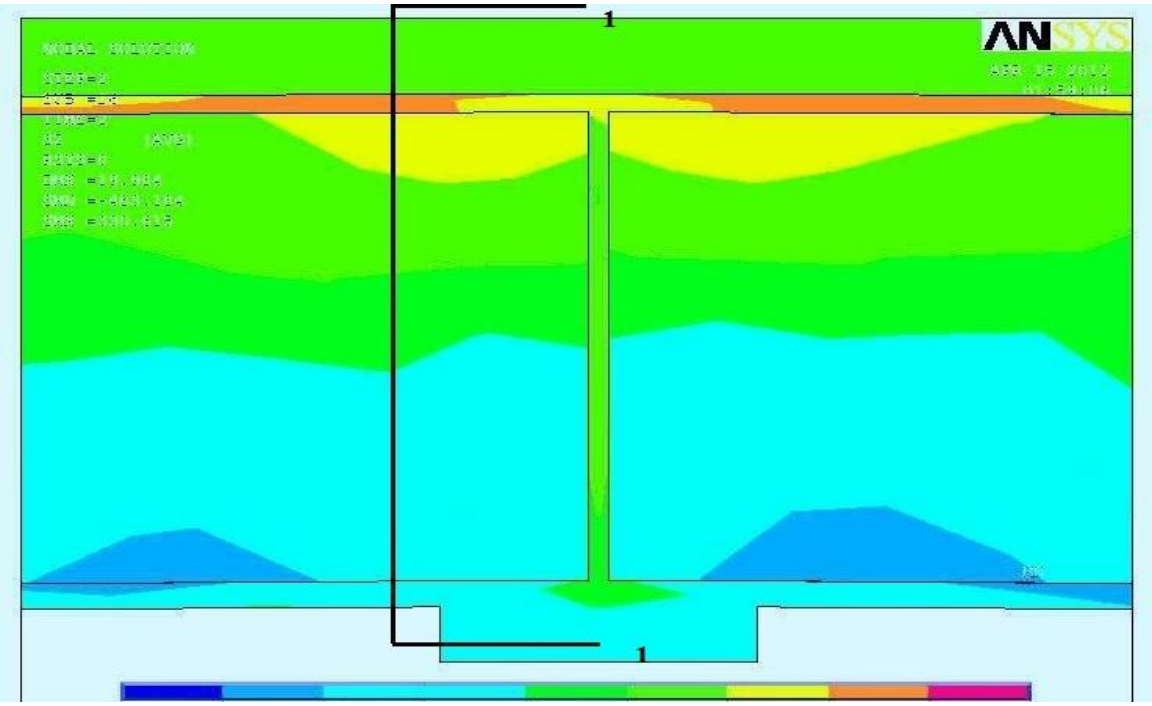

Figure 4-8 Stress distribution along negative moment region at ultimate capacity for CSC girder

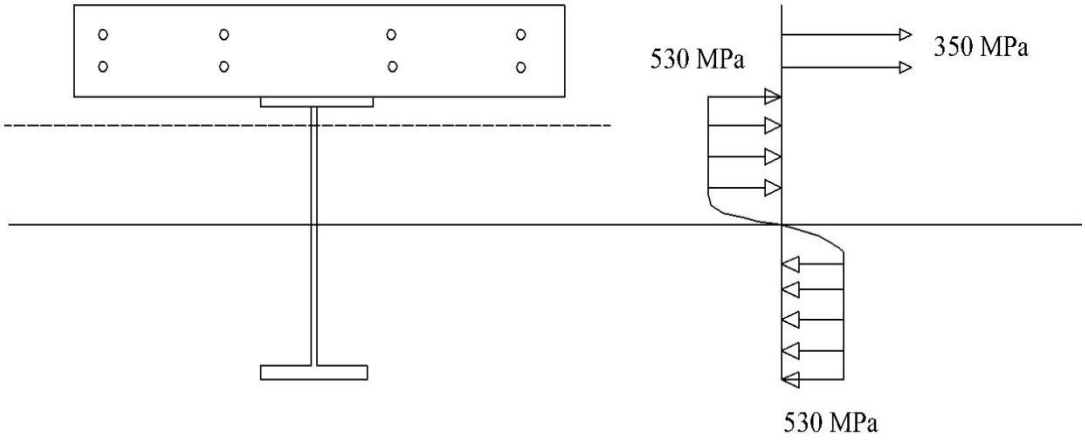

Figure 4-9 Stress distribution at section 1-1 at ultimate capacity for CSC girder

The stress distribution along mid-span and for section 2-2 at yielding of bottom steel flange at mid-span are shown in figures (4-10) and (4-11) respectively.

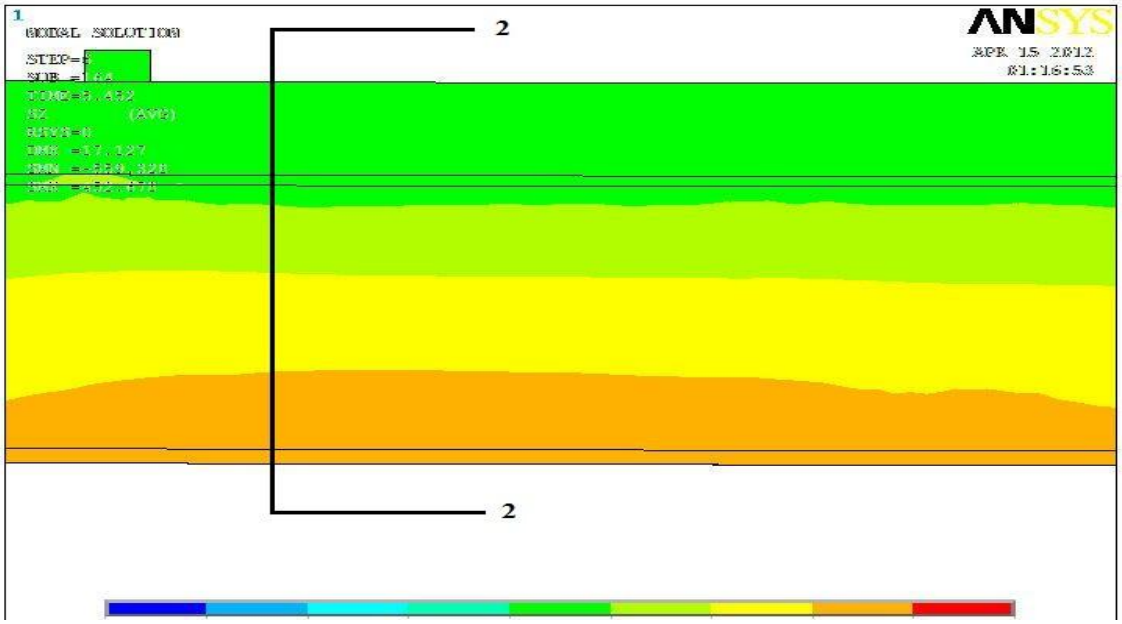

Figure 4-10 Stress distribution along mid-span at yielding of bottom steel flange for CSC girder

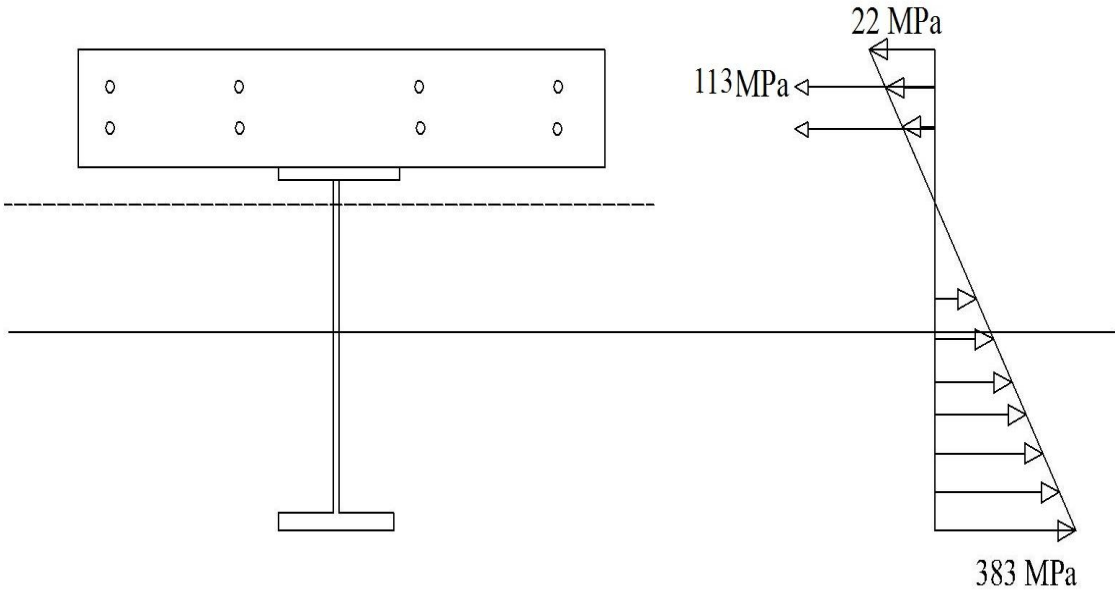

Figure 4-11 Stress distribution at section 2-2 at yielding of bottom steel flange for CSC girder

The stress distribution along mid-span and for section 2-2 at ultimate capacity are shown in figures (4-12) and (4-13) respectively.

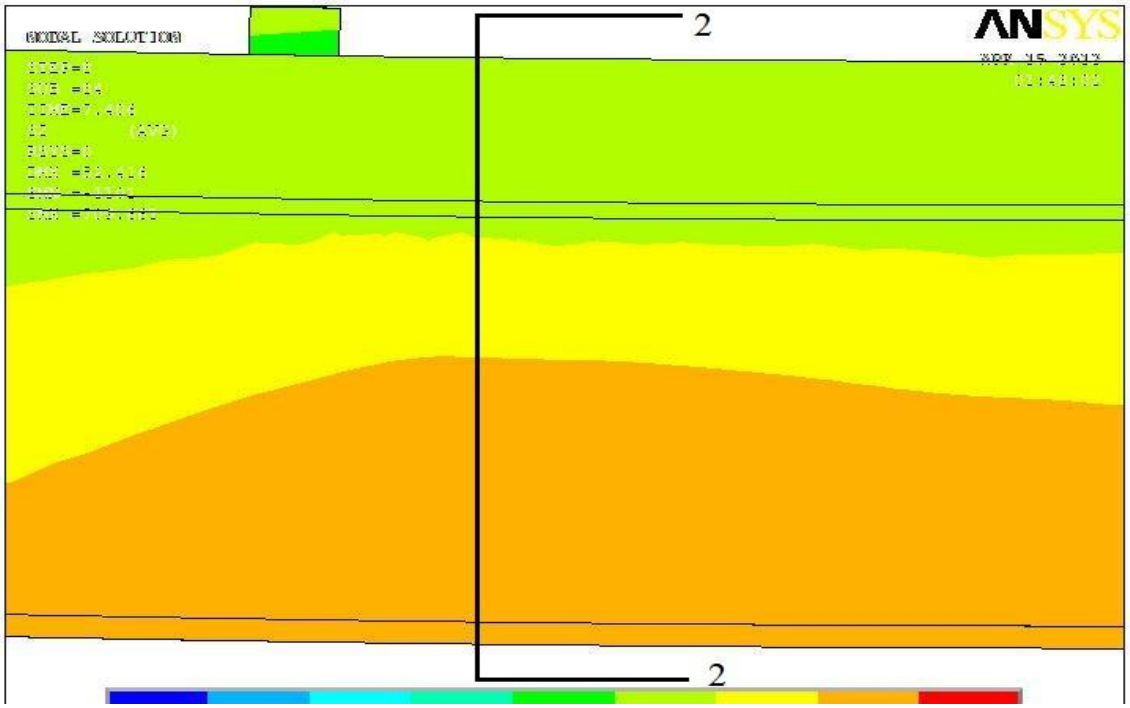

Figure 4-12 Stress distribution along mid-span at ultimate capacity of CSC girder

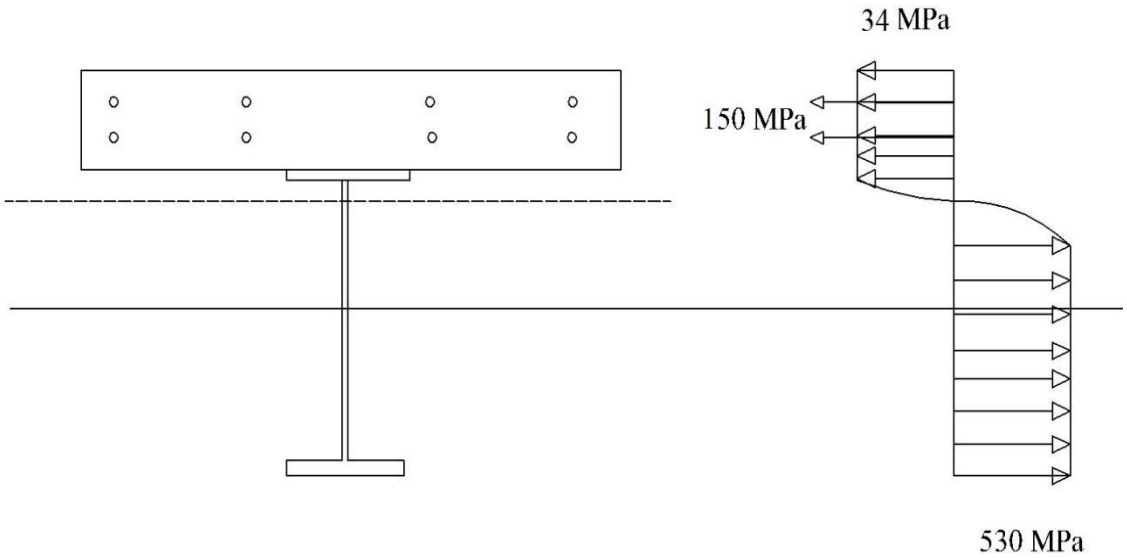

Figure 4-13 Stress distribution at section 2-2 at capacity of CSC girder

4.2 EFFECT OF BONDING CFRP OVER THE NEGATIVE MOMENT REGION

In this section, comparison between steel concrete continuous girder (CSC) and girder with CFRP sheet of 0.25 mm thickness and 2360 mm length (covers the total concrete slab at negative moment region) which named as CSCC2. The finite element results showed that bonding CFRP over the negative moment region increased the strength and stiffness of the girder significantly in addition to improve the ductility of girder as shown in figure (4-14).

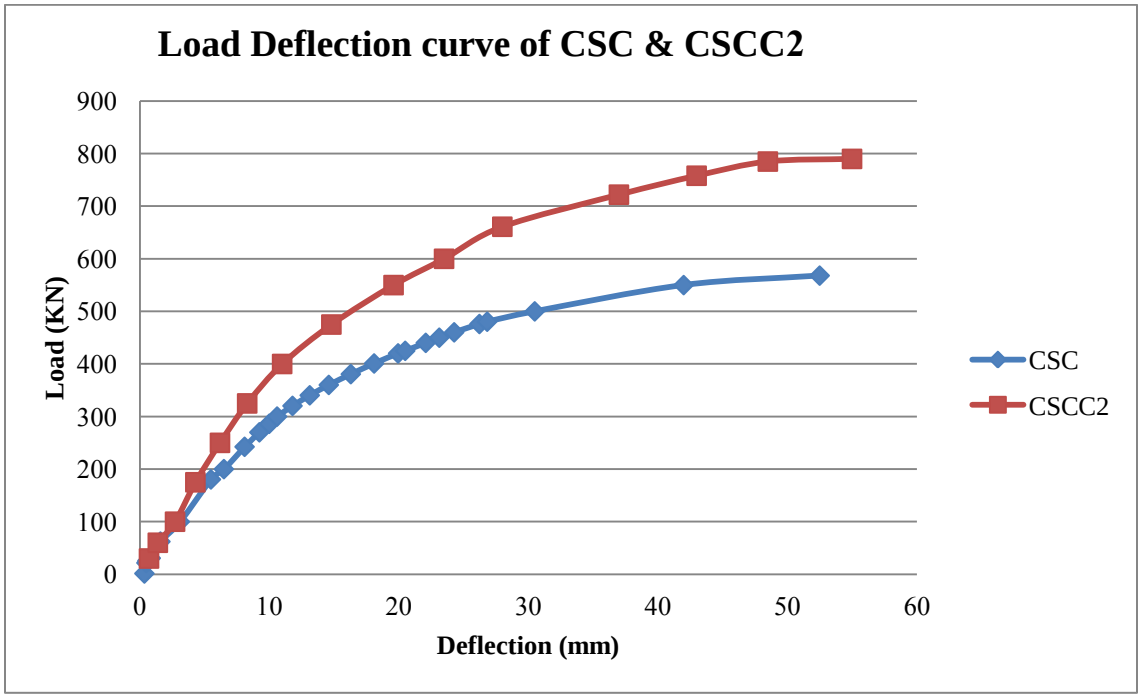

Figure 4-14 Load deflection curves of CSC and CSCC2

The ultimate load carrying capacity of CSC is increased by 39% by bonding 0.25 mm CFRP over the negative moment region. Strength and stiffness increases are mainly due to ability of CFRP to maintain the composite action at the negative moment region because CFRP has high tensile strength which prevents concrete cracking.

FE results showed that adding CFRP over the negative moment region prevented concrete cracking at that region. Small cracks observed at the edges of the concrete slab over the interior support which started at 65 KN as shown in figure (4-15).

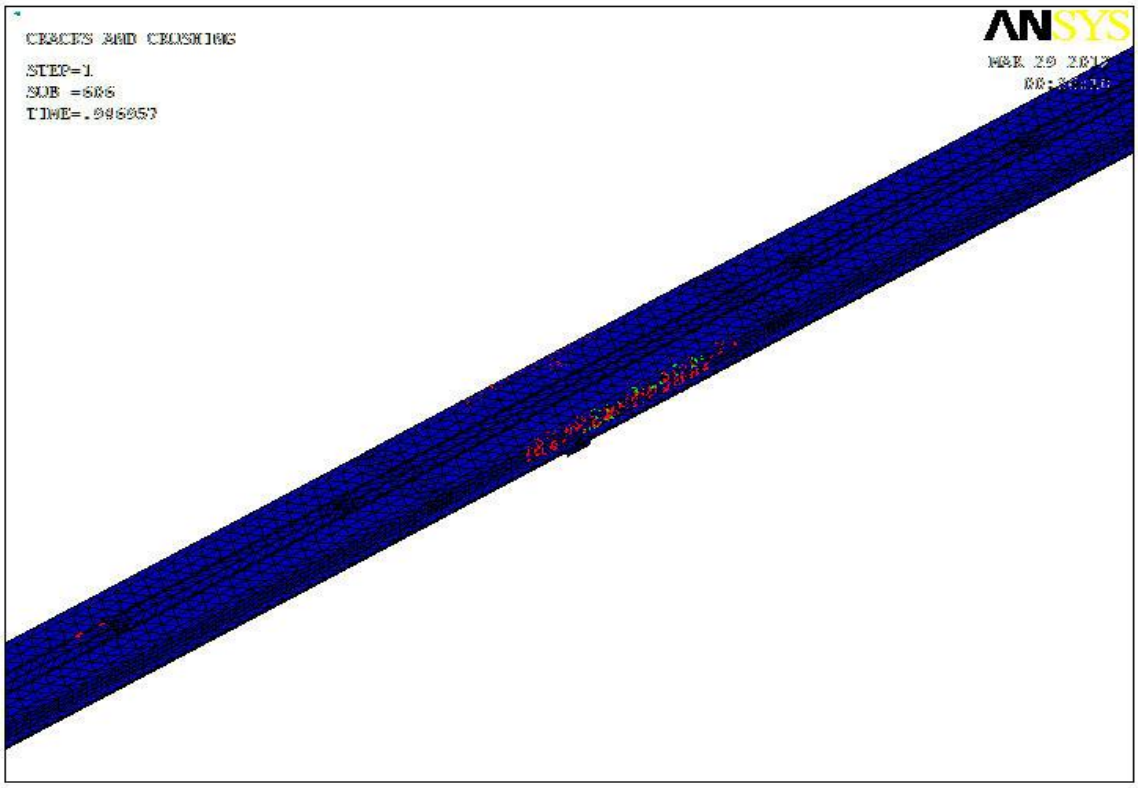

Figure 4-15 Cracks of girders with CFRP

The yielding of steel reinforcement started followed by yielding of bottom steel flange over the interior support. As the load increased yielding started at bottom flange close to exterior point load. Finally the girder reached its capacity over the interior support followed by the development of ultimate capacity of the section close to the exterior point loads.

The stress distribution along negative moment region and for section 1-1 at yielding of bottom steel flange over interior support of girder CSCC2 are shown in figures (4-16) and (4-17) respectively.

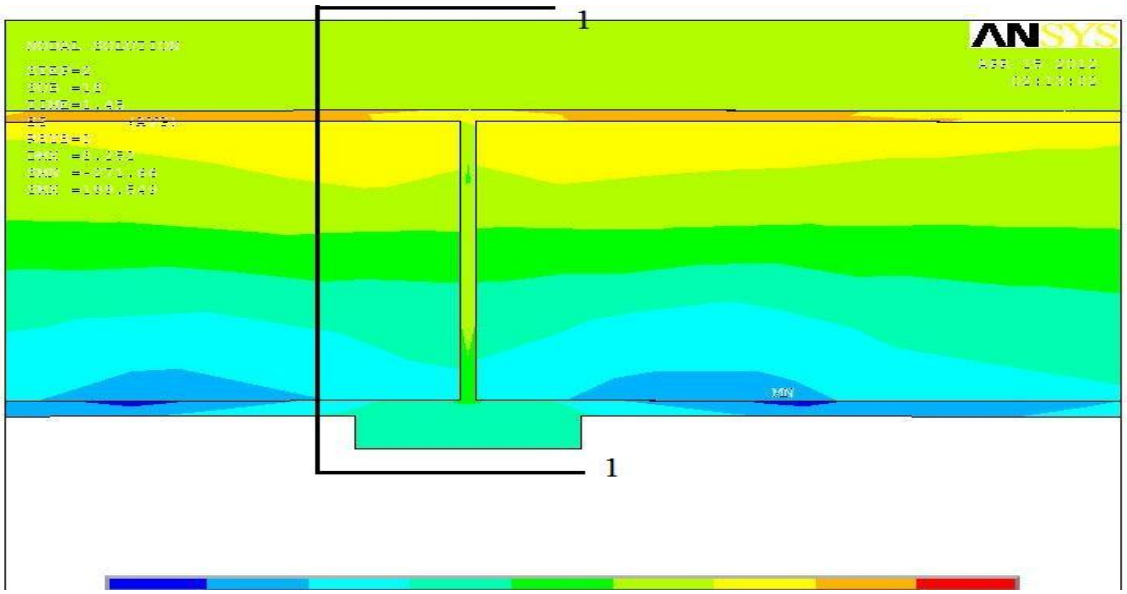

Figure 4-16 Stress distribution along negative moment region at yielding of bottom flange for CSCC2 girder

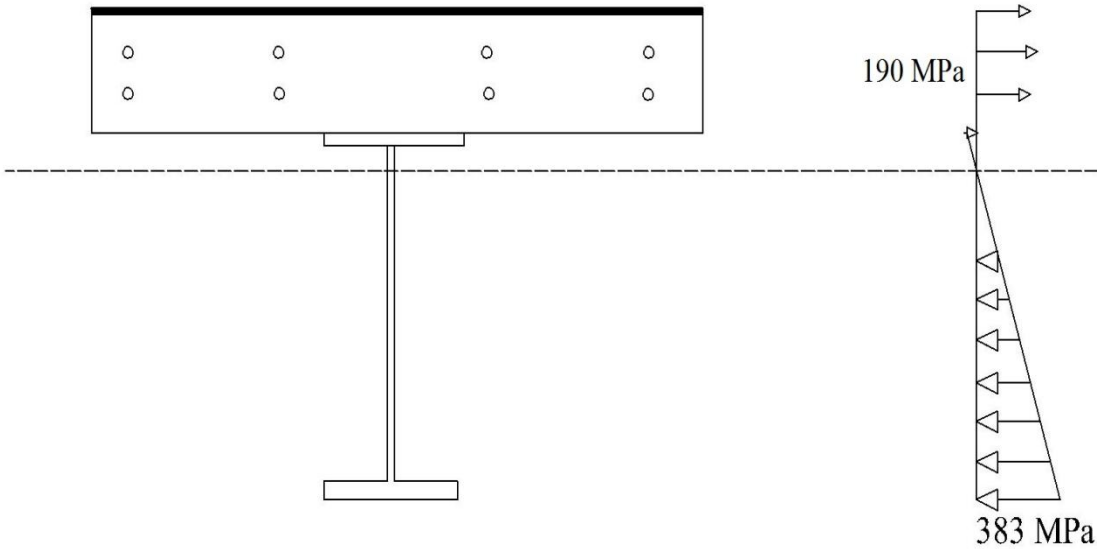

Figure 4-17 Stress distribution at section 1-1 at yielding of bottom steel flange for CSCC2 girder

The stress distribution along negative moment region and for section 1-1 at ultimate load of girder CSCC2 are shown in figures (4-18) and (4-19) respectively.

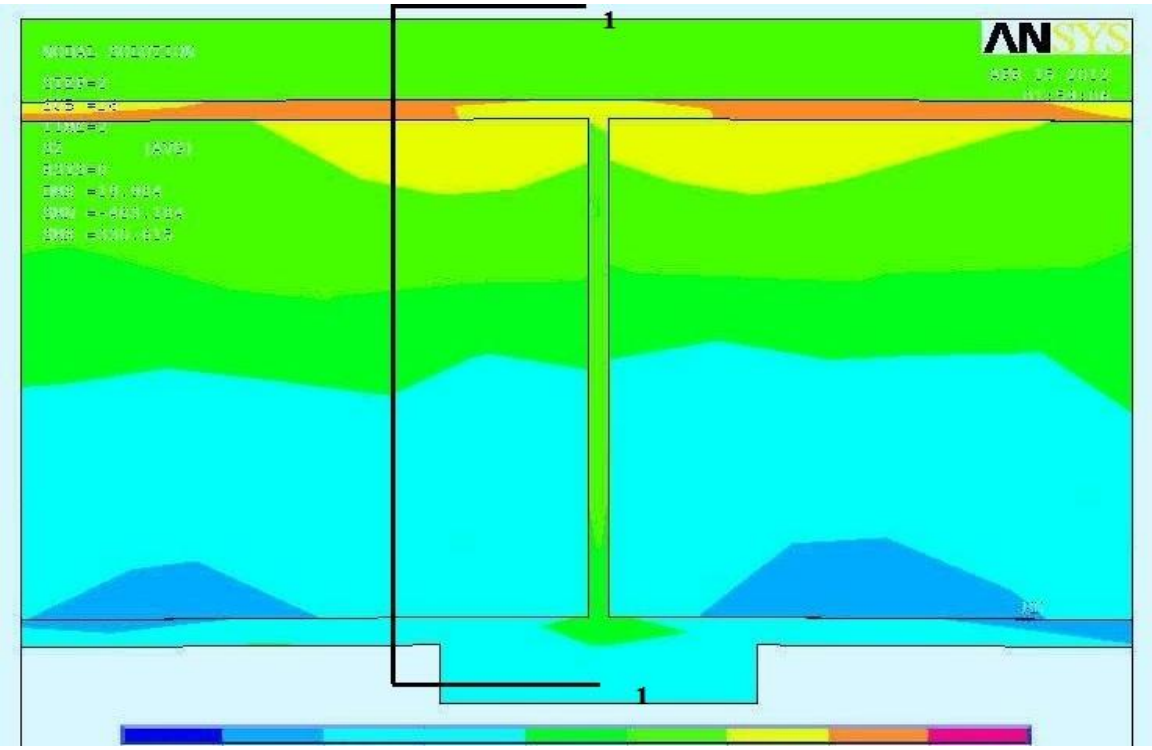

Figure 4-18 Stress distribution along negative moment region at ultimate capacity for CSCC2 girder

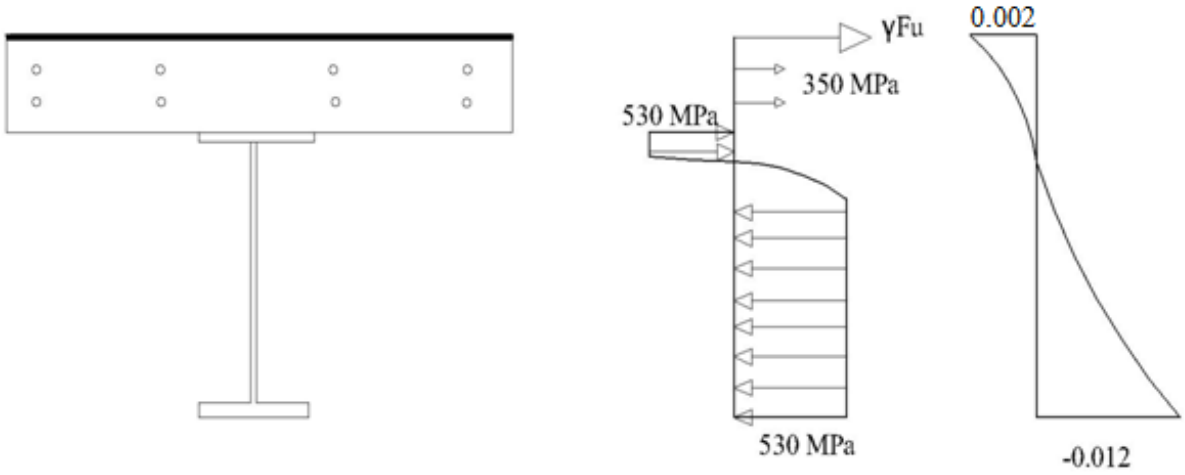

Figure 4-19 Stress and strain distributions at section 1-1 at ultimate capacity of section for CSCC2 girder

The stress distribution along positive moment region and for section 2-2 at yielding of bottom steel flange of CSCC2 are shown in figures (4-20) and (4-21) respectively.

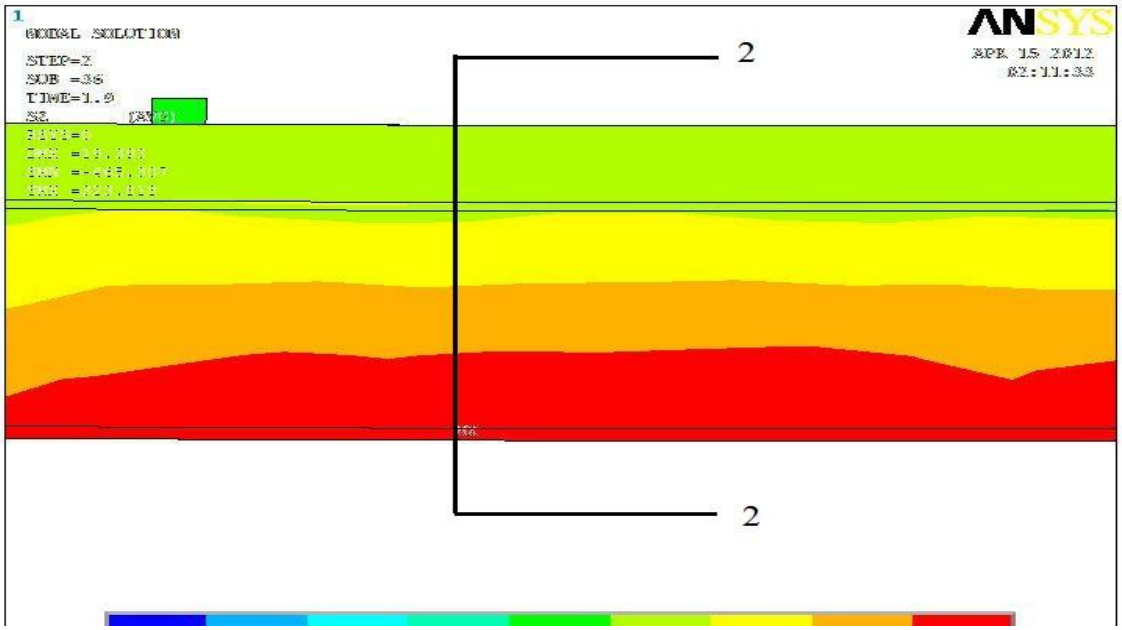

Figure 4-20 Stress distribution along mid-span at yielding of bottom steel flange for CSCC2girder

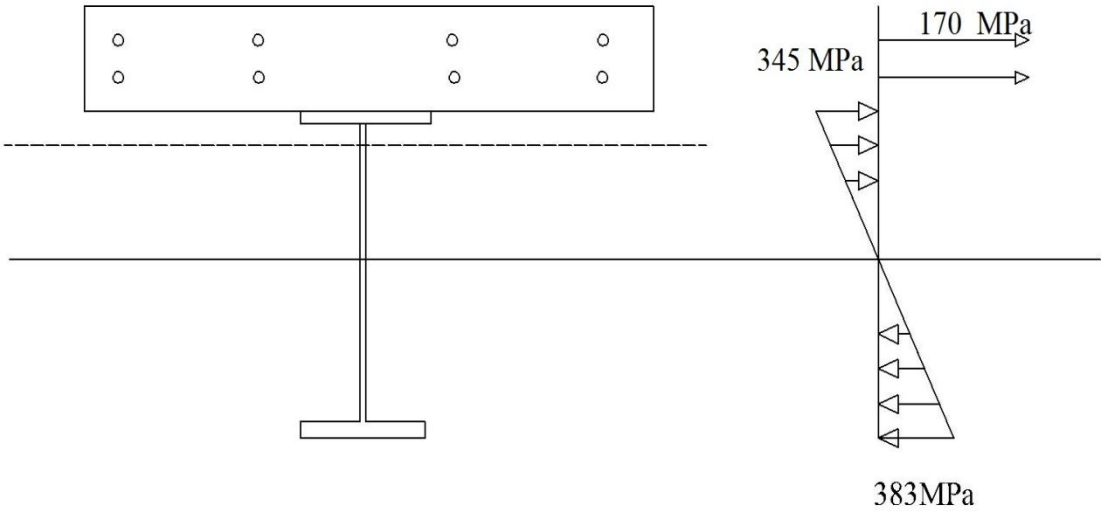

Figure 4- 21 Stress distribution at section 2-2 at yielding of bottom steel flange for CSCC2 girder

The stress distribution along positive moment region and for section 2-2 at yielding of bottom steel flange of CSCC2 are shown in figures (4-22) and (4-23) respectively.

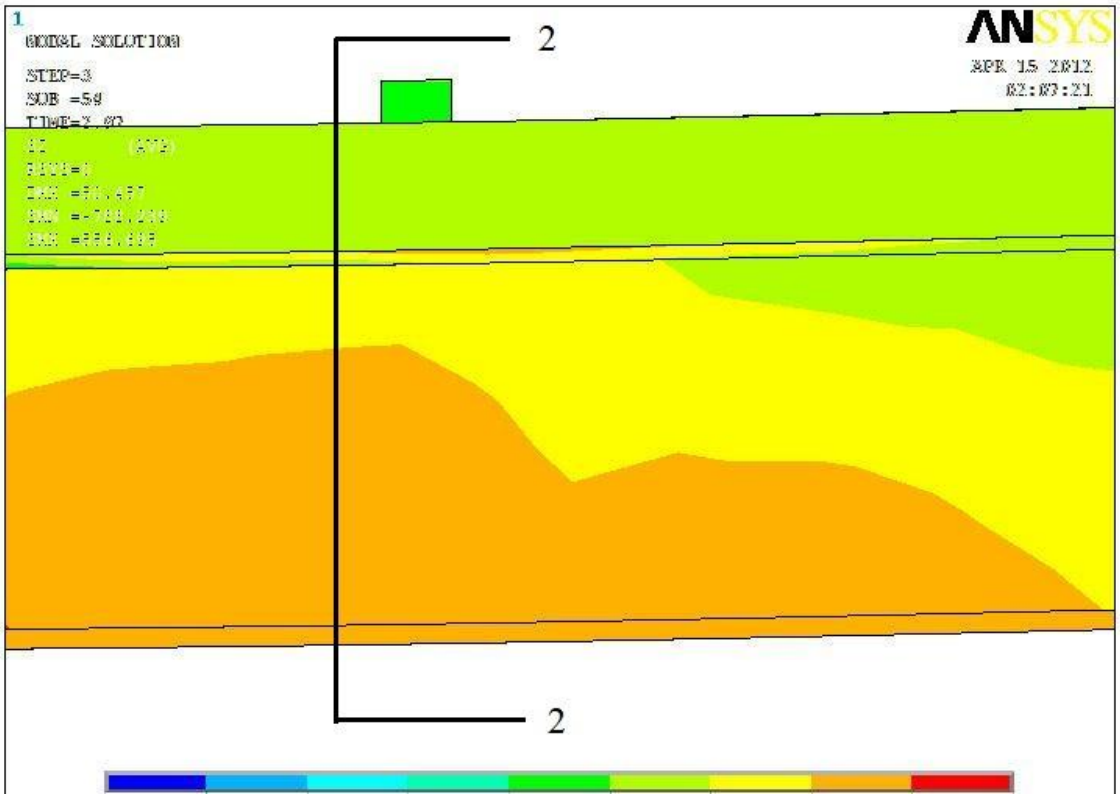

Figure 4-22 Stress distribution along mid-span at ultimate capacity for CSCC2 girder

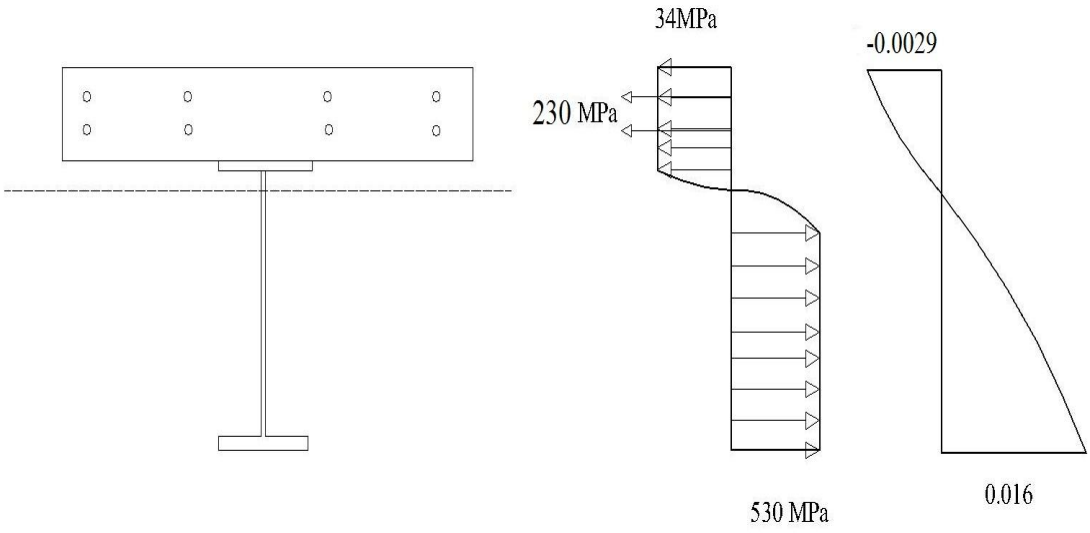

Figure 4-23 Stress and strain distributions at section 2-2 at ultimate load for CSCC2 girder

The main parameters were investigated in this research are thickness of CFRP, length of CFRP, and location of the neutral axis within the composite section. These parameters were investigated to see the ability of CFRP to maintain the composite action at the negative moment region, and the increase in the ultimate load carrying capacity of the continuous composite girder.

4.3 EFFECT OF CFRP THICKNESS

Composite steel-concrete girders with different five CFRP thicknesses were investigated in this study. These girders are CSCC1, CSCC2, CSCC3, CSCC4, and CSCC5 with 0.15, 0.25, 0.5, 1, and 3 mm CFRP thickness respectively. FE results showed that increasing thickness of CFRP increases the ultimate capacity of the girder and decreases the efficiency of using the tensile capacity of CFRP as shown in figure (4-24).

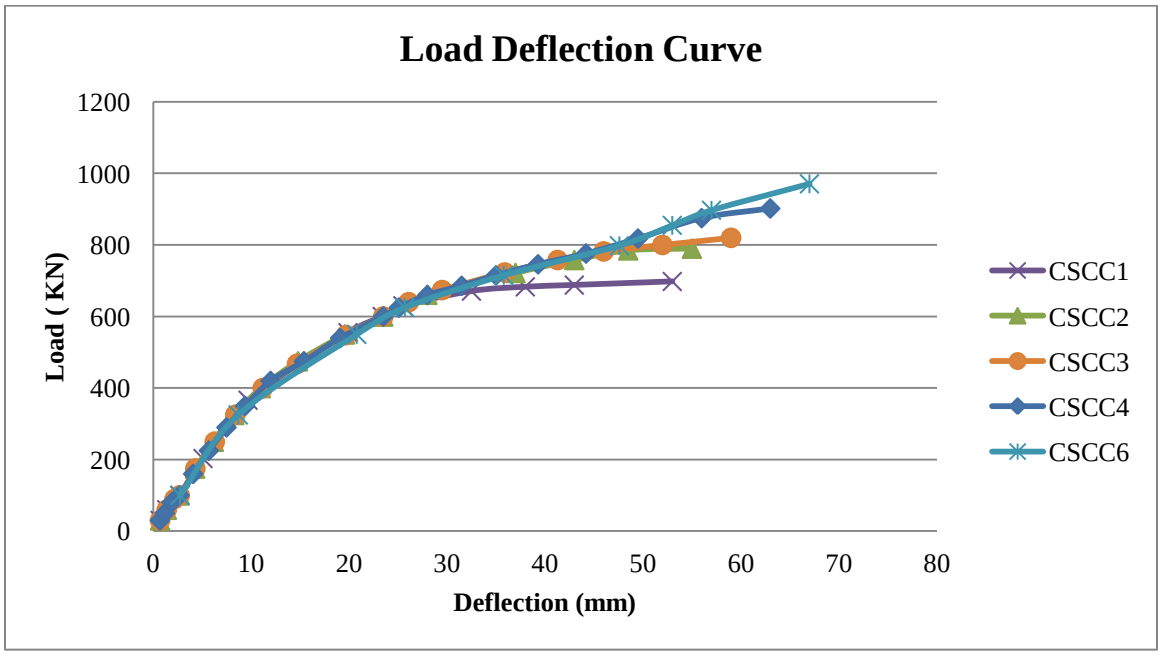

Figure 4-24 Load deflection curves of girders with different thicknesses of CFRP

It's clear that no change of the stiffness of girders with different CFRP thicknesses. All girders exhibit the same behavior up to reaching capacity of the steel section over the interior support as shown in figure (4-24). Thickness of CFRP changes the maximum deflection before failure. As thickness of CFRP increases, the maximum deflection at failure is increases.

Table (4-2) summarizes the ultimate capacity of girders with different CFRP thicknesses in addition to the increase in the ultimate capacity with respect to CSCC1. It includes the ratio of tensile stress in CFRP to the ultimate stress. Girder CSCC2 gives the best increase in capacity with the utilizing of CFRP as shown in figure (4-25) and Table (4-2). The results showed that as increasing capacity of steel section either by increasing ultimate stress or by increasing dimensions of section, this increases the tensile stress in CFRP.

Girder	CFRP thickness (mm)	Capacity	Capacity increase	Difference in capacity	% of CFRP tensile stress to Ultimate stress
CSCC1	0.15	698			11.3%
CSCC2	**0.25**	**790**	**13.2%**	**13.2%**	**10.8%**
CSCC3	0.5	820	17.5%	3.5%	7.9%
CSCC4	1.0	902	29.2%	11.7%	6.7%
CSCC5	3.0	971	39.1%	9.9%	5.7%
CSCC2Y	0.25	1091	56%	-	20%

Table 4-2 Comparison between girders with different CFRP thicknesses

The ultimate capacity of girders with different CFRP thicknesses and ratio of tensile stress to ultimate stress of CFRP are shown in chart (4-25).

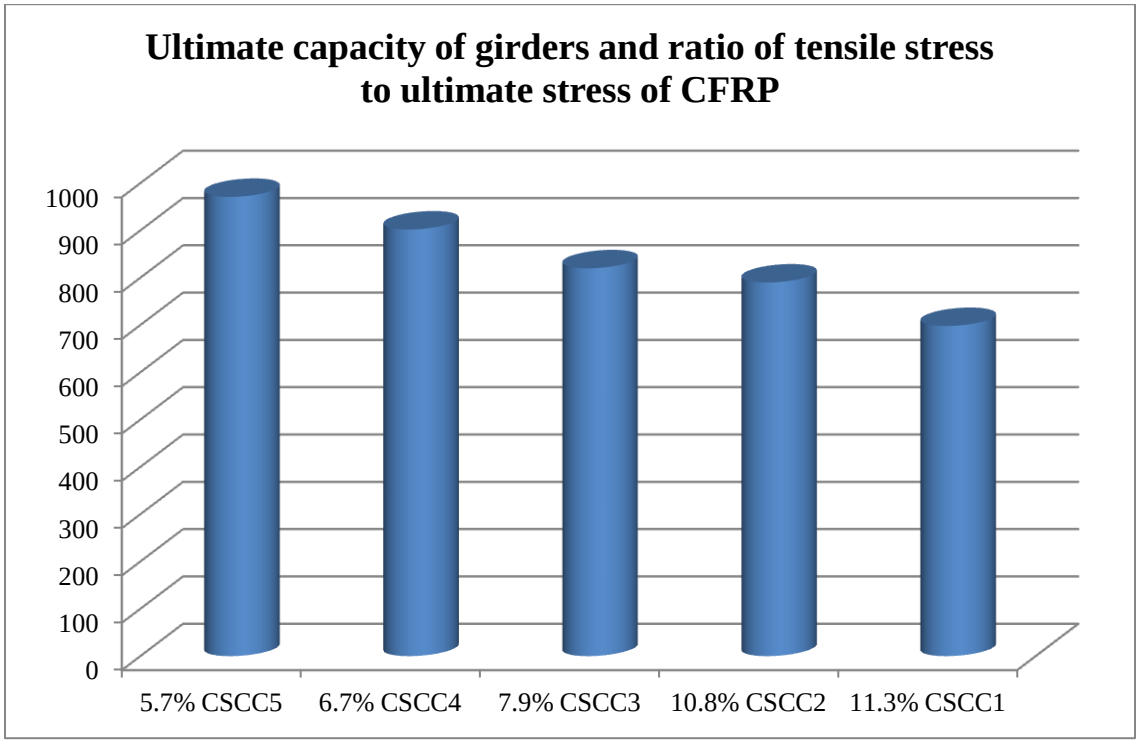

Figure 4-25 Ultimate capacities of Girders with different CFRP thicknesses and ratio of tensile stress to ultimate stress of CFRP

All girders with different thicknesses of CFRP showed the same failure mechanism. But different loads reached at each stage depending on the capacity of girder. Table (4-3) summarizes failure mechanism stages of girders with different thicknesses of CFRP and corresponding load at each stage.

Girder / Failure mechanism stage	CSCC1 (KN)	CSCC2 (KN)	CSCC3 (KN)	CSCC4 (KN)	CSCC5 (KN)
Yielding of steel reinforcement in the negative moment	407	432	448	496	515
Yielding of bottom steel flange (support)	454	462	468	472	482
Yielding of bottom steel flange (mid-span)	659	659	659	660	661
Ultimate capacity of section over interior support	523	601	643	723	821
Failure	698	790	820	902	971

Table 4-3 Loads corresponding to failure mechanism stages of Girder with CFRP

For girder CSCC4, and CSCC5 yielding of bottom flange at mid-span started before reaching the ultimate capacity of the section over the interior support. On the other hand, CSCC1, CSCC2, and CSCC3 yielding of bottom steel flange at the mid-span started before reaching capacity of section at the negative moment (over the interior support). This is mainly because capacity of section at the positive moment region is approximately constant, whereas capacity of section at the negative moment increased by increasing thickness of CFRP.

The steel reinforcement at the negative moment region started yielding at the same stage of loading of about 55% of the ultimate load for all girders with different thicknesses of CFRP as shown in table (4-4). Steel reinforcement at positive moment region reached higher compression stress at ultimate load as CFRP thickness increased as shown in table (4-5).

Stage of Loading / Girder	Load at yielding	Ultimate load	Ratio of yielding to ultimate load
CSCC1	407	698	0.583
CSCC2	432	790	0.546
CSCC3	448	820	0.546
CSCC4	496	902	0.549
CSCC5	535	971	0.55

Table 4-4 Yielding of steel reinforcement over interior support

Girder	Compression steel stress	% of yielding
CSCC1	226	65%
CSCC2	248	71%
CSCC3	255	73%
CSCC4	280	80%
CSCC5	326	93%

Table 4-5 Compression stress of steel reinforcement at positive moment region at ultimate load

Changing thicknesses of CFRP does not change the loads corresponding to yielding of bottom steel flange over interior support or at mid-span for girders significantly as shown in table (4-6). Small variation observed in this load due to small change of the neutral axis location.

Load / Girder	Load at yielding of bottom steel flange (support) (KN)	Load at yielding of bottom steel flange (mid-span) (KN)	Ultimate Load (KN)
CSCC1	454	659	698
CSCC2	462	659	790
CSCC3	468	659	820
CSCC4	472	660	902
CSCC5	482	661	971

Table 4-6 Yielding of steel section

4.4 EFFECT OF CFRP LENGTH

Four models with different CFRP lengths (CSCC2, CSCC2L1, CSCC2L2 and CSCC2L3). CFRP covers the negative moment region for all models except CSCC2L3. The results showed that extension of CFRP beyond the negative moment region does not affect the ultimate capacity of the girder as shown in Figure (4-26).

The ultimate load carrying capacity for girders that CFRP covers the negative moment region or extended beyond the inflection point is about 790 KN. Reduction of CFRP length within the negative moment region reduced the ultimate capacity of girder to 678 KN. The stiffness of these girders is the same whereas maximum deflection before failure reduced greatly if CFRP cut short of the inflection point.

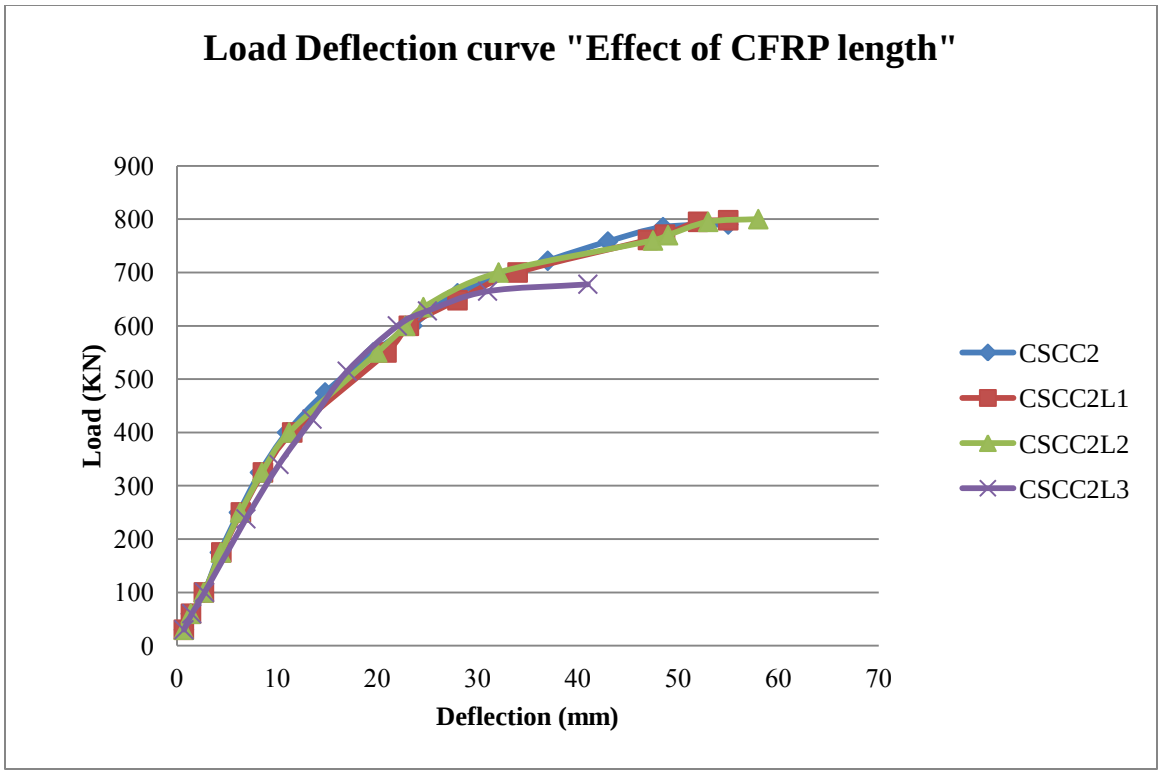

Figure 4-26 Load deflection curves of girders with different CFRP lengths

The shear and tensile stresses of the bonding material at the ends of CFRP plate were less than the maximum values at the ultimate capacity for all girders except CSCC2L3. When length of CFRP plate is cut short of the inflection point, such stresses exceeded the maximum shear and tensile stresses of the bonding material. Figure (4-27) shows reaching bonding material to the maximum allowable strain.

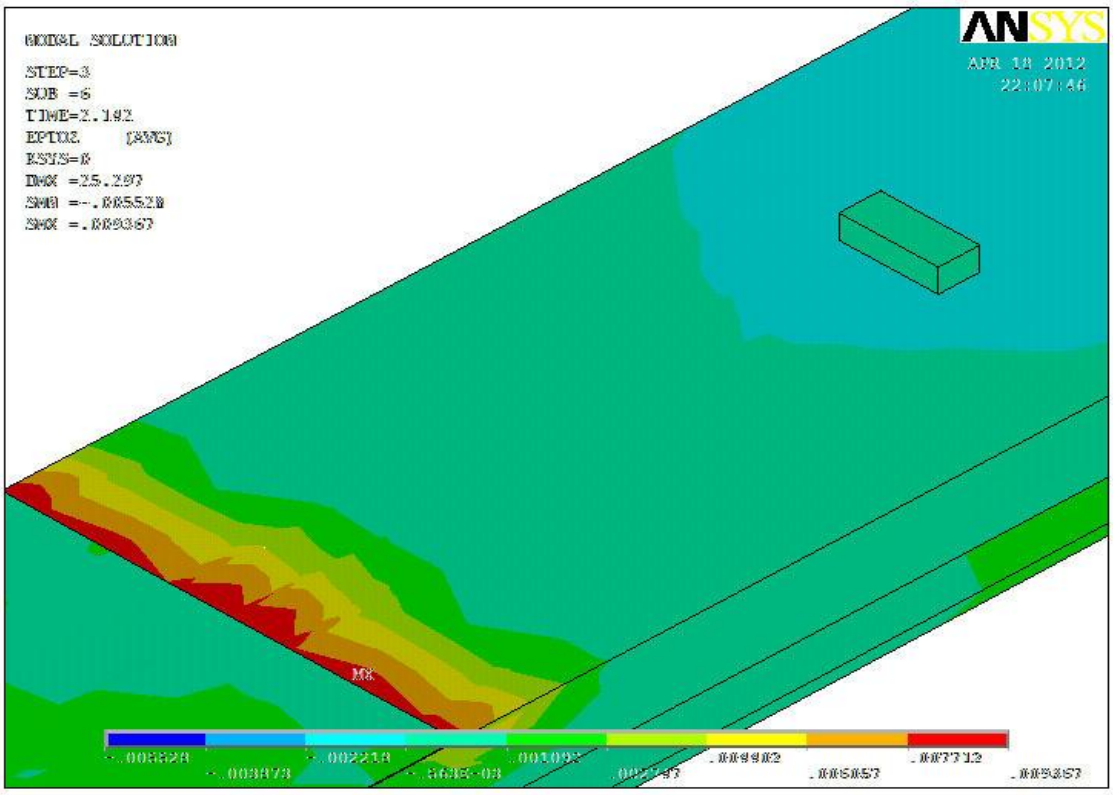

Figure 4-27 strain distribution at the end of CFRP sheet

The failure mechanism of girders CSCC2L1 and CSCC2L2 followed similar failure mechanism of girder CSCC2 as shown in table (4-7). No effect was noticed when CFRP extended beyond the inflection point. For girder CSCC2L3, the failure mechanism followed similar pattern to other girders up to reaching the ultimate capacity over the interior support. Beyond this loading, the bonding material reached the maximum shear and tensile stresses of bonding material at 620 KN. This is followed by yielding the bottom flange at mid-span. Finally girder failed by crushing of concrete at mid-span.

Failure mechanism stage	CSCC2L1 (KN)	CSCC2L2 (KN)	CSCC2L3 (KN)
Yielding of steel reinforcement in the negative moment region	436	437	430
Yielding of bottom steel flange over the interior support	461	460	451
Ultimate capacity of section over interior support	603	601	594
Yielding of bottom steel flange (mid-span)	667	667	635
Failure	800	798	673

Table 4-7 loads corresponding to failure mechanism stages of Girders with different lengths of CFRP

Bonding material of girder CSCC2L3 reached maximum tensile and shear stresses after reaching ultimate capacity over the interior support. Failure of bonding material causes exceeding capacity of the section and premature failure at mid-span. It's noted that CSCC2L3 doesn't reach full plastic capacity because of its premature failure.

4.5 EFFECT OF NEUTRAL AXIS LOCATION

Two models with different slab thicknesses were investigated in the study. Slab thickness of 90 mm (neutral axis in the steel section), and slab thickness of 120mm (neutral axis in the concrete slab). FE results showed that the ultimate load carrying capacity and stiffness of girder CSC1 is more than that of CSC as expected. The ductility of girder CSC1 is reduced compare to CSC because girder CSC1 is stiffer than CSC as shown in figure (4-28).

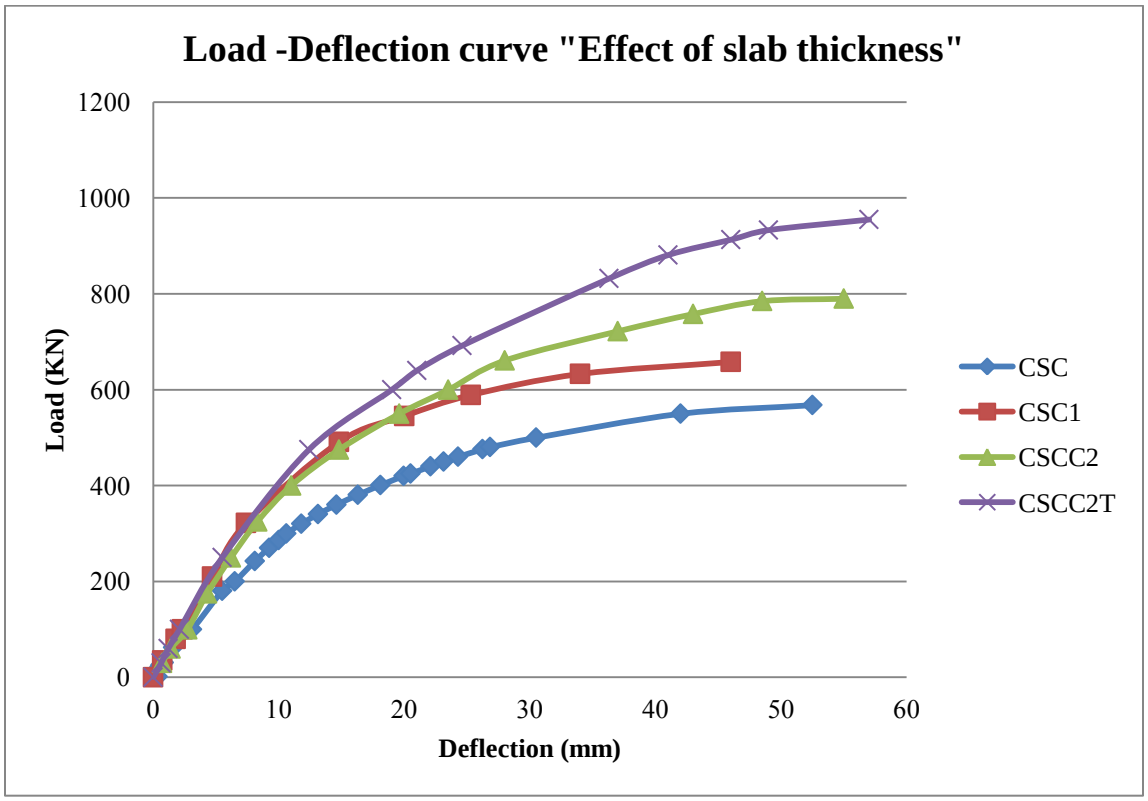

Figure 4-28 Load deflection curves of girders with different slab thicknesses

Load deflection curve shows that the ultimate load carrying capacity of CSCC2T is greatly increased compare to CSCC2. The stiffness and ductility of girder CSCC2T are improved compare to CSCC2. The efficiency of using tensile capacity of CFRP is

increased to 12.5% due to increasing the area of steel section in compression which increased the required tensile stress in CFRP.

Failure mechanism of CSCC2T followed the same mechanism of girders with CFRP. Steel reinforcement yielded at higher load compare to CSCC2. Steel reinforcement at the negative moment region started yielding at early stage of loading for CSCC2T compare to CSCC2 whereas steel reinforcement at positive moment region reached yielding at ultimate load.

4.6 COMPARISON BETWEEN CAPACITY OF SECTION AT THE NEGATIVE AND POSITIVE MOMENT REGIONS

The ratio of capacity of section at the negative moment region to the ultimate capacity at the positive moment region (collapse load) is given in table (4-8) for all girders. This ratio reflects the required rotational capacity of the section at the negative moment region.

Capacity of section at the negative moment region to the ultimate capacity at the positive moment region is increased by bonding CFRP over the negative moment region. The increase of this ratio is due to increasing the capacity of section over the negative moment region whereas no change in the capacity at positive moment region.

Stage of Loading / Girder	At Negative moment	At positive moment	Ratio
CSC	393	568	0.69
CSCC1	523	698	0.75
CSCC2	601	790	0.76
CSCC3	643	820	0.78
CSCC4	723	902	0.80
CSCC5	819	971	0.85
CSCC2L1	603	790	0.76
CSCC2L2	601	800	0.76
CSCC2L3	594	673	0.88
CSC1	423	658	0.64
CSCC2T	689	955	0.72

Table 4-8 Ultimate capacity of girders

Table (4-8) shows that increasing CFRP thickness over the negative moment region increased capacity of section at the negative moment region to the ultimate capacity at the positive moment region. Extending CFRP beyond the inflection point does not affect this ratio whereas cut of CFRP before the inflection point increased this ratio greatly due to premature failure.

Increasing concrete slab thickness increased the capacity of section at the positive moment significantly which decreases capacity of section at the negative moment region to the ultimate capacity at the positive moment region. This ratio is decreased for girder CSCC2T because capacity increase at positive moment region due to increasing slab thickness is more than capacity increase at negative moment region due to CFRP.

4.7 COMPARISON BETWEEN GIRDER WITH CFRP AND EXTERNAL PRESTRESSED CABLES

Increasing capacity of continuous steel-concrete girder using external prestressed tendons carried out experimentally by Chen et al [14]. This result used to compare using external prestressed tendons and using CFRP to increase capacity of continuous composite girder. The ultimate load carrying capacity of continuous composite girder prestressed with external tendons increased by 11% to 619 KN. Bonding CFRP of 0.25 mm thickness over the negative moment region increased the ultimate capacity of girder by 39% as shown in figure (4-29).

Improvement on stiffness for both girders with external prestressed tendons and CFRP was noticed. Figure (4-29) shows that stiffness of girder partially reinforced with CFRP improved more than girder strengthened by external prestressed tendons. Using external prestressed tendons reduced ductility of girder whereas using CFRP increased it. The increasing in the maximum deflection before failure is important to have enough rotation of section to achieve full plastic capacity of section.

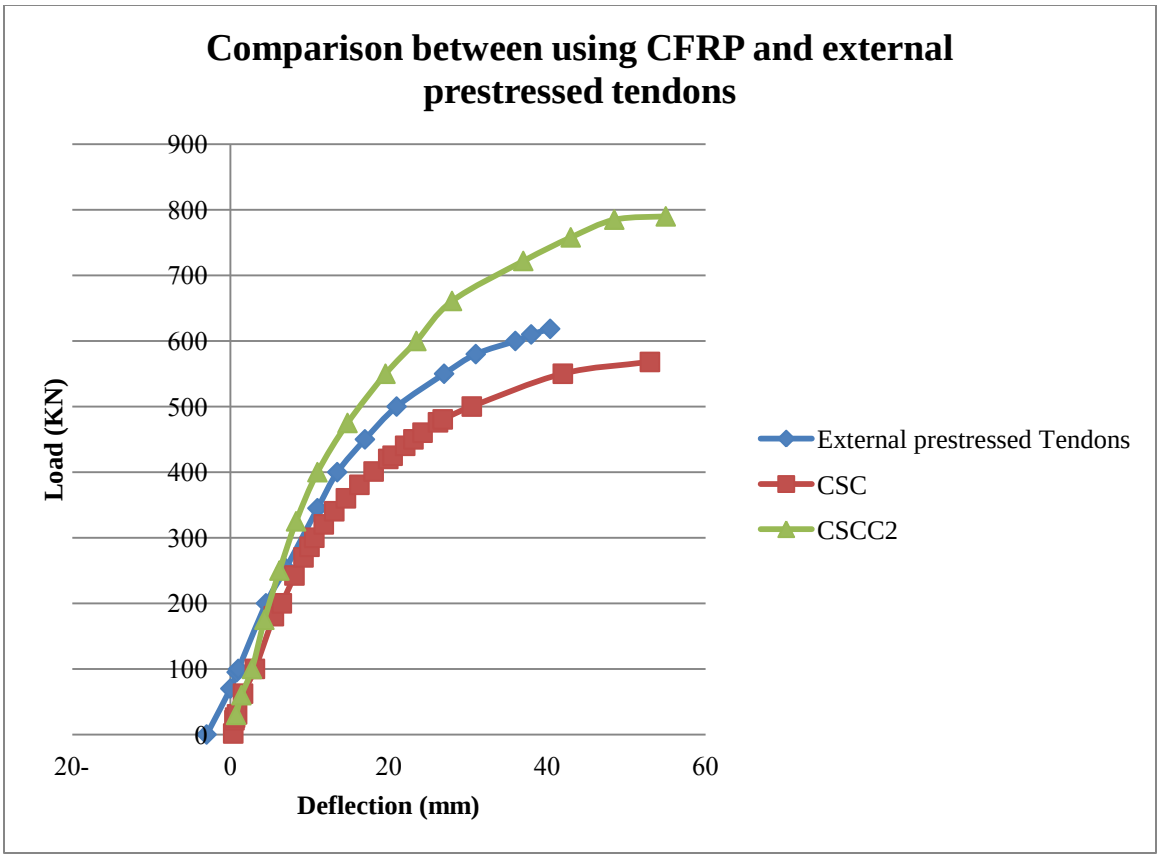

Figure 4- 29 Comparison between using CFRP and External prestressed tendons

External prestressed tendons did not improve the capacity of section over the internal support greatly, whereas it improves the total capacity of girder. The ultimate capacity of the section over the interior support becomes 51% of the capacity of section at positive moment region compare to 69% for CSC. On the other hand, using CFRP increased the ultimate capacity of section over the interior support. The capacity of section over the interior support becomes 76% of the ultimate load of girder.

Girder with external prestressed tendons has the same failure mechanism of CSC whereas the cracking load of concrete occurred at 95KN instead of 30.7 KN without prestressed tendons.

CHAPTER FIVE

PLSTIC ANALYSIS

The previous work discussed FE analysis of continuous composite girders with CFRP. Analysis conducted based on a multilinear stress-strain diagram. Both material and geometric non linearity were included in the modeling. This chapter presents a simple analytical solution to evaluate the ultimate capacity of the continuous composite steel-concrete girder partially reinforced with CFRP.

5.1 INTRODUCTION TO PLASTIC DESIGN

The ultimate load capacity of the structure s a whole considered as design criterion in the plastic analysis of structures. The ultimate capacity of the section is found from the strength of steel in the plastic range so that it's called plastic analysis. Economical sections provided by this method as regards the weight of steel since the required sections are smaller in size compare to sections required by elastic analysis. Analysis and design of statically indeterminate structures are the main application of plastic analysis. The selected section should reach its plastic moment capacity and then undergo considerable rotation at this moment.

For example, for a single span beam with fixed ended subjected to a uniform load (w). The elastic bending moment at the ends is $wl^2/12$ and at mid-span is $wl^2/24$, where "l" is the span length. The bending moment and the stresses at every section increase as (w) is increases gradually. As the load increases, the extreme fiber of section close to the end supports reaches yield stress, because the maximum bending moment is at supports. This moment called as first yield moment M_y. This moment does not mean reaching failure load, beam can continue to carry additional load. More and more fibers reach yield stress as the load continues to increase. Eventually the whole of the cross section reaches the yield stress. This moment corresponding to reach the whole section the yield stress called as plastic moment and denoted by Mp. Equilibrium equation used to find the fully plastic moment of a yielded section of a beam.

The ratio of the plastic moment to the yielding moment called the shape factor of section. It depends on cross section shape. After reaching the capacity of the sections at ends, the section is not capable to resist additional moment but it may maintain this moment with additional rotation like a plastic hinge. Based on that, beam is acting as simply supported beam with two Mp at ends. Beam continues to carry loads until forming a third plastic hinge at mid-span when the bending moment at that section reaches Mp. In this way, beam developed the collapse mechanism. The rotation capacity of the section is the ratio of the ultimate rotation to the yield rotation.

5.2 ENERGY METHOD "VIRTUAL WORK METHOD"

Plastic load (W) or required plastic moment Mp of a structure could be found using the principle of virtual work. "Consider that as the collapse mechanism load is reached the beam moves through the virtual displacement δ. For equilibrium, the external work done by the load moving through the virtual displacement must equal the internal strain energy due to plastic moment rotation through small angles" [28]. This requires evaluation of displacements and plastic hinge rotations.

.

It is assumed that the frame remains rigid between supports and hinge positions so that the plastic deformations at collapse load are considered larger than elastic deformations. All plastic rotation occurs at the plastic hinges. For a simply supported beam carried a point load at mid-span, the centre of the span has the maximum deflection where a plastic hinge will be formed once the full section reached yielding. The entire energy will be absorbed by the rotation of the plastic hinge because the remainder of the beam will remain straight.

5.3 ASSUMPTIONS

The simple analytical solution carried out based on material and geometrical assumptions.

5.3.1 Material assumptions

1) The tensile capacity of concrete slab is zero.
2) Idealize stress-strain diagram of steel. The steel considered as elastic-perfectly plastic material.
3) The compressive capacity of concrete is given as $0.85f'_c$.
4) The compressive and tensile stress capacity in steel reinforcement is yielding f_y.
5) Full composite action between concrete and steel, and between concrete and CFRP.

5.3.2 Geometrical Assumptions

1) Local buckling is prevented. Steel sections are consisting of thin plates assemble together. These plates may buckle before reaching the full capacity if they are subjected to large compressive stress as shown in figure (5-1). Buckling of these plates because they are slender prevents the member to reach the full plastic capacity. Therefore, local buckling becomes a limit state for the capacity of steel section subjected to compressive stress. So that it's assumed that the width to thickness ratio of plate elements is small which eliminate local buckling, this mean that section classified as plastic section as shown in figure (5-2) [28]. AISC manual contains specification limits and requirements for slenderness ratio of steel segments to achieve plastic capacity [29] [30].

Figure 5-1 Local buckling in the bottom flange of steel section

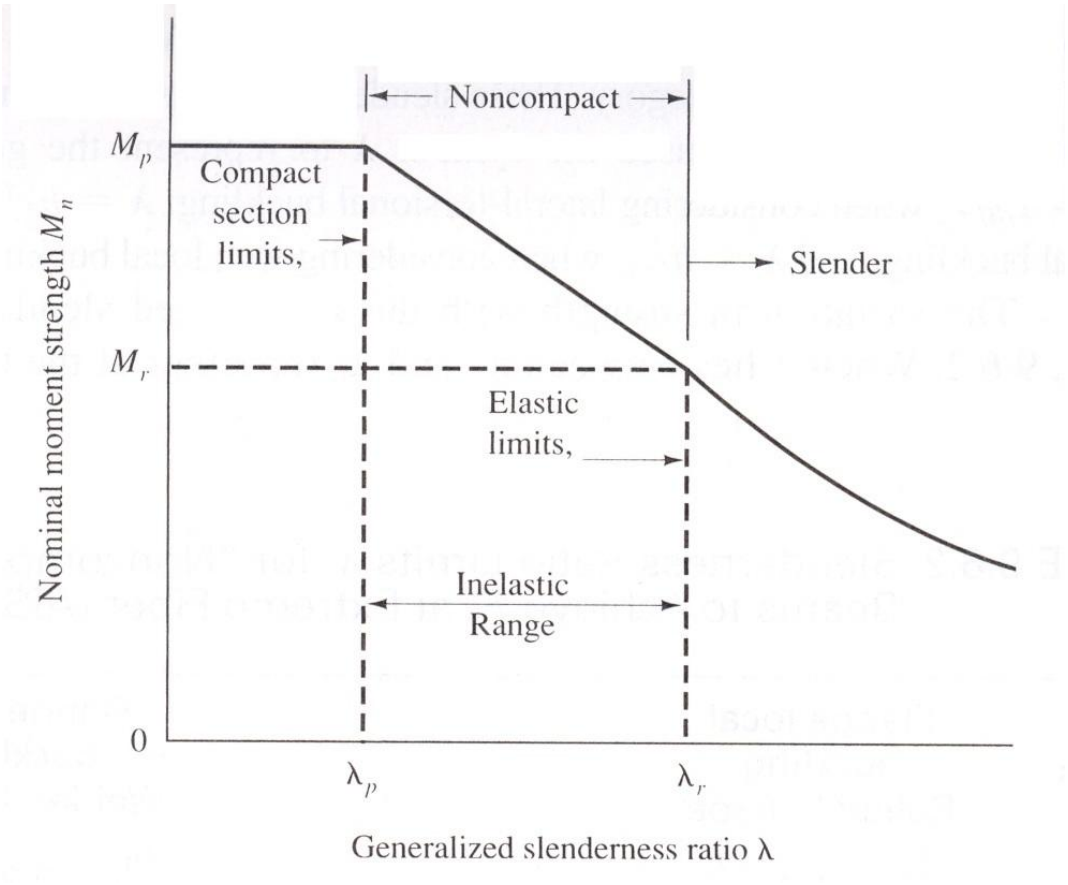

Figure 5-2 Slenderness ratio of section vs. Moment capacity

2) Lateral torsional buckling is prevented. Lateral torsional buckling occurred by flexural loading (M), and the buckling deformations are coupled in the lateral and torsional directions. Adequate lateral bracings at adequate intervals along the beam have to be used to prevent LTB [31]. Two limits for LTB (Lp and Lr) can be calculated for each section and compared to laterally unbraced length (L_b). AISC contains requirements to achieve full plastic capacity and to prevent LTB [29]. Depending on which limit state L_b sits at, the maximum moment for the beam can be calculated. Figure (5-3) shows slenderness of section versus moment capacity of the section.

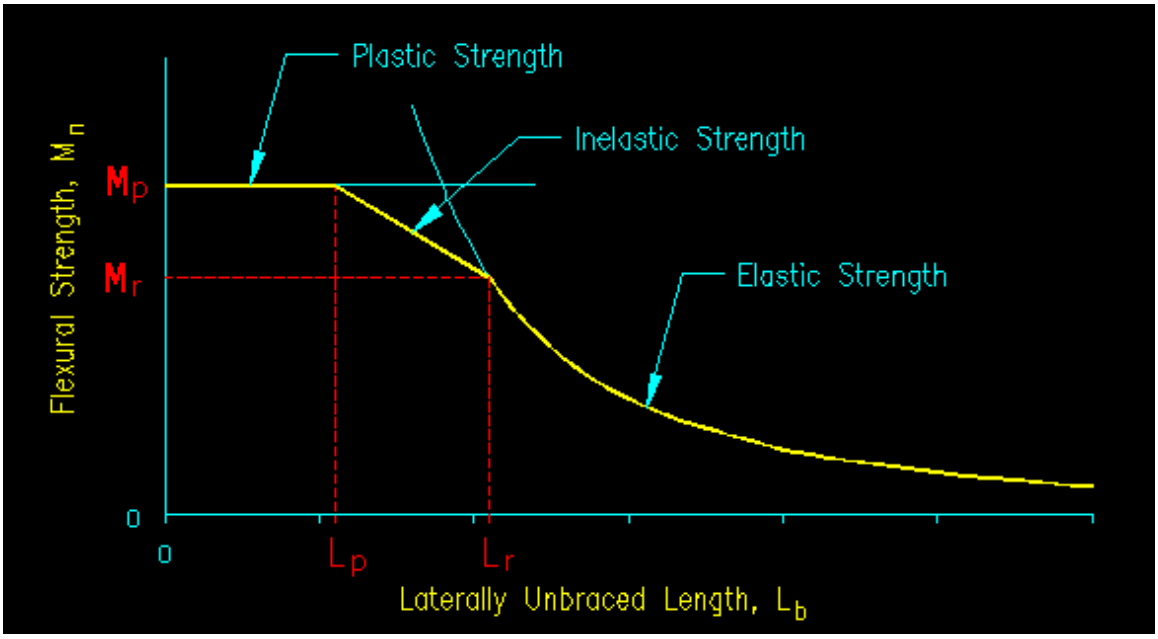

Figure 5-3 Effect of lateral unbraced length on moment capacity [30]

3) Proper stiffeners and bearing plates are provided so that concentrated load problems are prevented.

5.4 CAPACITY OF SECTION AT POSITIVE MOMENT

The ultimate load and failure mechanism depend on the location of the neutral axis. Equations for design obtained based on the neutral axis in

i) Concrete slab.

ii) Top flange of the steel section.

iii) Web of steel section.

Neutral axis in the concrete slab

At positive moment, the concrete slab subjects to compression stress whereas steel section subjects to tension. Figure (5-4) show stresses distribution at ultimate load.

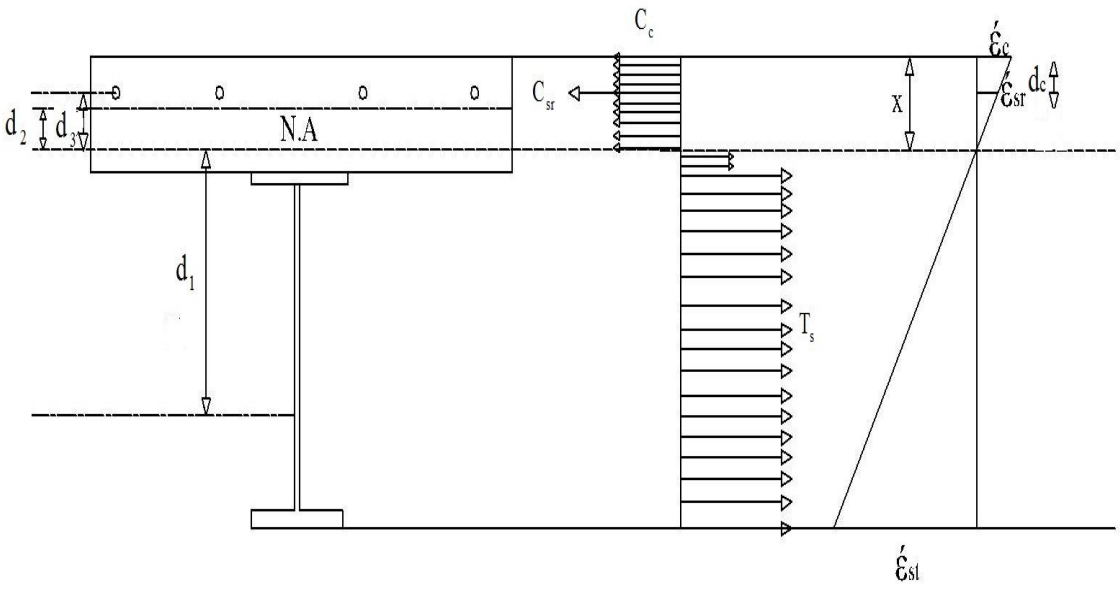

Figure 5-4 Stress and strain distributions at ultimate load, N.A in concrete slab

Using Equilibrium equation, then:

$$C_c + C_{sr} = T_c + T_s$$

$$C_c = 0.85 f'_c b a$$

$$C_{sr} = A_{sr} f_s$$

$$T_s = A_{st} f_y$$

Then, $$x = \frac{A_{st} f_y - A_{sr} f_y}{0.85 f'_c b}$$ .....equ(1)

The strain compatibility has to be checked so that the maximum strain in concrete "$\acute{\varepsilon}_c$" does not exceed 0.003. Then check if steel reinforcement reached yielding strain.

$$\varepsilon_{sr} = \frac{\varepsilon_c}{x} d_c$$ .....equ(2)

The moment Capacity is given by

$$M = A_{st} f_y d_1 + A_{sr} f_s d_3 + 0.85 f'_c b a d_2$$ .....equ(3)

The equation could be simplified if steel reinforcement in compression ignored to be:

$$M = A_{st} f_y d$$ .....equ(4)

Where:

d: distance between center of concrete in compression and center of steel section ($d_1 + d_2$)

Neutral axis in the steel section

The neutral axis could be in steel flange or steel web so that part of the steel section is under compression and another part in tension as shown in figures (5-5) and (5-6).

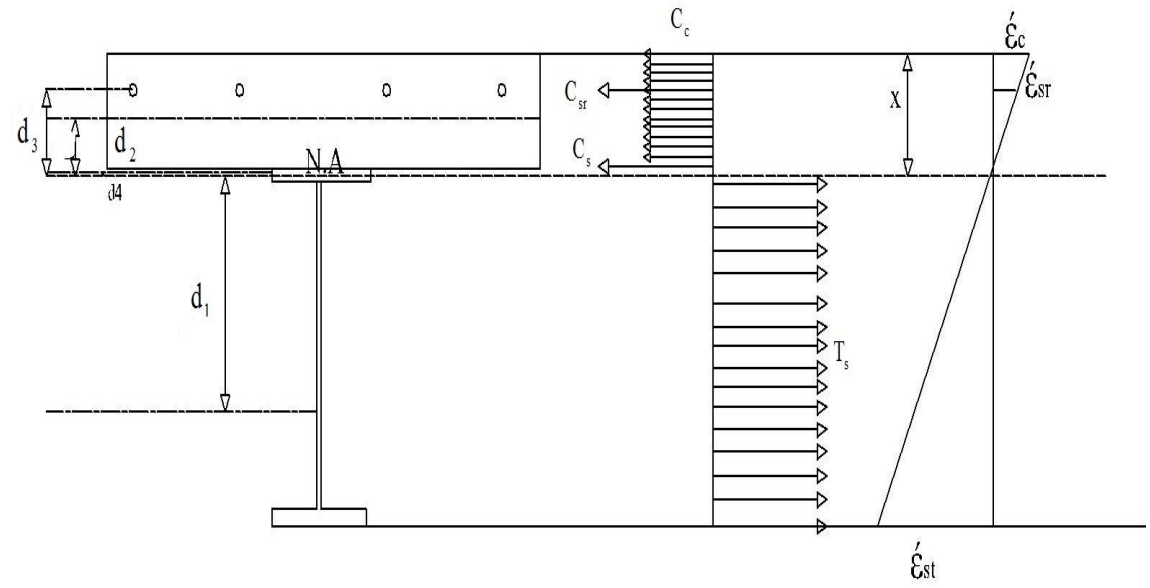

Figure 5-5 Stress and strain distributions at ultimate load, N.A in steel flange

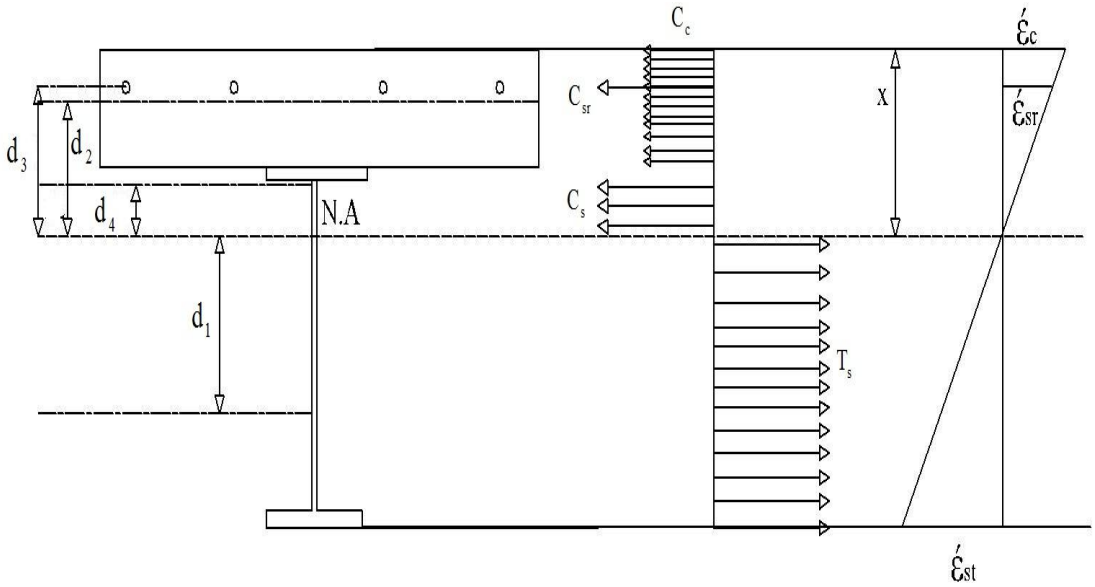

Figure 5-6 Stress and strain distributions at ultimate load, N.A in steel web

Using Equilibrium equation, then:

$$T_s = C_c + C_s + C_{sr}$$

$$C_c = 0.85 f'_c ba$$

$$C_{sr} = A_{sr} f_s$$

$$T_s = A'_{st} f_y$$

$$C_s = A''_{st} f_y$$

The strain compatibility has to be used to find the location of the neutral axis so that the maximum strain in concrete "$\acute{\varepsilon}_c$" does not exceed 0.003. Then check if steel reinforcement reached the yielding strain.

$$\varepsilon_{sr} = \frac{\varepsilon_c}{x} d_c$$

The moment capacity of section is

$$M = A'_{st} f_y d_1 + A''_{st} f_y d_4 + A_{sr} f_s d_3 + 0.85 f'_c b a d_2 \qquad \text{.....equ(5)}$$

5.5 CAPACITY OF SECTION AT THE NEGATIVE MOMENT

Neutral axis in the concrete slab

At ultimate load, the stress in the entire steel section is the yielding stress. Figure (5-7) shows stress and strain at the ultimate load.

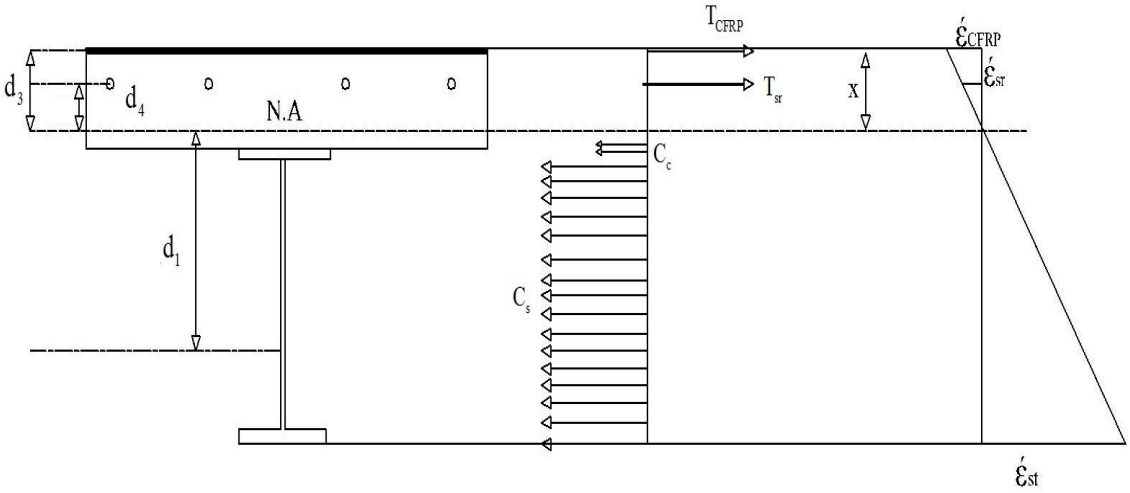

Figure 5-7 Stress and strain distributions at ultimate load in the negative moment, N.A in slab

Using Equilibrium equation, then:

$$T_{CFRP} + T_{sr} = C_s + C_c$$

The strain compatibility besides equilibrium equation should be used to find the location of the neutral axis and tensile stress in CFRP so that CFRP strain does not exceed maximum at the ultimate load. At the same time, the maximum strain in concrete at compression should not exceed maximum strain of concrete.

$$T_{sr} = A_{sr} f_{y1}$$

$$C_c = 0.85 f'_c ba$$

$$C_s = A_{st} f_{y2}$$

The strain in steel reinforcement is given by

$$\varepsilon_{sr} = \frac{\varepsilon_{CFRP}}{x} d_c$$

The strain at the bottom face of concrete slab should not exceed 0.003 and it is given by

$$\varepsilon_c = \varepsilon_{CFRP} \left(\frac{t - x}{x}\right) \quad \text{.....equ(6)}$$

The moment capacity is equal to

$$M = T_{CFRP} * d_3 + T_{sr} * d_4 + C_s * d_1 + C_c * d_2 \quad \text{.....equ(7)}$$

Note: Compression of concrete and tension of steel reinforcement are opposite to each other. For simplicity, neglect these two values.

$$T_{sr} = C_s$$

Then, the moment capacity of the section is

$$M = T_{CFRP} H \quad \text{.....equ(8)}$$

Where H: Distance between center of CFRP and center of steel section (d_1+d_3)

Neutral axis in the steel flange

If the neutral axis in the steel flange, then part of the steel section is under compression and other part in tension as shown in figure (5-8), then:

$$T_{CFRP} + T_{sr} + T_s = C_s$$

The strain compatibility besides equilibrium equation should be used to find the location of the neutral axis and tensile stress in CFRP so that CFRP strain does not exceed maximum at the ultimate load. Then it's required to check yielding of steel reinforcement.

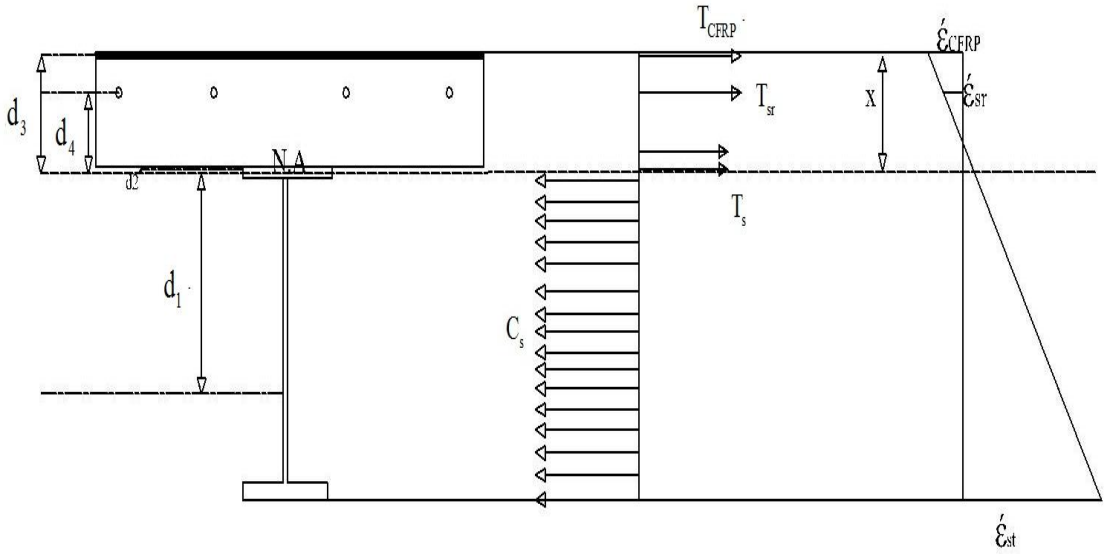

Figure 5- 8 Stress and strain distributions at ultimate load in the negative moment, N.A in steel flange

$$T_{sr} = A_{sr} f_{y1}$$

$$T_s = A'_{st} f_{y2}$$

$$C_s = A''_{st} f_{y2}$$

So that,

$$T_{CFRP} = A''_{st} f_{y2} - A'_{st} f_{y2} - A_{sr} f_{y1} \qquad \text{.....equ(9)}$$

The strain in steel reinforcement is given by

$$\varepsilon_{sr} = \frac{\varepsilon_{CFRP}}{x} d_c$$

Then, the moment capacity of the section is

$$M = C_s d_1 + T_{st} d_2 + T_{CFRP} d_3 + T_{sr} d_4 \qquad \text{.....equ(10)}$$

Neutral axis in the steel web

$$T_{CFRP} + T_{sr} + T_s = C_s$$

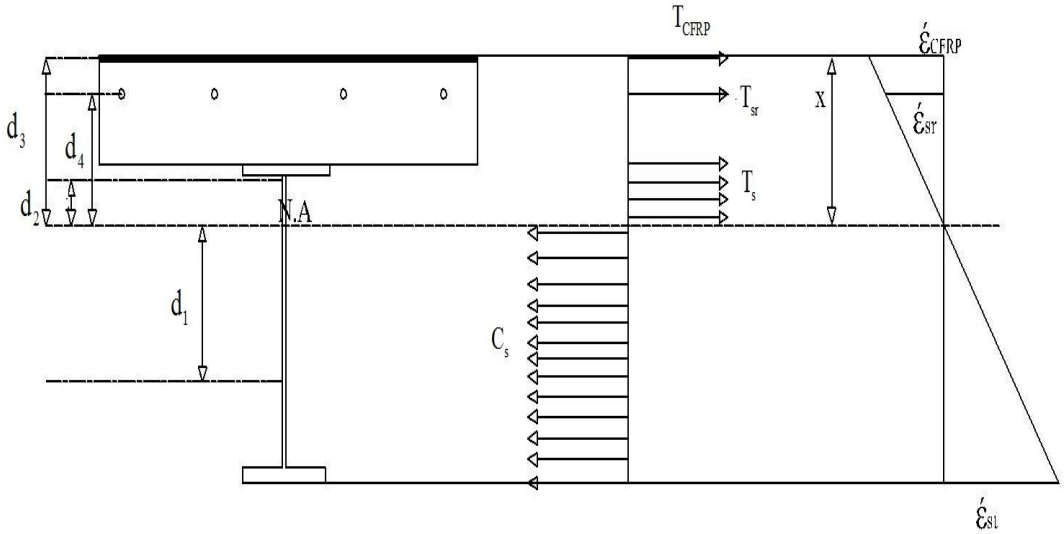

Figure 5- 9 Stress and strain distributions at ultimate load in the negative moment, N.A in steel web

The strain compatibility besides equilibrium equation should be used to find the location of the neutral axis and tensile stress in CFRP so that CFRP strain does not exceed maximum at the ultimate load. Then it's required to check yielding of steel reinforcement.

$$T_{sr} = A_{sr} f_{y1}$$

$$T_s = A'_{st} f_{y2}$$

$$C_s = A''_{st} f_{y2}$$

$$T_{CFRP} = A''_{st} f_{y2} - A'_{st} f_{y2} - A_{sr} f_{y1} \qquad \text{.....equ(11)}$$

The strain in steel reinforcement is given by

$$\varepsilon_{sr} = \frac{\varepsilon_{CFRP}}{x} d_c$$

$$M = C_s d_1 + T_{st} d_2 + T_{CFRP} d_3 + T_{sr} d_4 \qquad \text{.....equ(12)}$$

5.6 PLASTIC ANALYSIS FOR THE GIRDER

The plastic analysis conducted for the girder to obtain the plastic moment, and the ultimate load capacity of the girder. Two possible failure mechanism, the first one is the interior support and under the external load as shown in figure (5-10), whereas the second is the interior support and under the internal load as shown in figure (5-11).

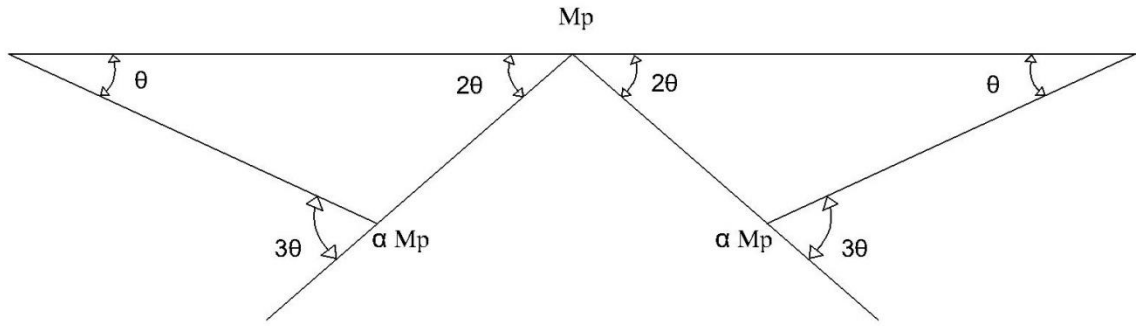

Figure 5-10 First possible failure mechanism

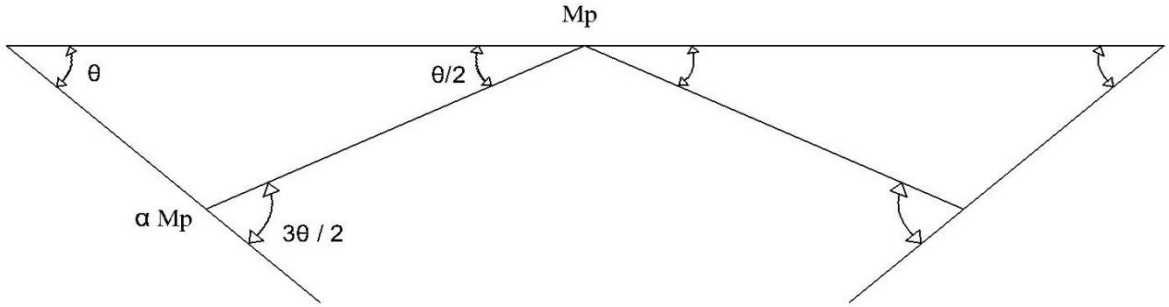

Figure 5-11 Second possible failure mechanism

First possible failure mechanism

Internal work = external work

$$2\theta M_p + 3\theta\alpha M_p = \frac{P}{2}(\Delta) + \frac{P}{2}(\frac{\Delta}{2}) \qquad \text{…..……equ(13)}$$

Where:

Δ: deflection under the internal point load

$$\Delta = 2\theta\frac{L}{3}$$

Then, $M_p = \frac{Pl}{4+6\alpha}$ …..……equ(14)

Second possible failure mechanism

Internal work = external work

$\frac{\theta}{2}M_p + \frac{3\theta}{2}\alpha M_p = \frac{P}{2}(\Delta) + \frac{P}{2}(\frac{\Delta}{2})$ …...……equ(15)

Where:

Δ: deflection under the external point load

$\Delta = \theta\frac{L}{3}$

Then, $M_p = \frac{Pl}{2+6\alpha}$ (Critical) …..……equ(16)

FE analysis showed that the second plastic hinge developed in the section close to the exterior point load.

5.7 ANALYTICAL SOLUTION FOR CSCC6

The finite element results showed that most of the concrete in the negative moment region not cracked by adding CFRP over the negative moment region. So that the neutral axis affected by concrete slab, the capacity of the girder calculated using the previous equations and plastic analysis as follow.

Check local buckling and Lateral torsional Buckling

Section plates of the steel section could be classified using AISC manual

- Web: $\frac{b}{t} = \frac{255}{6} = 42.5 < 3.76\sqrt{\frac{E}{f_y}} = 86$ (Compact)
- Bottom flange : $\frac{b}{2t} = \frac{120}{2*14} = 4.3 < 0.38\sqrt{\frac{E}{f_y}} = 8.7$ (Compact)
- Top flange: $\frac{b}{2t} = \frac{120}{2*10} = 6 < 0.38\sqrt{\frac{E}{f_y}} = 8.7$ (compact).

The length required to achieve plastic capacity of section with enough rotation is given by AISC manual

$$\frac{L_p}{r_y} = (0.12 + 0.076\frac{M_1}{M_p})\frac{E}{f_y}$$

$M_1 = M_p$ to develop plastic moment with enough rotation

Cross sectional area = 4410 mm^2 for the transformed section

Radius of gyration about y-axis (r_y) is given by

$$r_y = \sqrt{\frac{I_{yy}}{A}}$$

Moment of Inertia about y-axis

$$I_{yy} = \frac{1}{12}*14*120^3 + \frac{1}{12}*10*120^3 + \frac{1}{12}*255*6^3 + \frac{1}{12}*90*87^3 = 8399363\,\text{mm}^4$$

Radius of gyration about y-axis = $\sqrt{\frac{8399363}{4410}} = 43.6$

$$L_p = (0.12 + 0.076)\frac{29000}{60}*43.6 = 4.9\text{m}$$ (Compare to L_b = 4.8 m)

$L_p > L_b$

Calculate capacity of section at negative moment

The depth of the neutral axis has to be found by iterative procedure using equilibrium equation and strain compatibility. CFRP strain at ultimate load is 0.0164.

Assume that depth of neutral axis is 254 mm from bottom flange and tensile stress of CFRP is 0.25 F_u.

A''_{st} = 14*120 + 240*6 = 3120 mm^2

A'_{st} = 10*120 + 15*6 = 1290 mm^2

A_{CFRP} = 137.5 mm^2

A_{st} = 1610 mm^2

Center of steel in tension

$$\frac{10*120*5 + 15*6*17.5}{(10*120) + (15*6)} = 5.9\text{mm}$$

Center of steel in compression

$$\frac{14*120*7 + 240*6*134}{(14*120) + (240*6)} = 65.6\text{mm}$$

Then,

d_1 = 188.4 mm

d_2 = 19.1 mm

d_3 = 115 mm

d_4 = 70 mm

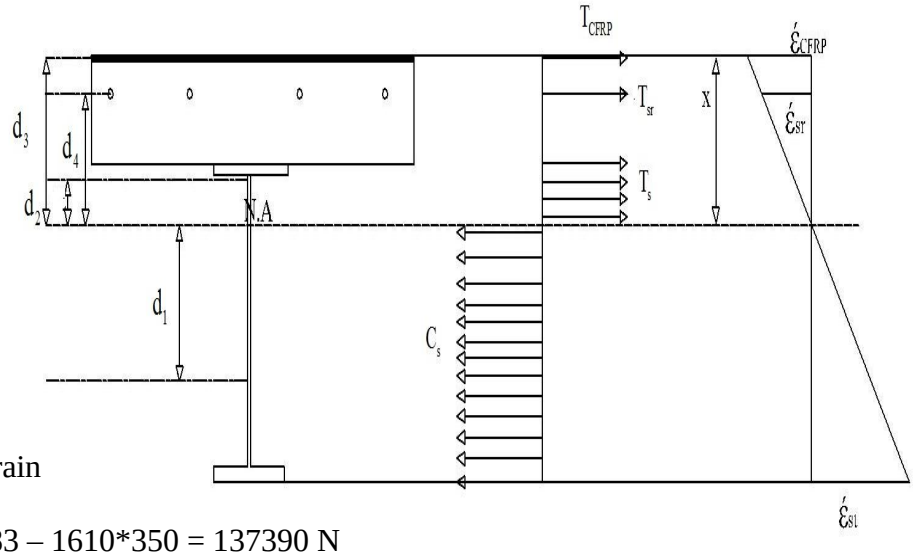

Calculate T_{CFRP} and check strain

T_{CFRP} = 3120*383 – 1290*383 – 1610*350 = 137390 N

Stress of CFRP = 995 N/mm^2 (0.255 F_u)

Strain of CFRP = 0.00433 OK

Strain of steel reinforcement > yielding strain

The capacity of section at the negative moment is given in equation (12),

M= 3120 *188.4 * 383 + 1290*19.1*383 + 137390*115 + 1610 * 350 *70 = 290 *10^6

N.mm = 290 KN.m

Calculating capacity of section at positive moment

The neutral axis located using equilibrium equation and strain compatibility. Assume the neutral axis 293 mm from the bottom steel flange and yielding of steel reinforcement.

d_1 =154 mm

d_2=38 mm

d_3= 31 mm

d_4= 0 mm

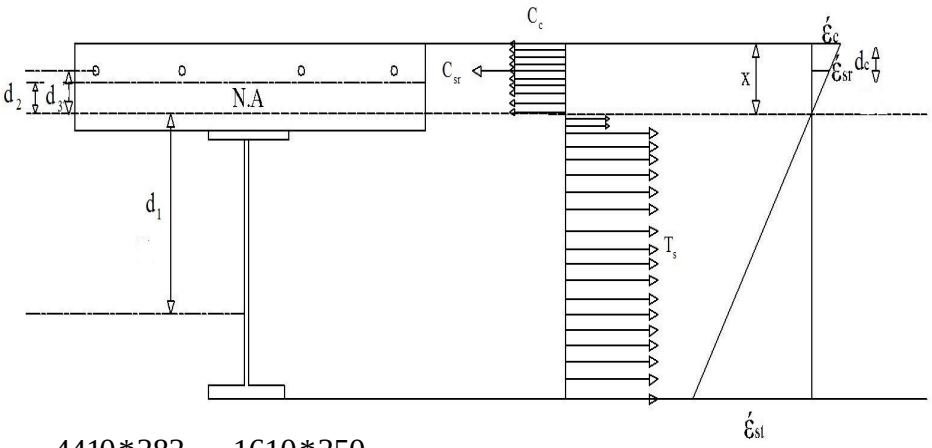

Stress in concrete= $\frac{4410*383 - 1610*350}{550*77}$ = 27.2 MPa (close to 0.85 f'$_c$)

Maximum strain of concrete " έ$_c$=0.003 ", then strain in steel reinforcement is more than yielding strain (0.00175).

$$M = A'_{st} f_y d_1 + A''_{st} f_y d_4 + A_{sr} f_s d_3 + 0.85 f'_c b t d_2$$

M = 4410*383*154 + 0 +1610*350*31 + 550*90*28.9*31 =325*10^6 N.m

M=325KN.m

The plastic moment capacity of the girder is given by equation (16)

$$M_p = \frac{Pl}{2+6\alpha}$$

$$\alpha = \frac{325}{290} = 1.13$$

$$290 = \frac{P*4.72}{2+6*(1.13)}$$

So that, P = 540 KN.

This result compared to the ultimate capacity of CSCC6 using FE software ANSYS. The ultimate load carrying capacity of CSCC6 is 635 KN by ANSYS. The following figure shows load deflection curve of CSCC6 using ANSYS.

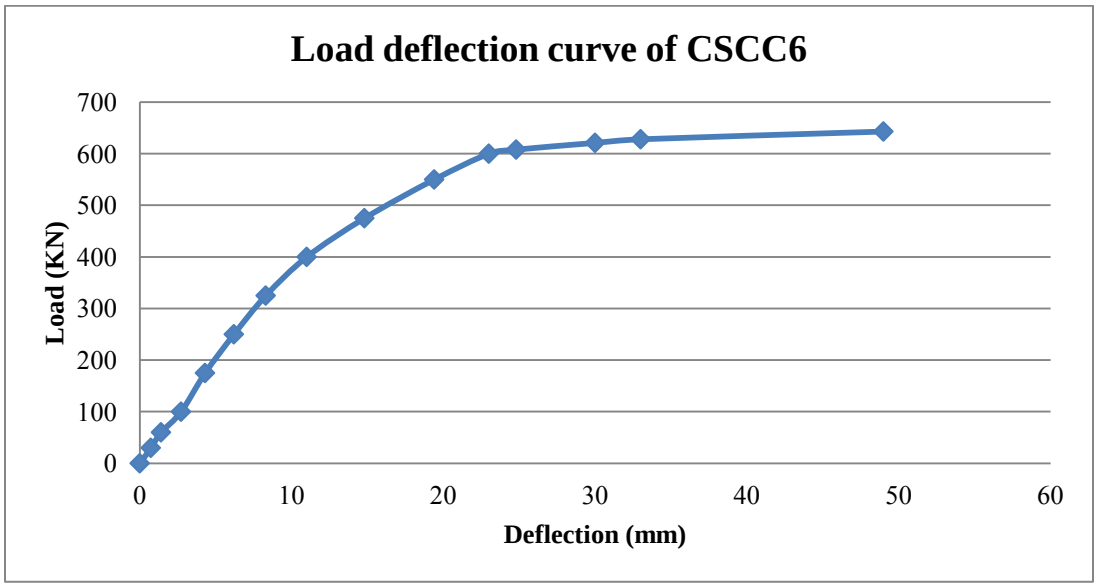

Figure 5- 12 Load deflection curve of CSCC6

Appendix includes design of continuous two spans girder partially reinforced with CFRP, and carried a uniform load.

5.8 NOMENCLATURE

C_c : Compression of concrete

C_s : Compression of steel

T_{st} : Tension of steel.

T_{CFRP} : Tension of CFRP

T_{sr} : Tension of steel Reinforcement.

C_{sr} : Compression of steel Reinforcement.

A_{st} : Area of steel section

A'_{st} : Area of steel section in tension.

A''_{st} : Area of steel section in compression.

A_{CFRP}: Cross sectional area of CFRP.

A_{sr} : Area of steel reinforcement.

f_{y1} : Yielding strength of steel reinforcement.

f_{y2} : Yielding strength of Steel.

f_s : Tensile stress of steel.

f'_c : Compressive capacity of concrete.

F_u : Ultimate strength of CFRP.

$\acute{\varepsilon}_{CFRP}$: Strain in CFRP.

$\acute{\varepsilon}_c$: Strain in concrete.

$\acute{\varepsilon}_{sr}$: Strain in steel reinforcement.

$\acute{\varepsilon}_{st}$: Strain in steel.

α: Capacity of section under the point load/ Capacity of section over support

t_{CFRP}: Thickness of CFRP

b: Width of concrete slab

t: Thickness of slab

t_c: Thickness of slab in tension.

a: Concrete compression block.

CHAPTER SIX

CONCLUSION AND FUTURE WORK

6.1 CONCLUSION

- Finite Element result showed that bonding CFRP over the negative moment region of continuous composite steel-concrete girder maintains the composite action between concrete and steel up to failure. This extremely improves ultimate capacity and stiffness in addition to the ductility of the composite continuous girder.

- The tensile stress of CFRP controlled by different factors such as
  - ✓ Capacity of the steel section. Once the steel section reached the ultimate capacity, then based on the equilibrium equation, CFRP cannot go for higher tensile load.
  - ✓ Location of the neutral axis. This will determine if the steel section acting totally in compression, or part in compression and another in tension.
  - ✓ Thickness of CFRP.

- Increasing CFRP thickness reduces utilization the CFRP.

- Increasing CFRP thickness has negligible effect on the stiffness of the continuous girder up to reaching capacity of steel section over the interior support, but it affects ductility of girder.

- Extension of CFRP beyond the inflection point has negligible effect on the capacity and stiffness of continuous composite girder. Reduction of CFRP length decreases the ultimate capacity and causes premature failure.

- The ratio of the capacity of section at negative moment region to that at positive moment region decreases as slab thickness increases

6.2 FUTURE WORK

Following are some suggestions for future research.

1) Investigating ability of CFRP to maintain the composite action under cyclic loading for continuous composite steel-concrete girder.

2) Experimental Program for girder partially reinforced with CFRP at the negative moment region to validate the results.

3) Finite element analysis of girder partially reinforced with CFRP at the negative moment region using different construction methods "Shored and Unshored system".

4) Investigate different shapes of steel section such as box section. Shape of steel section affect the stiffness of girder and the location of the neutral axis, it also affect local failure such as local buckling and lateral torsional buckling.

APPENDIX

DESIGN A CONTINUOUS GIRDER PARTIALLY REINFORCED WITH CFRP

Continuous two spans composite steel concrete girder carried total load of 50 KN/m^2. The span length is 10 m and the cross section is shown in the following figure. Lateral supports are provided to prevent lateral torsional buckling. The compressive capacity of concrete f'_c= 34 MPa and yielding strength of steel 383 MPa whereas yielding strength of steel reinforcement 350 MPa

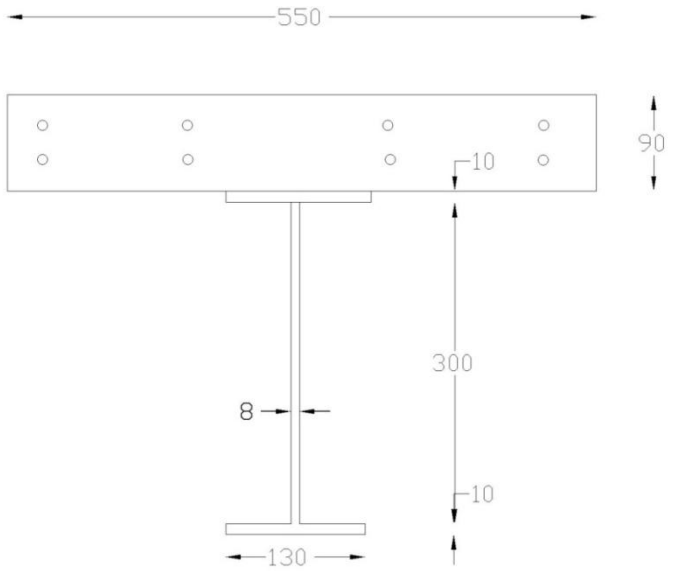

Plastic analysis using virtual work method used to find the plastic moment Mp as shown in the following figure.

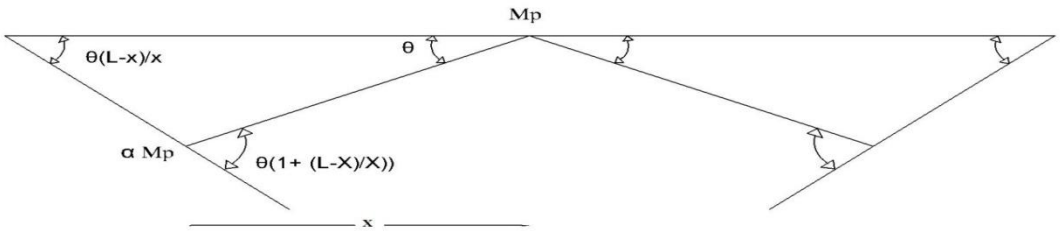

$$\theta Mp + \theta\,(1+ (L/X)/X)\ \ \alpha Mp = \frac{W_u L}{2}\,(L-X)\theta$$

$$\text{Then, } Mp = \frac{W_u L}{2}\,\Delta\,(L-X) / (X+ \alpha\, L)$$

$$\partial\, Mp/\partial\, X = 0$$

$$X= 0.414\ \alpha\ L$$

$$Mp = \frac{W_u L}{2}\,(0.293\ L - 0.121\,\alpha\ L)$$

Note: All plates of steel section are compact section.

Capacity of sections at positive and negative moment region calculated using equations in chapter five.

Calculate capacity of section at negative moment

Assume that N.A is 293 mm from the bottom flange and stress in CFRP is 0.25 F_u

$A''_{st} = 3564\ mm^2$

$A'_{st} = 1436\ mm^2$

$A_{sr} = 1610\ mm^2$

Center of steel in tension

$$\frac{10*130*5+17*8*18.5}{(10*130)+(17*8)} = 6\text{mm}$$

Center of steel in compression

$$\frac{10*130*5+283*8*151.5}{(10*130)+(283*8)} = 98\text{ mm}$$

T_{CFRP} = 3564*383 – 1436*383 – 1610*350 = 251524 N

Assume thickness of CFRP is 0.5 mm

Stress in CFRP is 915 MPa (0.24 F_u)

Strain in CFRP is 0.004

So that, steel reinforcement reached yielding

Then,

d_1 = 195 mm

d_2 = 21 mm

d_3 = 117 mm

d_4 = 72 mm

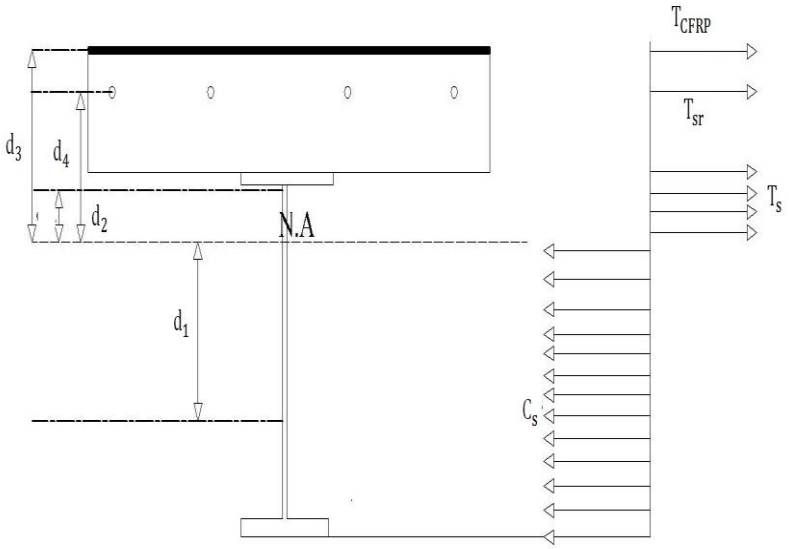

The capacity of section at the negative moment is

M= 3564 *195 * 383 + 1436*21*383 + 251524*117 + 1610 * 72* 350 =

330 *10^6 N.mm = 330KN.m (define as Mp)

Calculating capacity of section at positive moment

Assume that N.A is 325 mm from the bottom flange

Stress in concrete= $\frac{5000*383 - 1610*350}{550*85}$ = 29 MPa (close to 0.85 f'_c)

d_1 =165 mm

d_2= 43 mm

d_3= 40mm

d_4= 0 mm

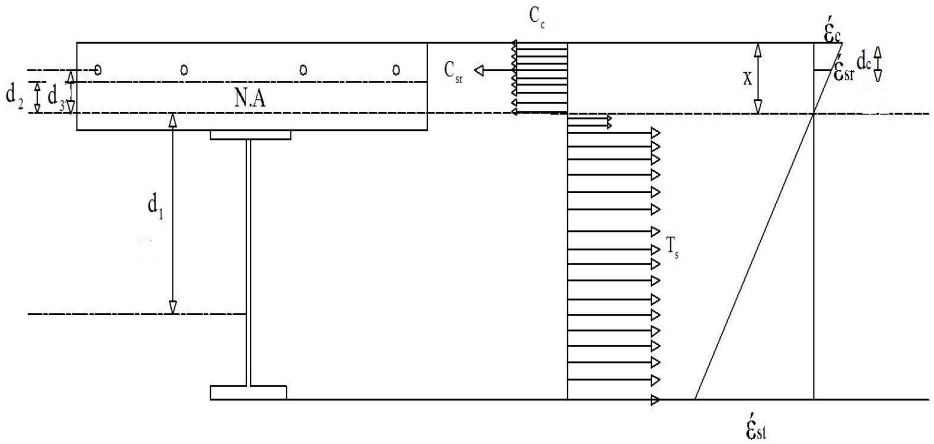

Capacity of section in the positive moment is

M = 5000*383*165 + 0 + 1610*350*40 + 550*85*29*43

M= 440 *10^6 N.mm = 440KN.m

α = 1.35

Mp = $\frac{50*10}{2}$ (0.293 * 10 – 0.121*1.15*10) = 327 KN.m< 330 KN.m (OK)

If not, need to increase CFRP thickness

Length of CFRP covers total negative moment region and extended for 5 m symmetry over the interior support.

REFERENCES

[1] B. Jurkiewiez, C. Meaud, and L. Michel, "Non linear behaviour of steel-concrete epoxy bonded composite beams," *Journal of Constructional Steel Research,* vol. 67, pp. 389–397, 2011.

[2] Y. Luo, A. Li, and Z. Kang, "Parametric study of bonded steel–concrete composite beams by using finite element analysis," *Engineering Structures,* vol. 34, pp. 40-51, 2012.

[3] L. Bouazaoui, G. Perrenot, Y. Delmas, and A. Li, "Experimental study of bonded steel concrete composite structures," *Journal of Constructional Steel Research,* vol. 63, pp. 1268-1278, 2007.

[4] H. R. Valipour and M. A. Bradford, "A steel-concrete composite beam element with material nonlinearities and partial shear interaction," *Finite Elements in Analysis and Design,* vol. 45, pp. 966-972, 2009.

[5] A. Ayoub, "A force-based model for composite steel–concrete beams with partial interaction," *Journal of Constructional Steel Research,* vol. 61, pp. 387-414, 2005.

[6] A. J. Yakel and P. Atorod Azizinamini, "Improved moment strength prediction of composite steel plate girders in positive bending," *Journal of bridge engineering,* vol. 10, p. 28, 2005.

[7] G. Ranzi and A. Zona, "A steel-concrete composite beam model with partial interaction including the shear deformability of the steel component," *Engineering Structures,* vol. 29, pp. 3026-3041, 2007.

[8] A. Vasseghi, "Improving strength and ductility of continuous composite plate girder bridges," *Journal of Constructional Steel Research,* vol. 65, pp. 479-488, 2009.

[9] F. Tahmasebinia and G. Ranzi, "Three-Dimensional FE Modelling of Simply-Supported and Continuous Composite Steel-Concrete Beams," *Procedia Engineering,* vol. 14, pp. 434-441, 2011.

[10] G. Porco, G. Spadea, and R. Zinno, "Finite element analysis and parametric study of steel-concrete composite beams," *Cement and Concrete Composites,* vol. 16, pp. 261-272, 1994.

[11] H. Sallam, A. Badawy, A. Saba, and F. Mikhail, "Flexural behavior of strengthened steel–concrete composite beams by various plating methods," *Journal of Constructional Steel Research,* vol. 66, pp. 1081-1087, 2010.

[12] G. Fabbrocino, G. Manfredi, and E. Cosenza, "Modelling of continuous steel–concrete composite beams: computational aspects," *Computers & structures,* vol. 80, pp. 2241-2251, 2002.

[13] S. Chen and Y. Jia, "Required and available moment redistribution of continuous steel-concrete composite beams," *Journal of Constructional Steel Research,* vol. 64, pp. 167-175, 2008.

[14] S. Chen, X. Wang, and Y. Jia, "A comparative study of continuous steel-concrete composite beams prestressed with external tendons: Experimental investigation," *Journal of Constructional Steel Research,* vol. 65, pp. 1480-1489, 2009.

[15] S. Nakamura, Y. Momiyama, T. Hosaka, and K. Homma, "New technologies of steel/concrete composite bridges," *Journal of Constructional Steel Research,* vol. 58, pp. 99-130, 2002.
[16] K. HAYASHI, S. ONO, and S. NAKAMURA, "Experimental Studies on Retrofit by Partially Encased Concrete to the Steel I-Girder subjected to Buckling Deformation," *Technical Memorandum of Public Works Research Institute,* pp. 229-236, 2003.
[17] J. Nie, M. Tao, and S. Li, "Analytical and Numerical Modeling of Prestressed Continuous Steel-Concrete Composite Beams," *Journal of Structural Engineering,* vol. 1, p. 305, 2011.
[18] D. H. Choi, Y. S. Kim, and H. Yoo, "External Post-tensioning of Composite Bridges by a Rating Equation Considering the Increment of a Tendon Force Due to Live Loads," *International Journal of Steel Structures,* vol. 8, pp. 109-118, 2008.
[19] A. M. Ibrahim and M. S. Mahmood, "Finite Element Modeling of Reinforced Concrete Beams Strengthened With FRP Laminates," *European Journal of Scientific Research,* vol. 30, pp. 526-541, 2009.
[20] M. Tavakkolizadeh, "Strengthening of steel-concrete composite girders using carbon fiber reinforced polymers sheets," *Journal of Structural Engineering-ASCE,* vol. 129, 2003.
[21] S. Khudeira, "Strengthening of Deteriorated Concrete Bridge Girders Using an External Posttensioning System," *Practice Periodical on Structural Design and Construction,* vol. 15, p. 242, 2010.
[22] T. C. Miller, M. J. Chajes, D. R. Mertz, and J. N. Hastings, "Strengthening of a steel bridge girder using CFRP plates," *Journal of bridge engineering,* vol. 6, p. 514, 2001.
[23] M. M. A. Kadhim, "Effect of CFRP plate length strengthening continuous steel beam," *Construction and Building Materials,* vol. 28, pp. 648-652, 2012.
[24] X. Liu, P. Silva, and A. Nanni, "Rehabilitation of steel bridge members with FRP composite materials," *strain,* vol. 11, p. 13, 2001.
[25] K. Galal, H. M. S. ElDin, and L. Tirca, "Flexural Performance of Steel Girders Retrofitted Using CFRP Materials," *Journal of Composites for Construction,* vol. 1, p. 212, 2011.
[26] K. Lau, P. Dutta, L. Zhou, and D. Hui, "Mechanics of bonds in an FRP bonded concrete beam," *Composites Part B: Engineering,* vol. 32, pp. 491-502, 2001.
[27] A. J. Wolanski, "Flexural behavior of reinforced and prestressed concrete beams using finite element analysis," Faculty of the Graduate School, Marquette University, 2004.
[28] C. G. Salmon, "Steel Structures: Design And Behavior Author: Charles G. Salmon, John E. Johnson, Faris A. Malhas, Publisher," 2008.
[29] A. AISC, "Steel Construction Manual; American Institute of Steel Construction," *Inc.–,* 2005.
[30] http://www.bgstructuralengineering.com/
[31] http://www.cnx.org
[32] ANSYS
[33] Structural Analysis Program (SAP 2000)

VITAE

NAME	MOHAMMAD A. SAMAANEH
PLACE OF BIRTH	NABLUS, PALESTINE
PERMANENT ADRESS	Beit Iba- Nablus - Palestine
E-mail	mohammad_samaaneh@yahoo.com samaaneh@kfupm.edu.sa
PHONE NUMBER	+970599355666

EDUCATIONAL QUALIFICATION

M.S (Civil Engineering-Structures)

King Fahd University of Petroleum and Minerals, Dhahran, Saudi Arabia

B.S (Civil Engineering)

An-Najah National University, Nablus,

Palestine